

Supplementary Information

Synthesis, pharmacological and structural studies of 5-substituted-3-(1-arylmethyl-1,2,3,6-tetrahydropyridin-4-yl)-1*H*-indoles as multi-target ligands of aminergic GPCRs

Magda Kondej¹, Tomasz M. Wróbel^{1,2}, Andrea G. Silva³, Piotr Stępnicki¹, Oliwia Koszła¹,
Ewa Kędzierska⁴, Agata Bartyzel⁵, Grażyna Biała⁴, Dariusz Matosiuk¹, Maria I. Loza³,
Marián Castro³, Agnieszka A. Kaczor^{1,6*}

¹*Department of Synthesis and Chemical Technology of Pharmaceutical Substances, Faculty of Pharmacy with Division of Medical Analytics, Medical University of Lublin, 4A Chodźki St., PL-20093 Lublin, Poland*

²*Department of Drug Design and Pharmacology, Faculty of Health and Medical Sciences, University of Copenhagen, Universitetsparken 2, 2100 Copenhagen, Denmark*

³*Department of Pharmacology, Universidade de Santiago de Compostela, Center for Research in Molecular Medicine and Chronic Diseases (CIMUS), Avda de Barcelona, E-15782 Santiago de Compostela, Spain*

⁴*Department of Pharmacology and Pharmacodynamics, Faculty of Pharmacy with Division of Medical Analytics, Medical University of Lublin, 4A Chodźki St., PL-20093 Lublin, Poland*

⁵*Department of General and Coordination Chemistry, Maria Curie-Skłodowska University, M. Curie-Skłodowskiej Sq. 2, PL-20031 Lublin, Poland*

⁶*School of Pharmacy, University of Eastern Finland, Yliopistonranta 1, P.O. Box 1627, FI-70211 Kuopio, Finland*

*Corresponding author: agnieszka.kaczor@umlub.pl

Content:

Fig. S1. Partial packing diagram of compound **9** viewed along the axes a (**a**) and c (**b**) showing N–H···N hydrogen bonds.

Fig. S2. Crystal packing of compound **9** showing the formation of N–H···H hydrogen bonds (dotted lines).

Fig. S3. Competition binding curves of compounds in radioligand binding assays at human D₂ receptors.

Fig. S4. Competition binding curves of compounds in radioligand binding assays at human 5-HT_{1A} receptors.

Fig. S5. Competition binding curves of compounds in radioligand binding assays at human 5-HT_{2A} receptors.

Fig. S6. Concentration-response curves of selected compounds antagonizing dopamine response in functional assays of cAMP signalling at human D₂ receptors.

Table S1. Lipophilicity calculated using ALOGPS 2.1 software and blood-brain permeability (BBB) calculated using On-line BBB predictor.

Table S2. Crystal data and structure refinement of the compound **9**.

Table S3. Interatomic distances and selected bond angles for the compound **9**.

Table S4. Experimental conditions employed in radioligand binding assays.

¹H NMR, ¹³C NMR and HRMS spectra of reported compounds.

Fig. S1. Partial packing diagram of compound **9** viewed along the axes **a** (a) and **c** (b) showing N–H···N hydrogen bonds.

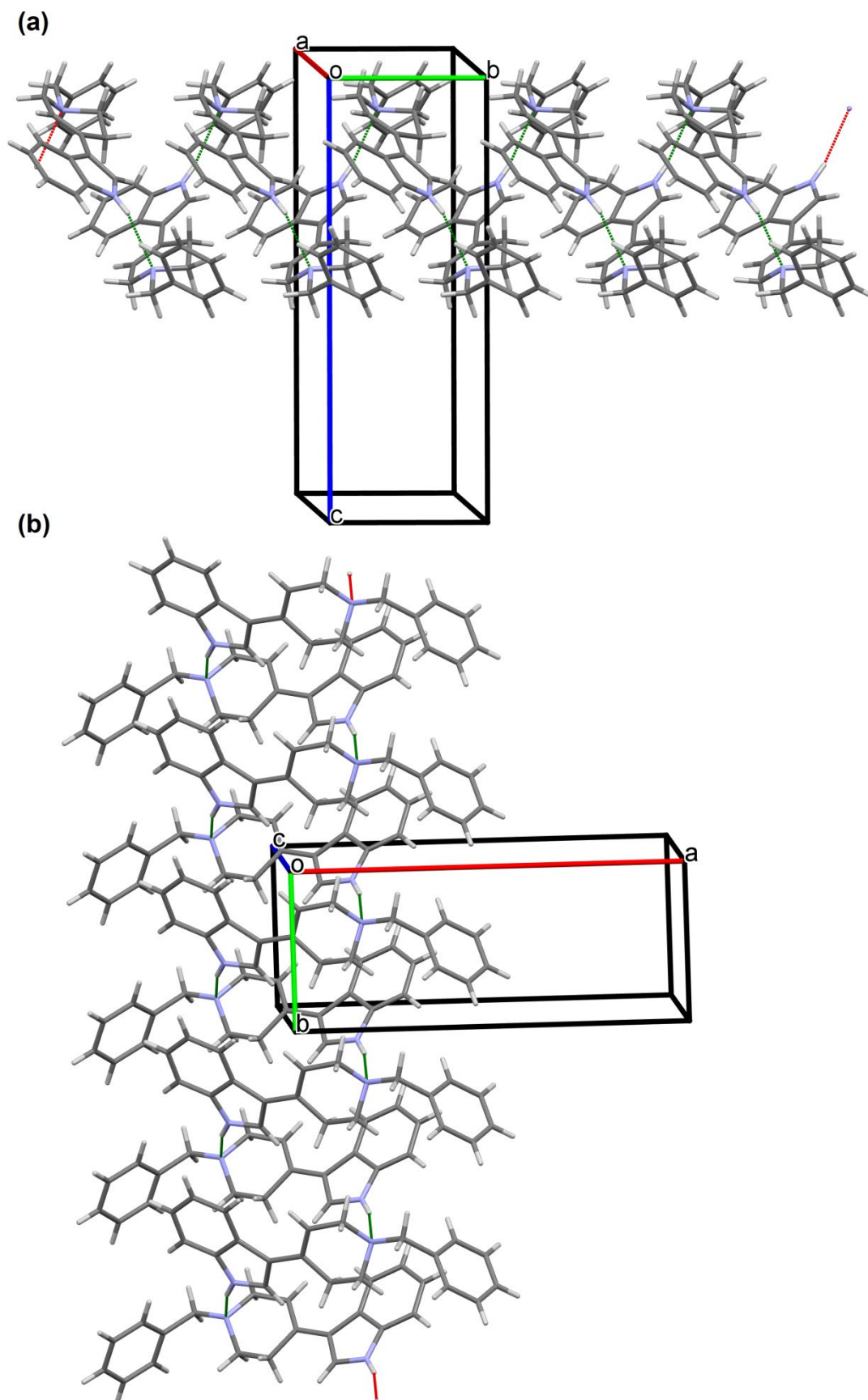


Fig. S2. Crystal packing of compound **9** showing the formation of N–H···H hydrogen bonds (dotted lines).

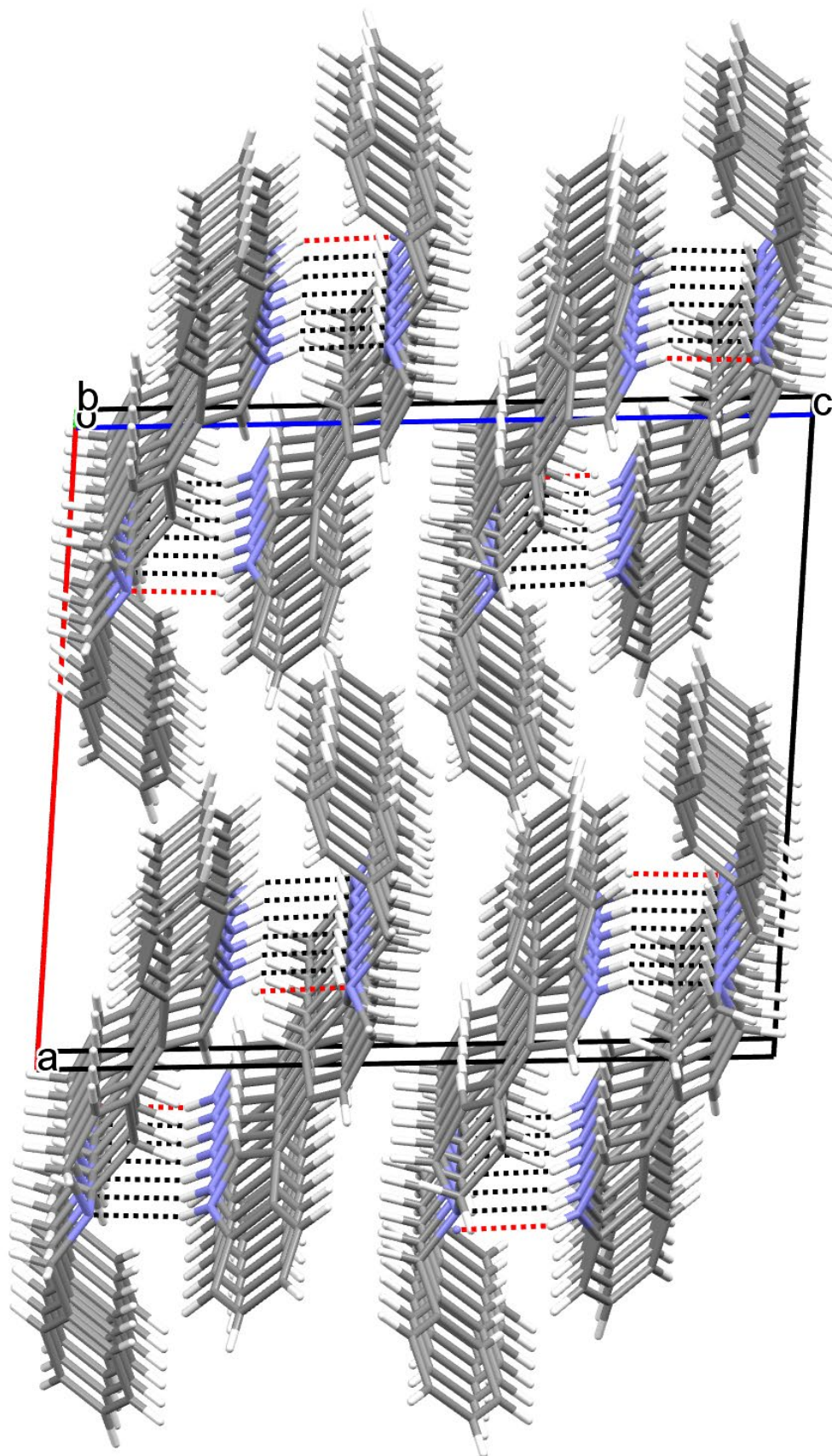
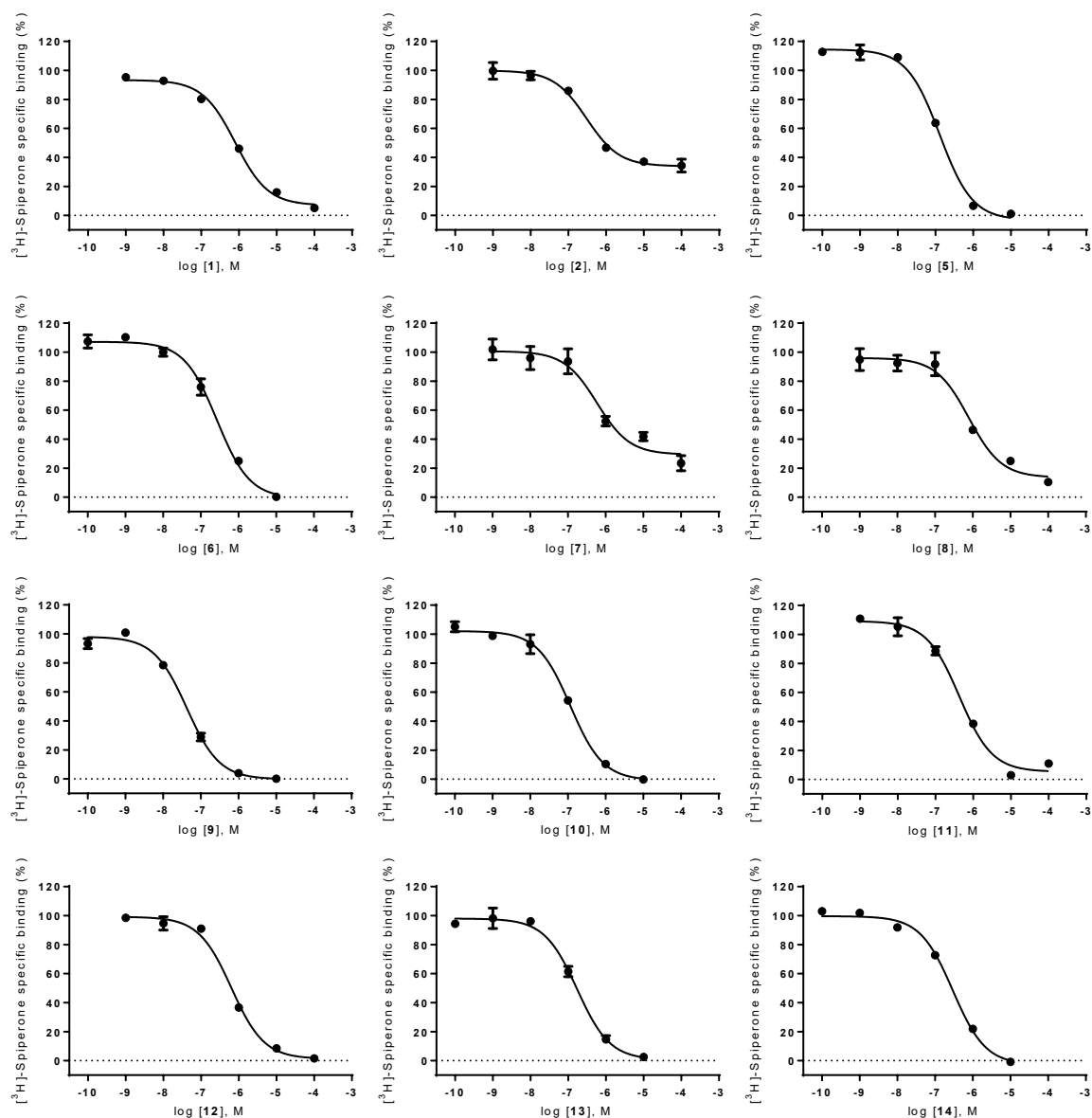


Fig. S3. (Continues on the following page). **Competition binding curves of compounds in radioligand binding assays at human D₂ receptors.** Concentration-dependent displacement of the specific binding of the D₂ antagonist radioligand [³H]-Spiperone by compounds **1**, **2**, and **5–14** (present page) (compound **11** [1]), and **15–20** and reference compound haloperidol (following page) in membranes from CHO-K1 cells overexpressing the human cloned dopamine D₂ receptor (isoform D_{2short}). The graphs show the data (media ± SEM) of a representative experiment out of 2-3 independent experiments performed in duplicate.



(Fig. S3. Continues from previous page).

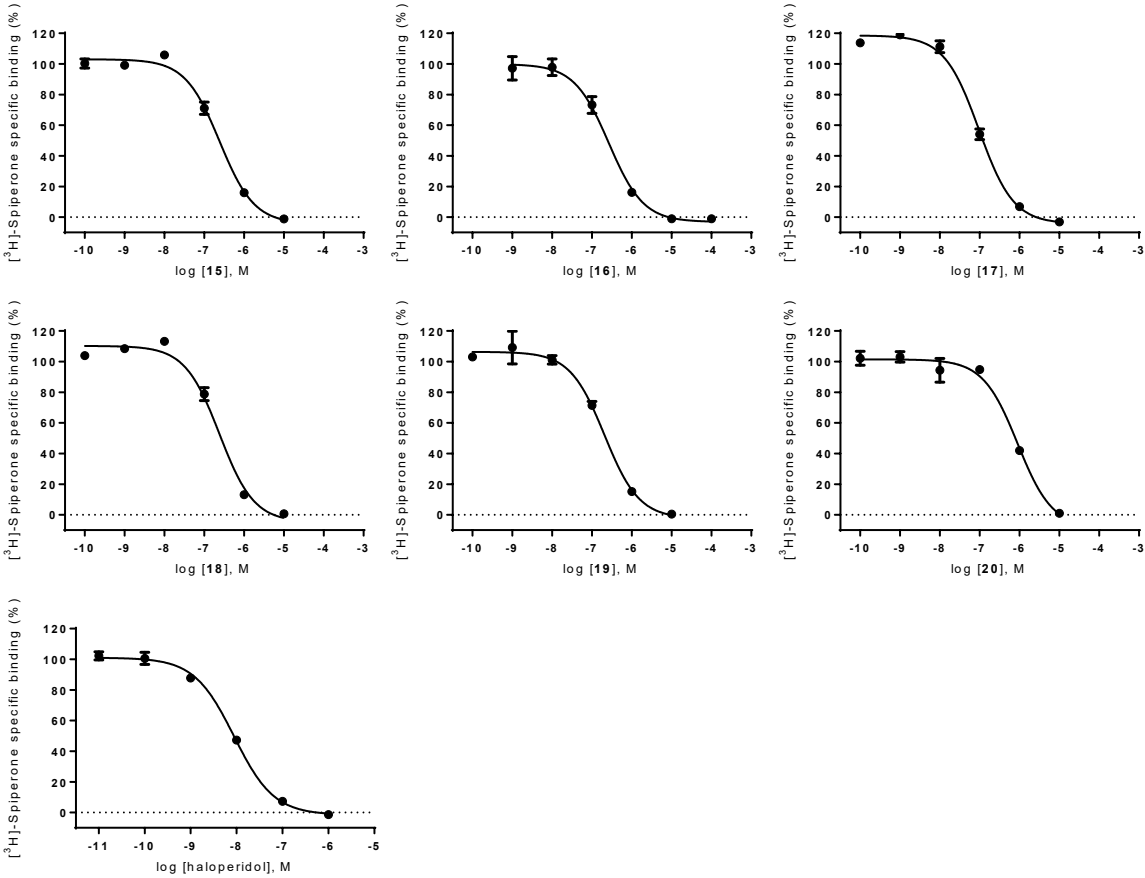
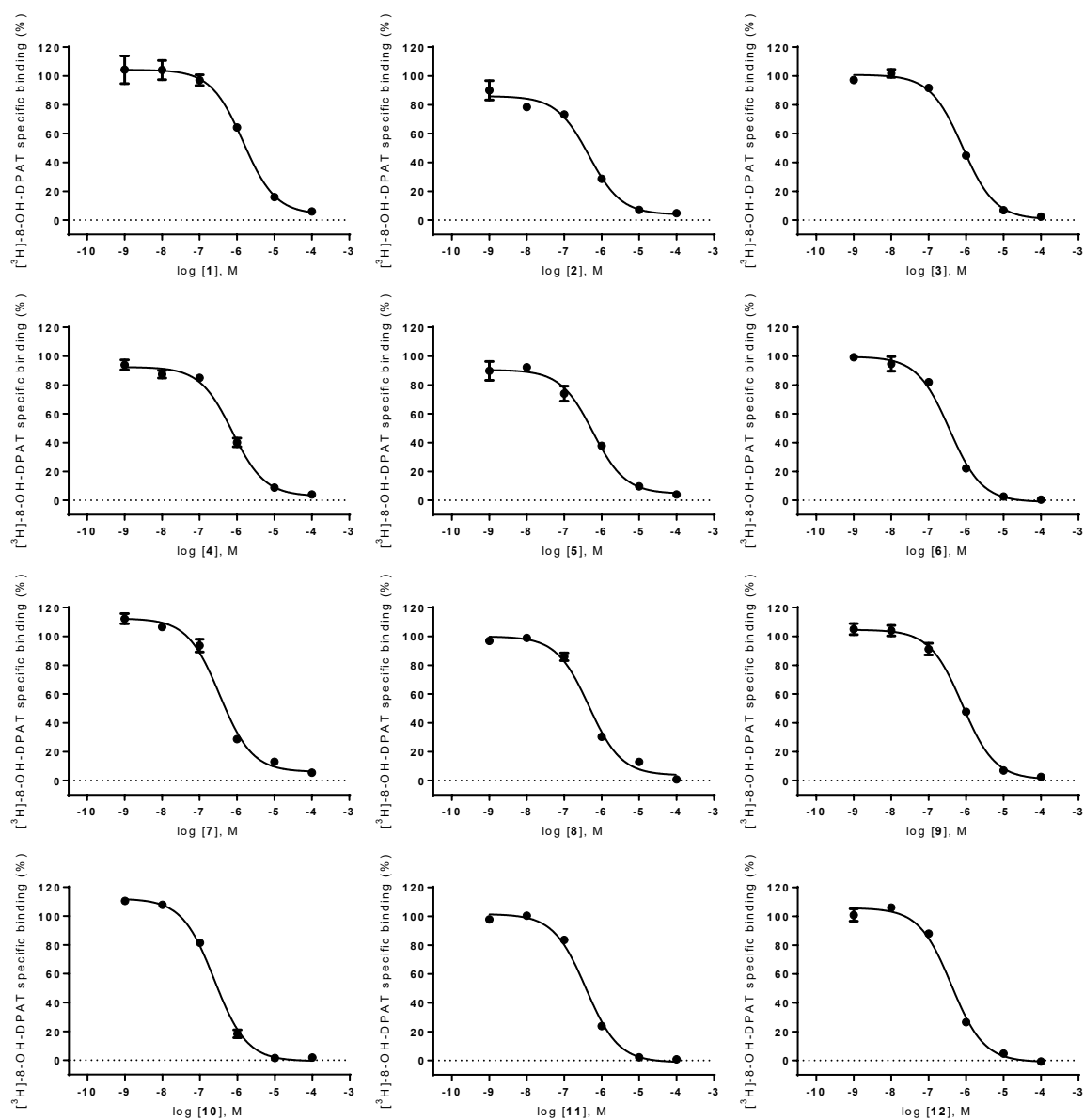


Fig. S4. (Continues on the following page). **Competition binding curves of compounds in radioligand binding assays at human 5-HT_{1A} receptors.** Concentration-dependent displacement of the specific binding of the 5-HT_{1A} agonist radioligand [³H]-8-OH-DPAT by compounds 1–12 (present page), and 13–20 and reference compound 5-carboxamidotryptamine (5-CT) (following page) in membranes from HEK293 cells overexpressing the human cloned serotonin 5-HT_{1A} receptor. The graphs show the data (media ± SEM) of a representative experiment out of 2-3 independent experiments performed in duplicate.



(Fig. S4. Continues from previous page).

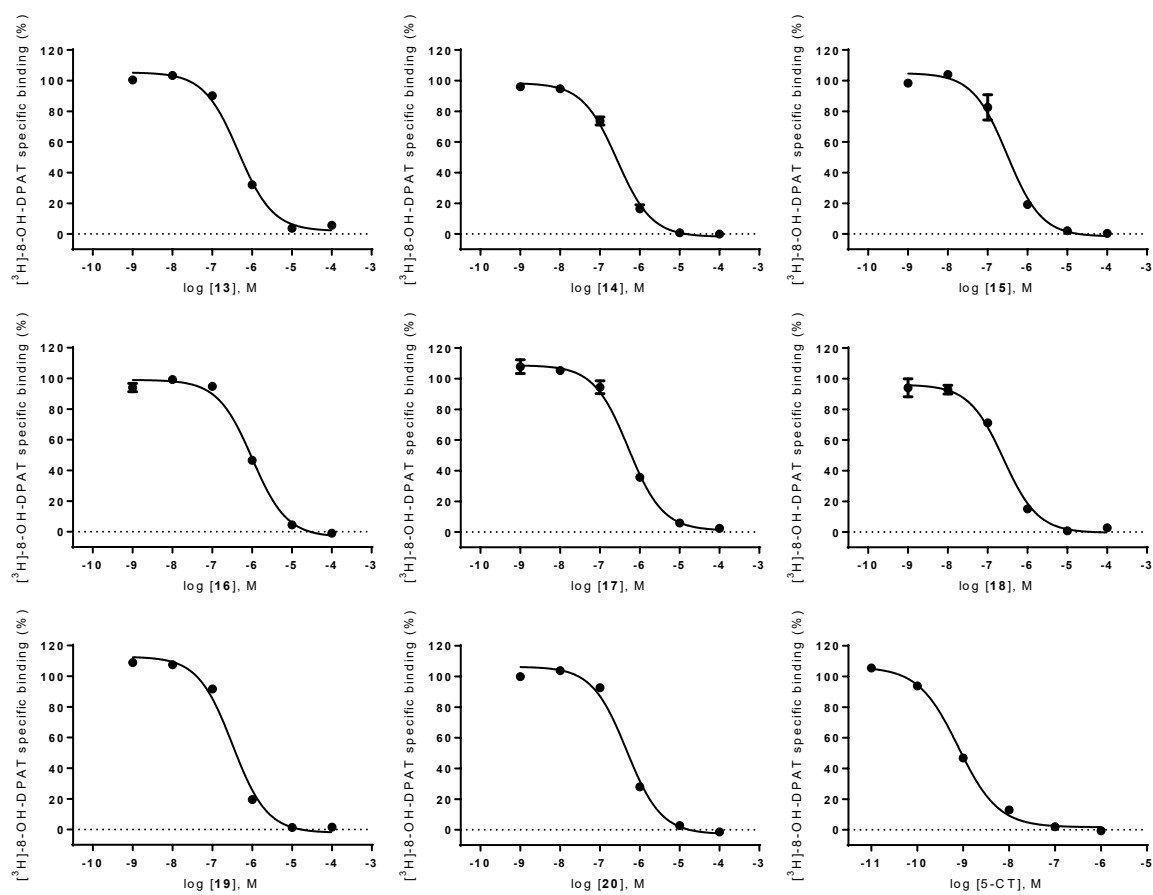


Fig. S5. Competition binding curves of compounds in radioligand binding assays at human 5-HT_{2A} receptors. Concentration-dependent displacement of the specific binding of the 5-HT_{2A} antagonist radioligand [³H]-Ketanserin by compounds **1**, **5**, **6**, **9**, **11**, **17** and reference compound risperidone in membranes from CHO-K1 cells overexpressing the human cloned serotonin 5-HT_{2A} receptor. The graphs show the data (media ± SEM) of a representative experiment out of 2-3 independent experiments performed in duplicate.

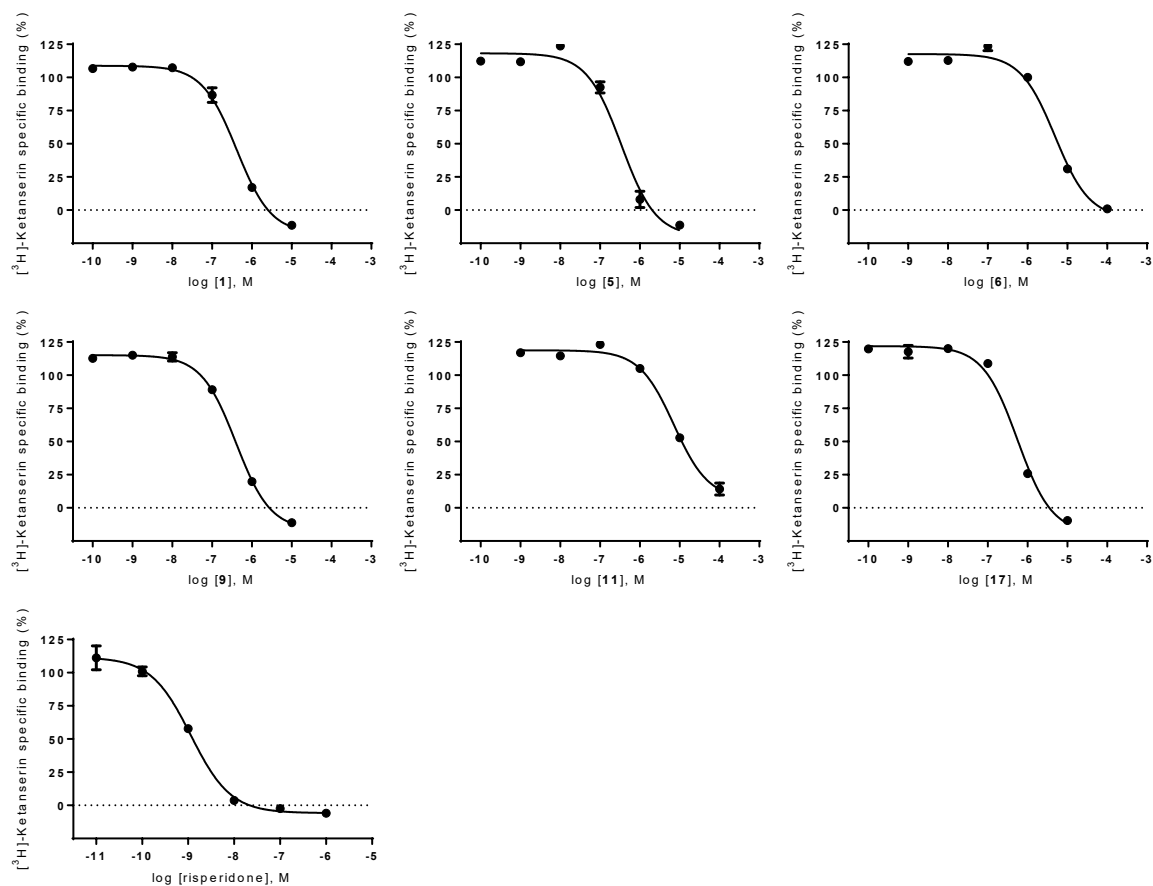


Fig. S6. Concentration-response curves of selected compounds antagonizing dopamine response in functional assays of cAMP signalling at human D₂ receptors. Concentration-response (inhibition of forskolin-stimulated cAMP production) curves of compounds **5**, **9**, **17** and reference antagonist haloperidol in CHO-K1 cells expressing human D₂ receptors. The graph shows data (mean \pm SEM) of one experiment performed in duplicate.

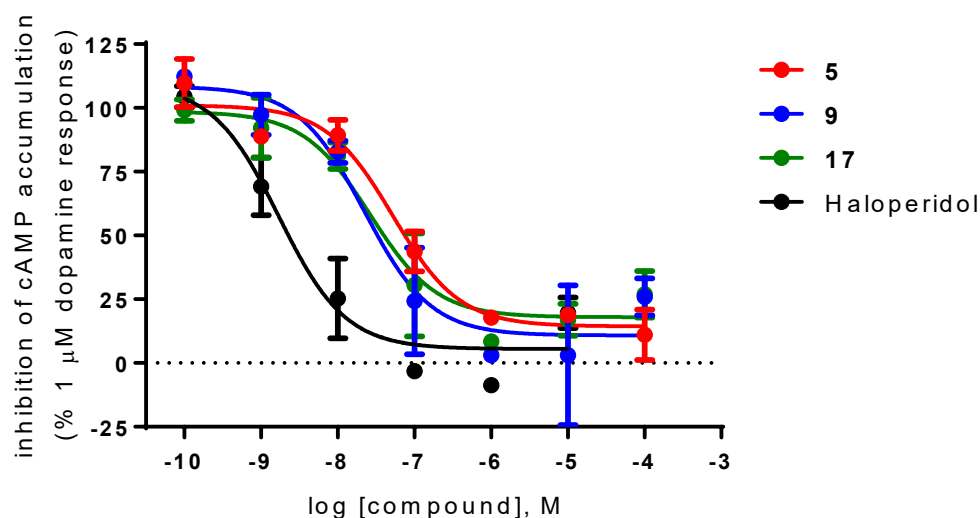


Table S1. Lipophilicity calculated using ALOGPS 2.1 software [2] and blood-brain permeability (BBB) calculated using On-line BBB predictor [3].

Compound	BBB		Lipophilicity	
	Value	Classification	AlogP	MlogP
1	0.104	BBB+	3.68	2.19
2	0.108	BBB+	3.66	1.88
3	0.086	BBB+	4.01	2.11
4	0.079	BBB+	4.39	2.34
5	0.092	BBB+	4.24	3.03
6	0.087	BBB+	4.22	2.69
7	0.073	BBB+	4.57	2.92
8	0.057	BBB+	4.95	3.14
9	0.100	BBB+	4.28	3.41
10	0.097	BBB+	4.27	3.07
11	0.079	BBB+	4.62	3.28
12	0.069	BBB+	4.99	3.50
13	0.097	BBB+	4.27	3.07
14	0.109	BBB+	4.25	2.74
15	0.103	BBB+	4.60	2.96
16	0.081	BBB+	4.98	3.17
17	0.097	BBB+	4.27	3.07

18	0.109	BBB+	4.25	2.74
19	0.103	BBB+	4.60	2.96
20	0.081	BBB+	4.98	3.17

Table S2. Crystal data and structure refinement of the compound **9**.

Formula	C ₂₀ H ₂₀ N ₂
Formula weight	288.38
Temperature K	298(2)
Crystal system	monoclinic
Space group	<i>P2₁/c</i>
a (Å)	15.0016(12)
b (Å)	6.0904(5)
c (Å)	17.1365(12)
β	94.510(7)
Volume (Å ³)	1560.8(2)
Z	4
Calculated density (g cm ⁻³)	1.227
μ (mm ⁻¹)	0.072
Absorption correction	multi-scan
F(000)	616
Crystal size (mm)	0.50 x 0.30 x 0.08
θ range (°)	2.651 to 26.103
Reflections collected/unique	10590/3206
R _{int}	0.0505
Data/restraints/parameters	3206/0/203
Goof on F ²	1.052
Final R indices[I > 2σ(I)]	R ₁ = 0.0557, wR ₂ = 0.1161
R indices(all data)	R ₁ = 0.1049, wR ₂ = 0.1399
Largest diff. peak/hole, e Å ⁻³	0.147/-0.151

Table S3. Interatomic distances and selected bond angles for the compound **9**.

Bond lengths (Å)

C(1)-N(1)	1.358(3)	C(10)-C(11)	1.488(3)
C(1)-C(2)	1.367(2)	C(11)-N(2)	1.465(2)
C(2)-C(3)	1.446(2)	C(12)-C(13)	1.514(2)
C(2)-C(9)	1.463(2)	C(13)-N(2)	1.462(2)
C(3)-C(4)	1.396(3)	C(14)-N(2)	1.472(2)
C(3)-C(8)	1.411(2)	C(14)-C(15)	1.493(3)
C(4)-C(5)	1.370(3)	C(15)-C(21)	1.366(3)

C(5)-C(6)	1.382(3)	C(15)-C(16)	1.371(3)
C(6)-C(7)	1.368(3)	C(16)-C(17)	1.376(4)
C(7)-C(8)	1.385(3)	C(17)-C(18)	1.333(5)
C(8)-N(1)	1.365(3)	C(18)-C(19)	1.366(6)
C(9)-C(10)	1.328(2)	C(19)-C(20)	1.384(5)
C(9)-C(12)	1.502(2)		

Bond angles (°)

C(1)-C(2)-C(9)	123.94(17)	N(2)-C(13)-C(12)	110.57(15)
C(3)-C(2)-C(9)	130.59(16)	N(2)-C(14)-C(15)	114.80(16)
C(10)-C(9)-C(2)	124.70(17)	C(21)-C(15)-C(14)	121.0(3)
C(10)-C(9)-C(12)	118.23(17)	C(16)-C(15)-C(14)	121.5(2)
C(2)-C(9)-C(12)	116.90(15)	C(19)-C(17)-C(16)	119.6(4)
C(9)-C(10)-C(11)	124.47(18)	C(13)-N(2)-C(11)	108.20(15)
N(2)-C(11)-C(10)	112.80(15)	C(13)-N(2)-C(14)	111.17(15)
C(9)-C(12)-C(13)	113.43(15)	C(11)-N(2)-C(14)	107.95(15)

Torsion angles (°)

C(12)-C(9)-C(10)-C(11)	0.6(3)	C(9)-C(12)-C(13)-N(2)	-47.0(2)
C(9)-C(10)-C(11)-N(2)	18.1(3)	C(12)-C(13)-N(2)-C(11)	65.2(2)
C(10)-C(9)-C(12)-C(13)	13.7(3)	C(10)-C(11)-N(2)-C(13)	-50.0(2)

Table S4. Experimental conditions employed in radioligand binding assays.

	<i>hD₂</i>	<i>h5-HT_{1A}</i>	<i>h5-HT_{2A}</i>
Protein per well	10 µg	10 µg	80 µg
Assay buffer	50 mM Tris-HCl, 120 mM NaCl, 5 mM KCl, 5 mM MgCl ₂ , 1 mM EDTA (pH = 7.4)	50 mM Tris-HCl, 5 mM MgSO ₄ (pH = 7.4)	50 mM Tris-HCl (pH = 7.5)
Wash buffer	50 mM Tris-HCl, 0.9% NaCl (pH = 7.4)	50 mM Tris-HCl (pH = 7.4)	50 mM Tris-HCl (pH = 6.6)
Plate	GF/C	GF/C	GF/B
Radioligand	0.2 nM [³ H]- Spiperone ^a	1 nM [³ H]-8-OH-DPAT ^b	1 nM [³ H]-Ketanserin ^c
Nonspecific binding	10 µM Sulpiride	10 µM Serotonin	1 µM Methysergide
Incubation	25 °C/120 min	37 °C/120 min	37 °C/30 min

^a PerkinElmer NET1187250UC. ^b PerkinElmer NET929250UC. ^c PerkinElmer NET791250UC.

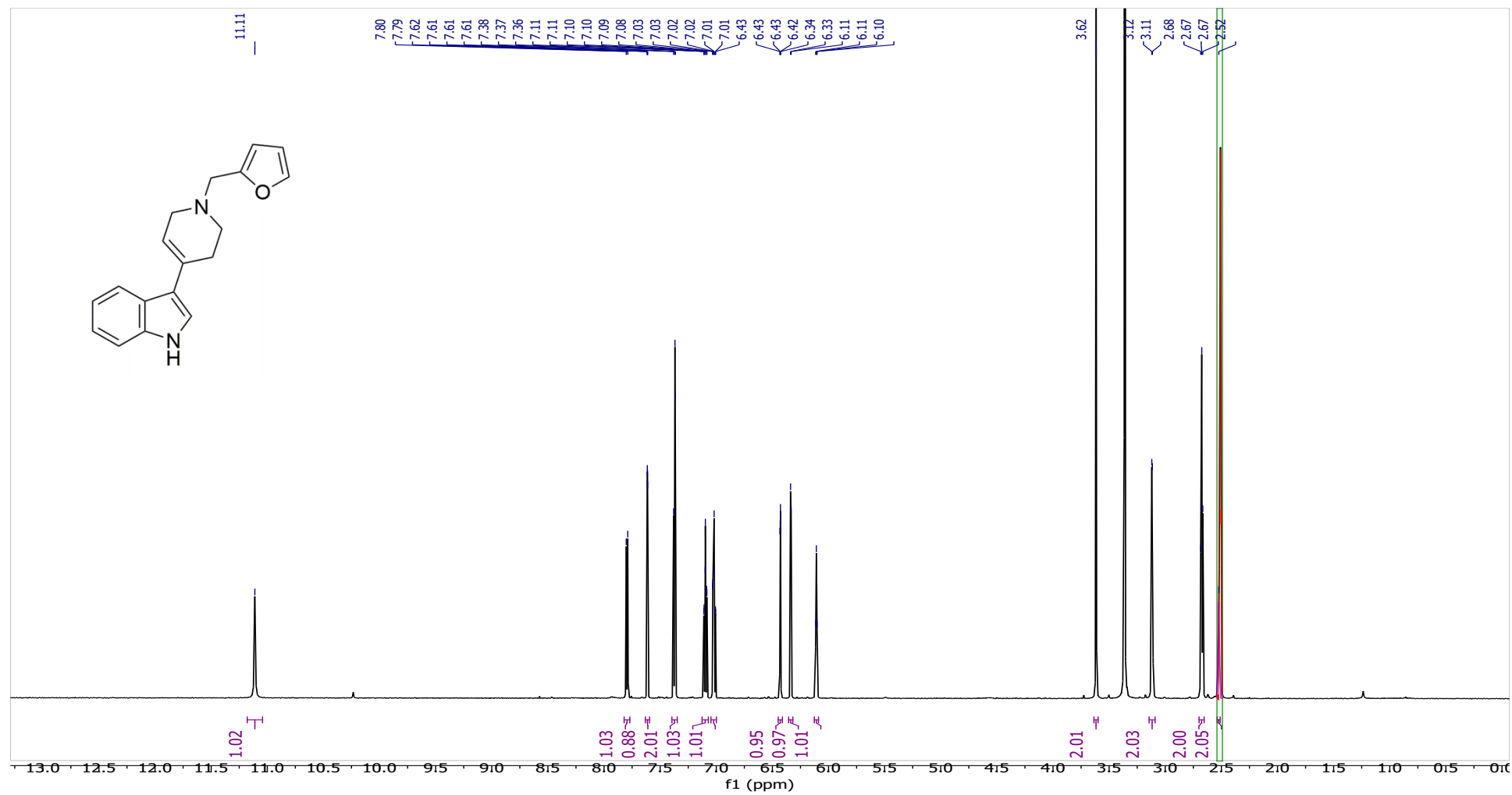
References:

[1] Kondej, M.; Bartyzel, A.; Pitucha, M.; Wróbel, T.M.; Silva, A.G.; Matosiuk, D.; Castro, M.; Kaczor, A.A. Synthesis, structural and thermal studies of 3-(1-Benzyl-1,2,3,6-tetrahydropyridin-4-yl)-5-ethoxy-1H-indole (D2AAK1_3) as dopamine D₂ receptor ligand. *Molecules* **2018**, *23*, pii: E2249, DOI: 10.3390/molecules23092249.

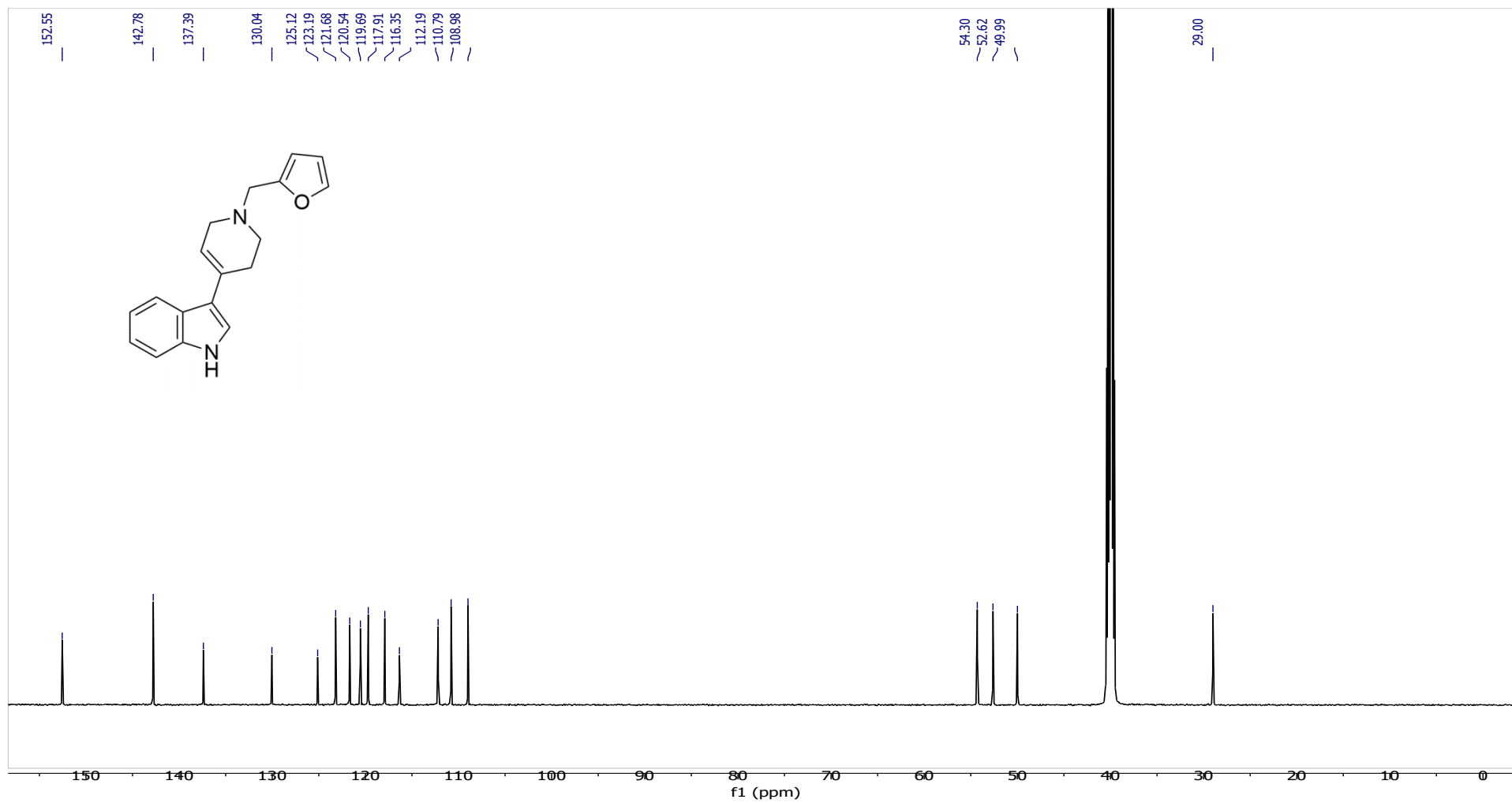
[2] Tetko, I. V.; Tanchuk, V. Y. Application of associative neural networks for prediction of lipophilicity in ALOGPS 2.1 program. *J. Chem. Inf. Comput. Sci.*, **2002**, *42*, 1136-1145, DOI: 10.1021/ci025515j.

[3] <https://www.cbligand.org/BBB/>.

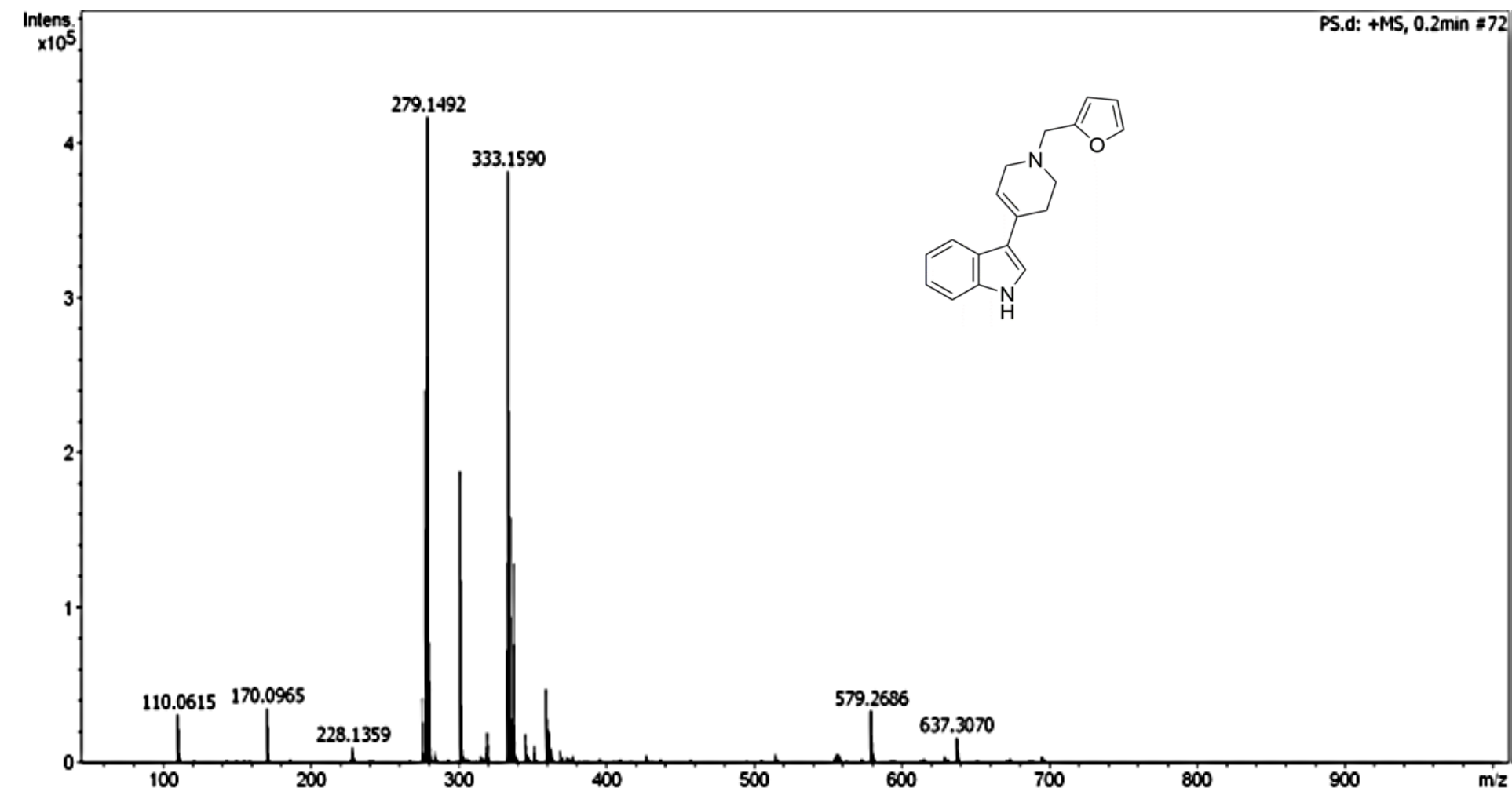
3-(1-(furan-2-ylmethyl)-1,2,3,6-tetrahydropyridin-4-yl)-1H-indole (1)



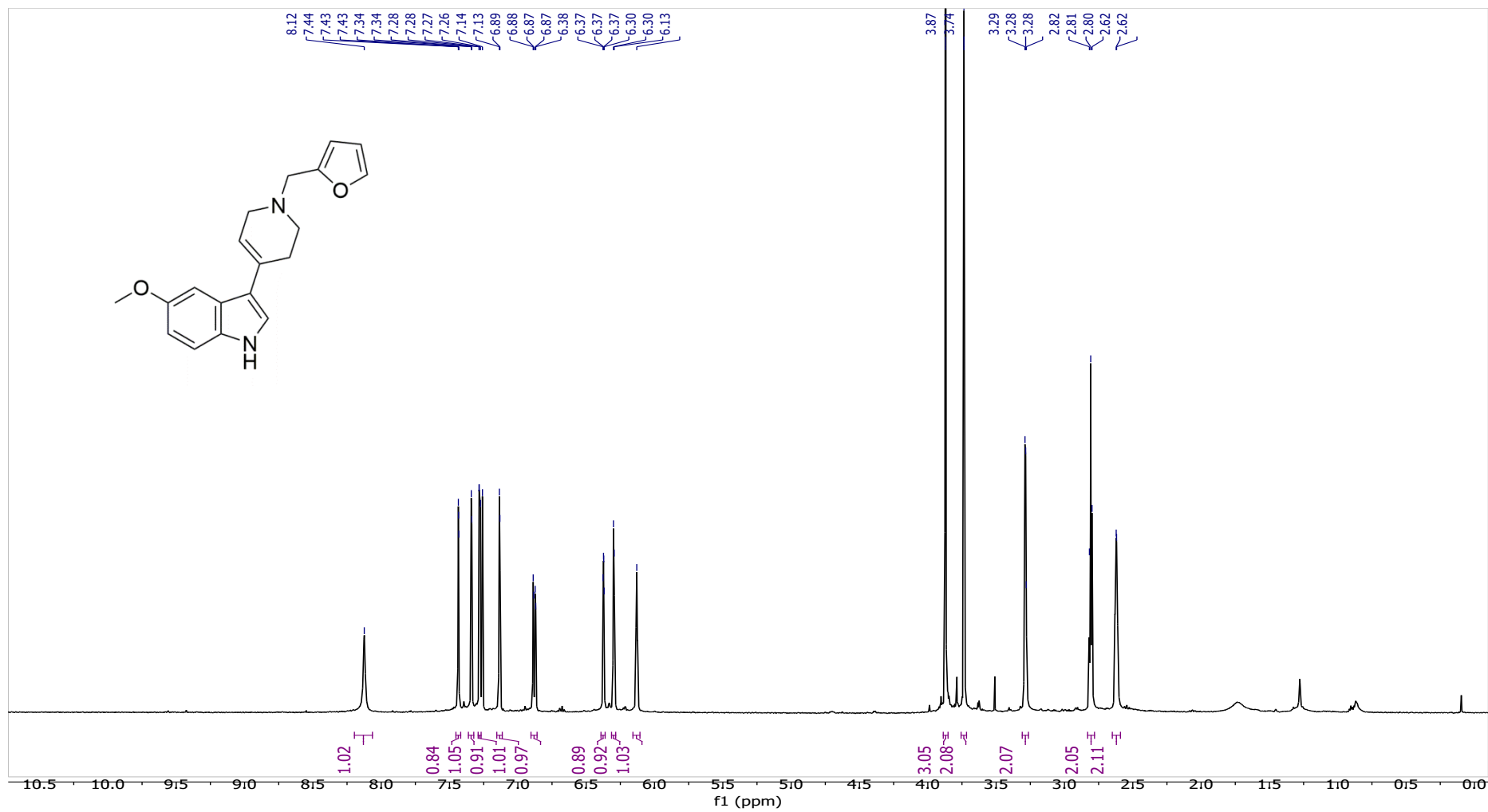
3-(1-(furan-2-ylmethyl)-1,2,3,6-tetrahydropyridin-4-yl)-1*H*-indole (1)



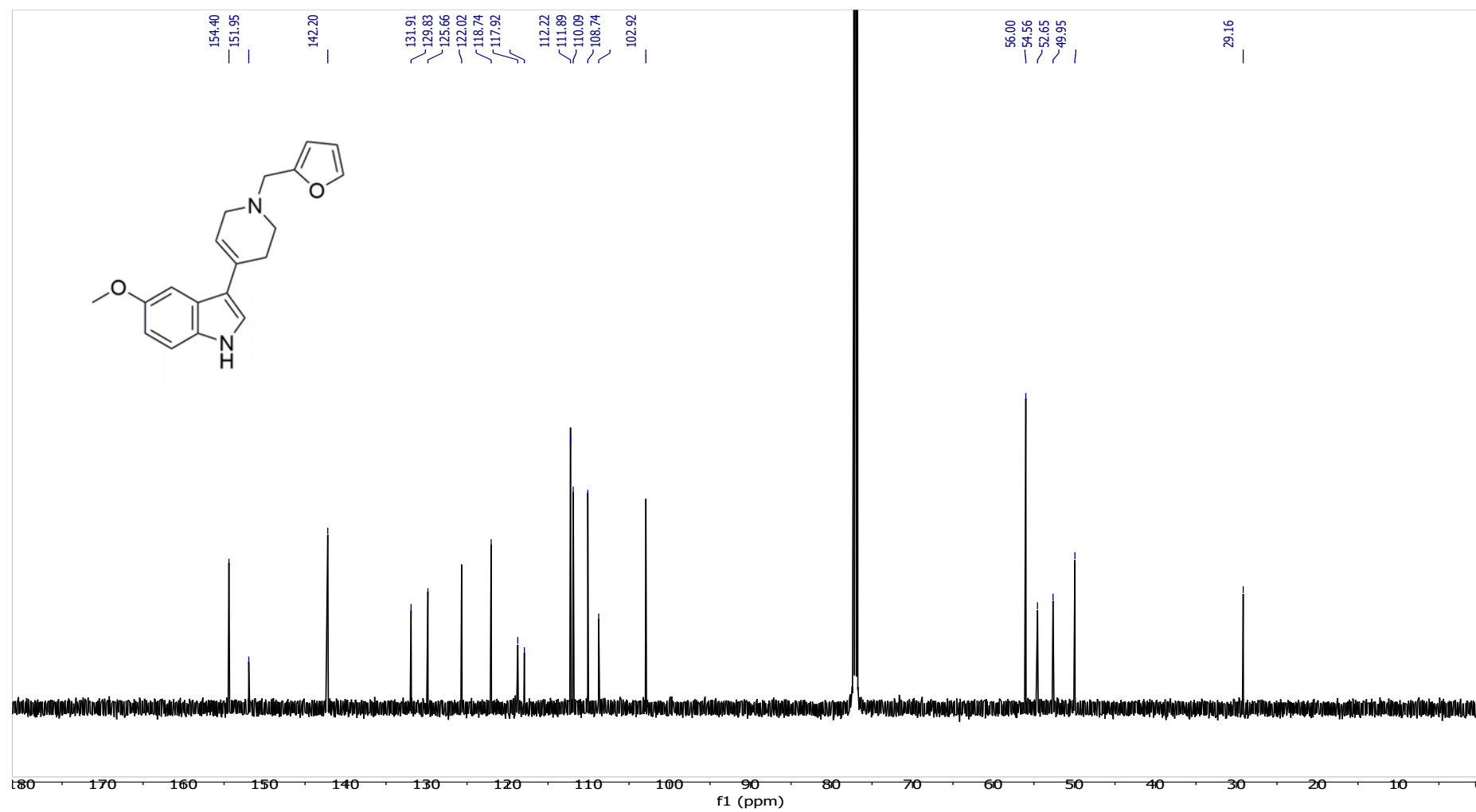
3-(1-(furan-2-ylmethyl)-1,2,3,6-tetrahydropyridin-4-yl)-1*H*-indole (1)



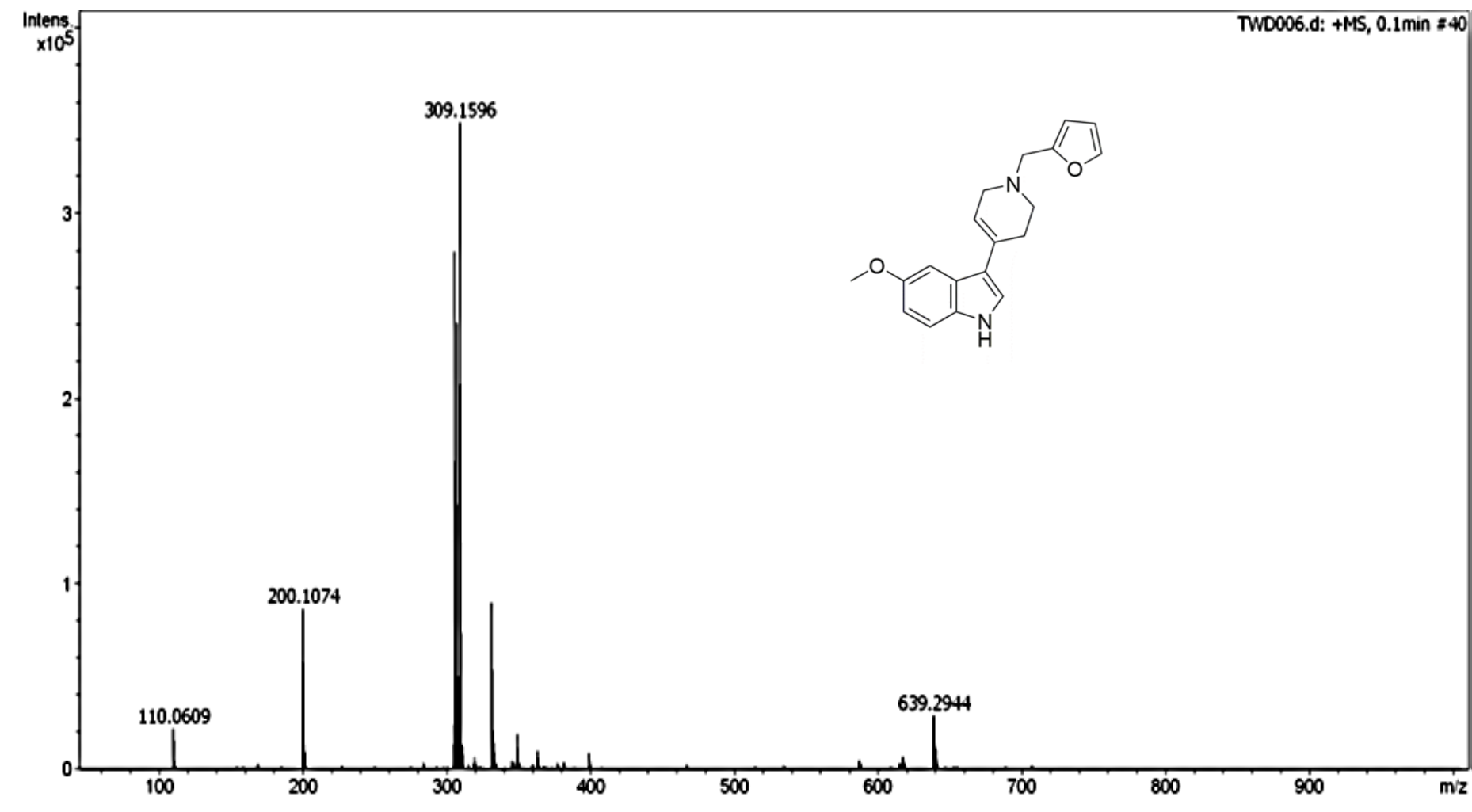
3-(1-(furan-2-ylmethyl)-1,2,3,6-tetrahydropyridin-4-yl)-5-methoxy-1H-indole (2)



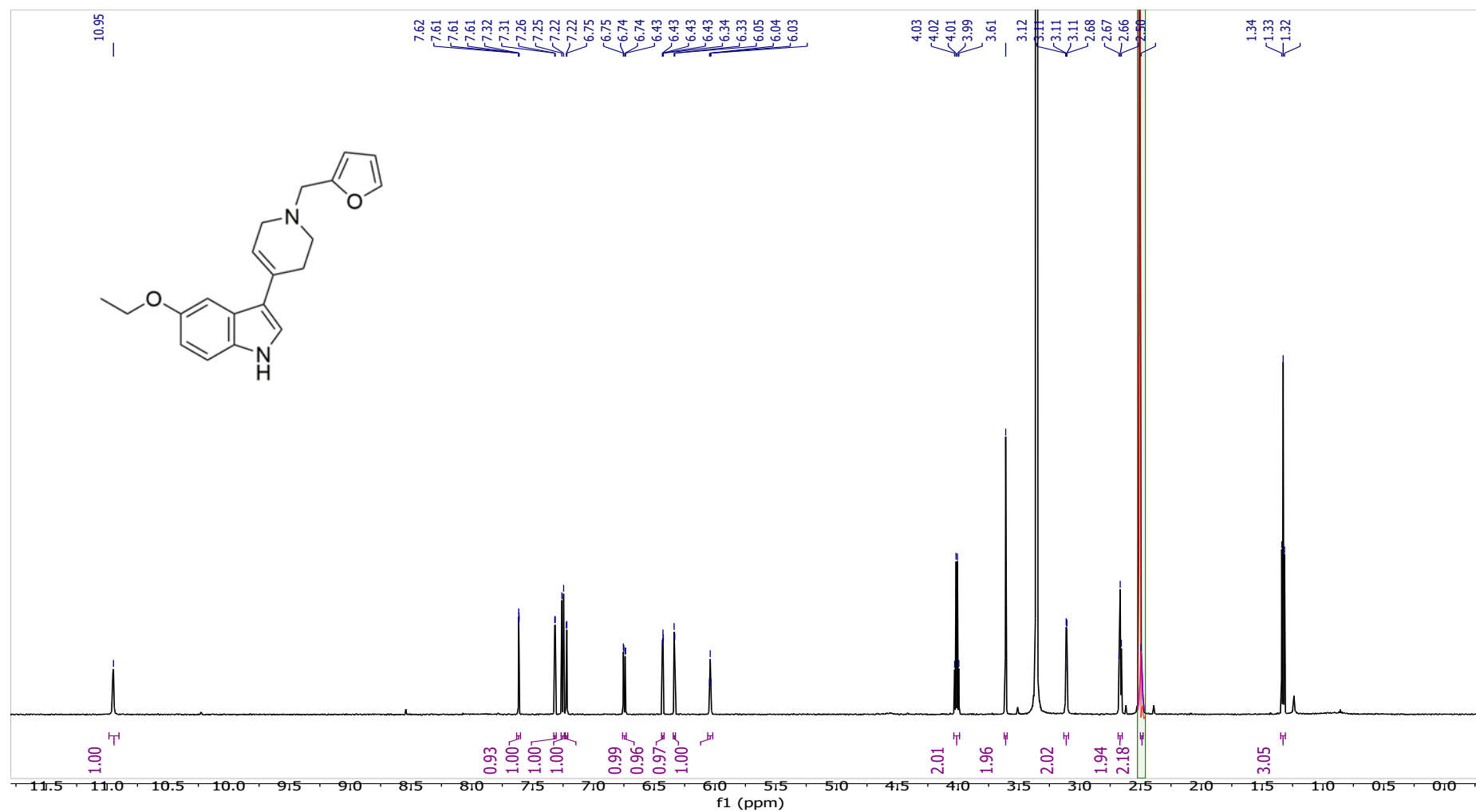
3-(1-(furan-2-ylmethyl)-1,2,3,6-tetrahydropyridin-4-yl)-5-methoxy-1H-indole (2)



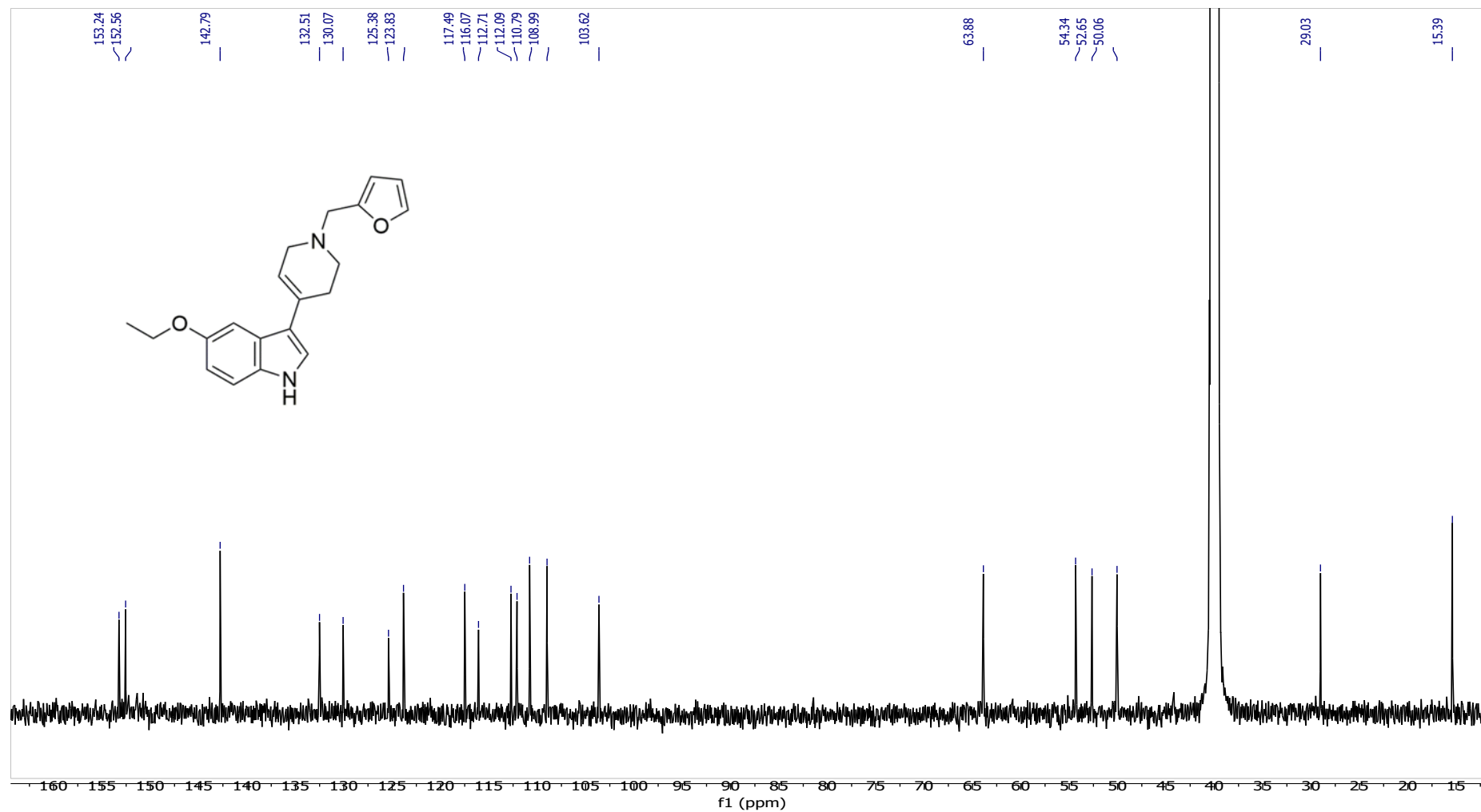
3-(1-(furan-2-ylmethyl)-1,2,3,6-tetrahydropyridin-4-yl)-5-methoxy-1H-indole (2)



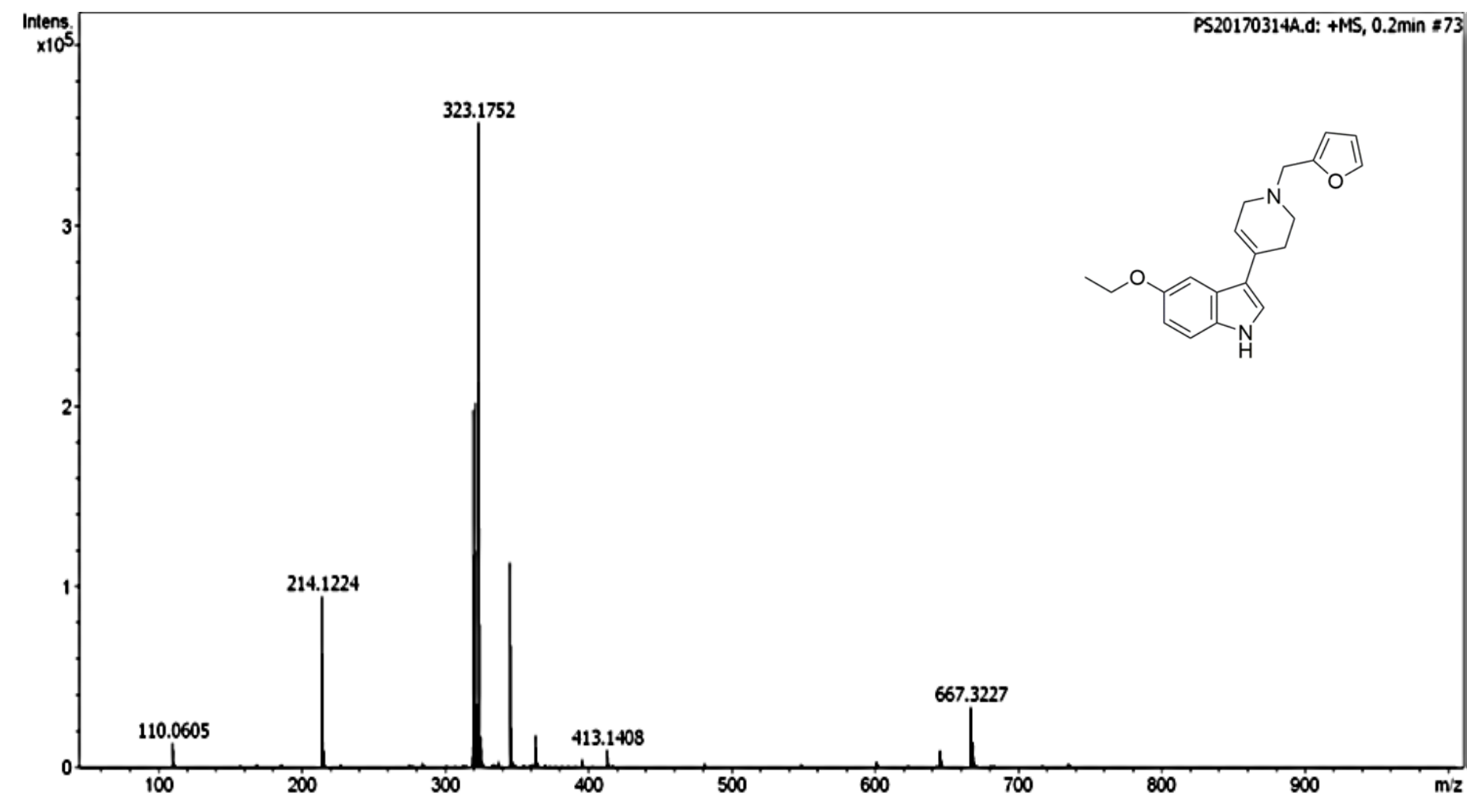
5-ethoxy-3-(1-(furan-2-ylmethyl)-1,2,3,6-tetrahydropyridin-4-yl)-1H-indole (3)



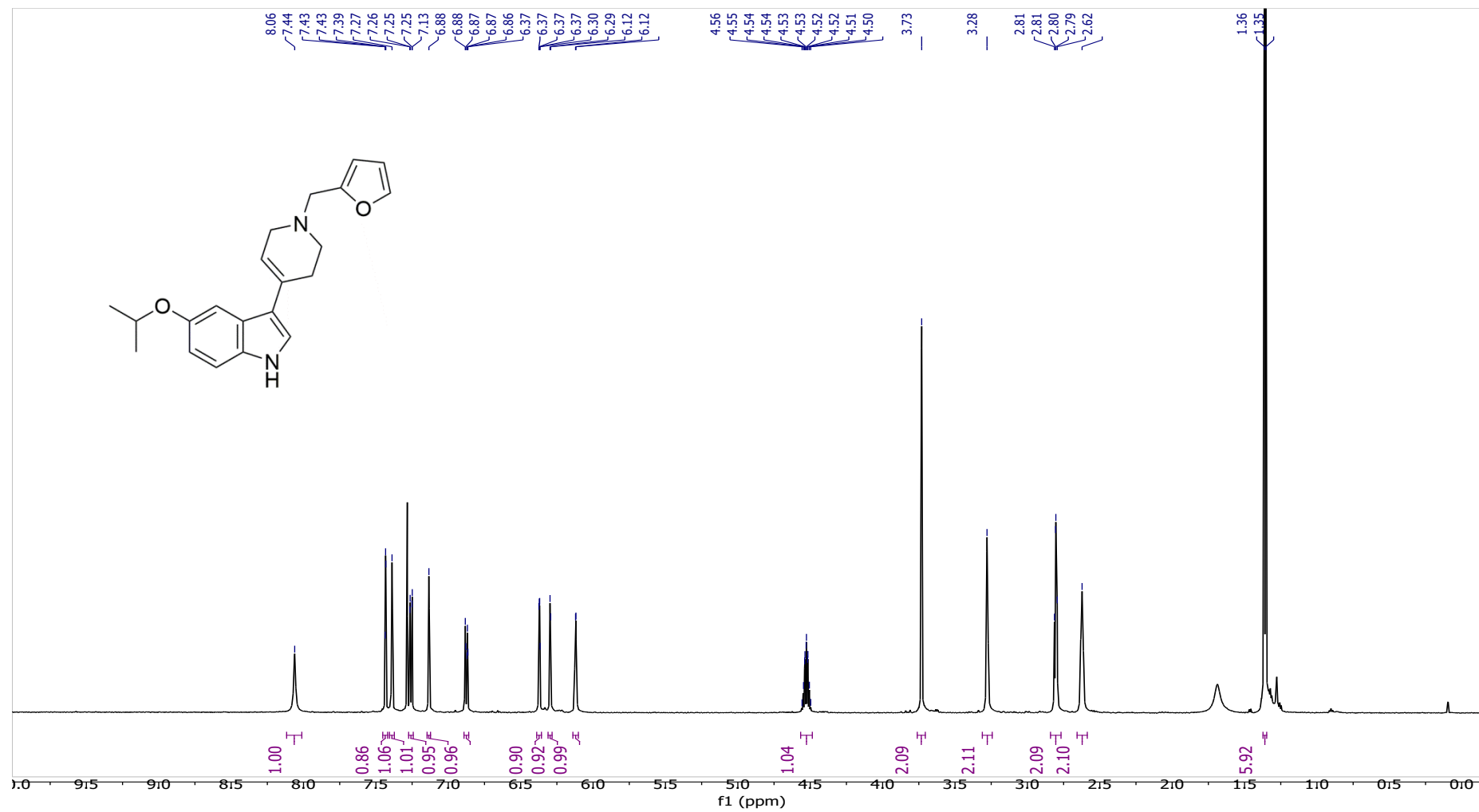
5-ethoxy-3-(1-(furan-2-ylmethyl)-1,2,3,6-tetrahydropyridin-4-yl)-1H-indole (3)



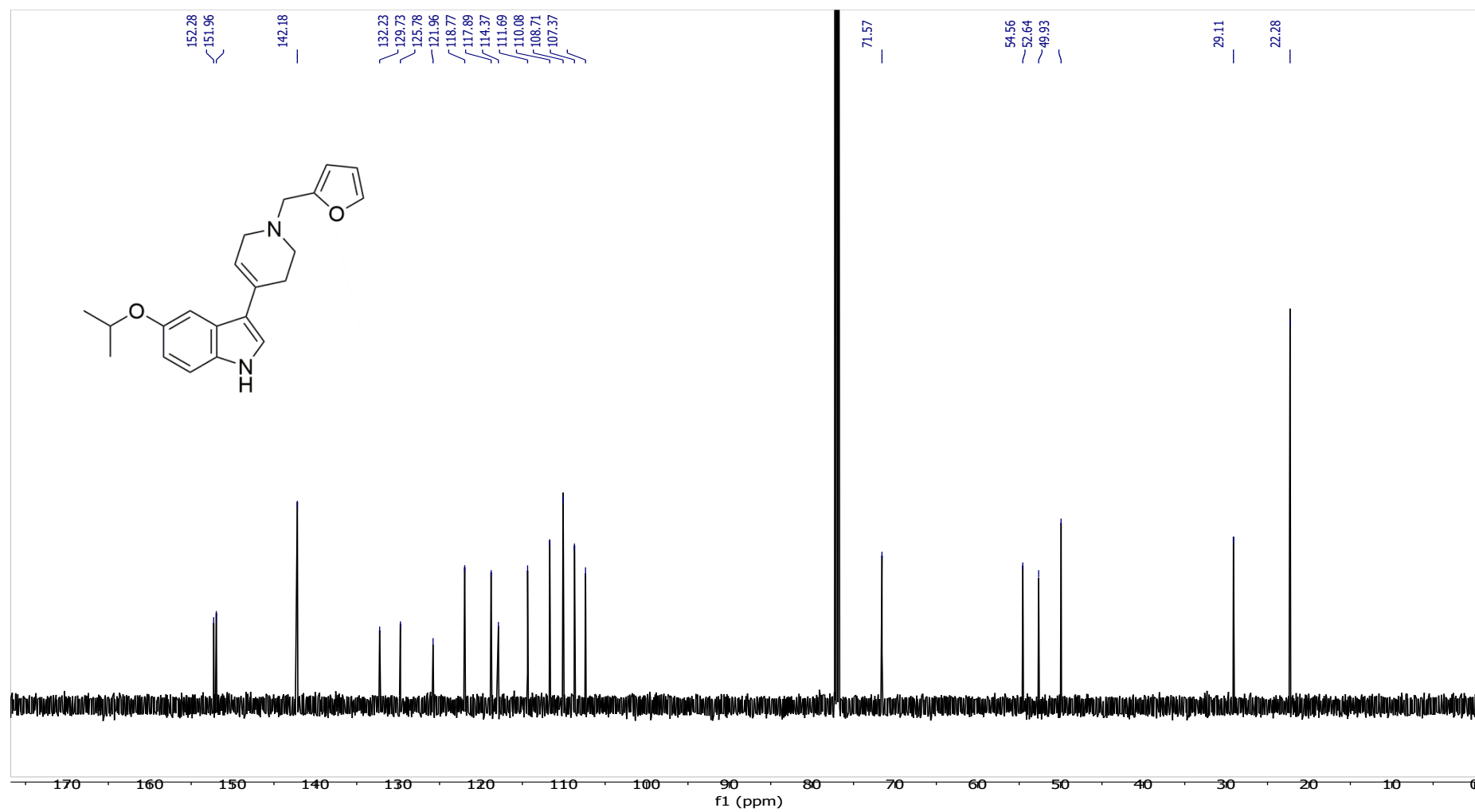
5-ethoxy-3-(1-(furan-2-ylmethyl)-1,2,3,6-tetrahydropyridin-4-yl)-1H-indole (3)



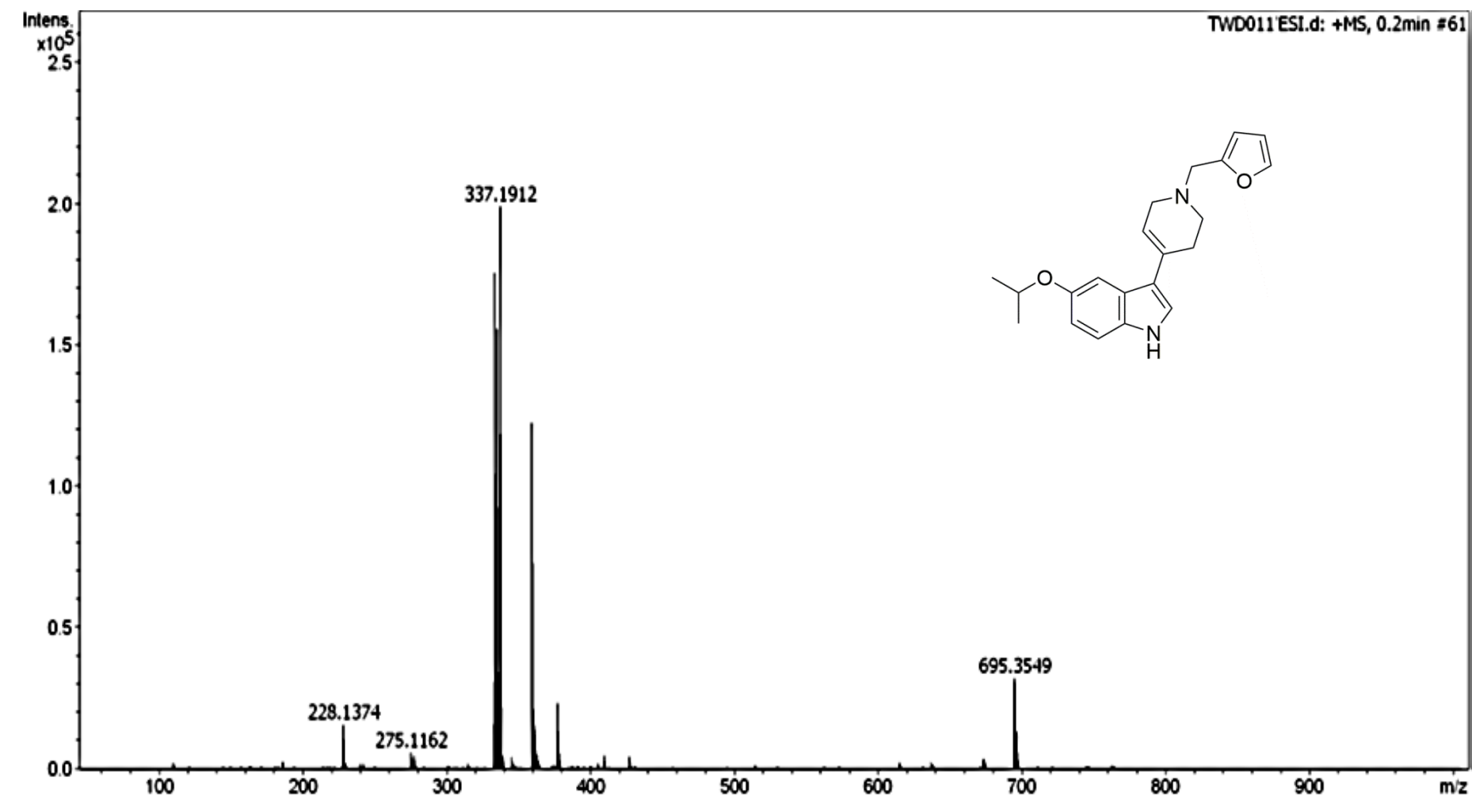
3-(1-(furan-2-ylmethyl)-1,2,3,6-tetrahydropyridin-4-yl)-5-isopropoxy-1*H*-indole (4)



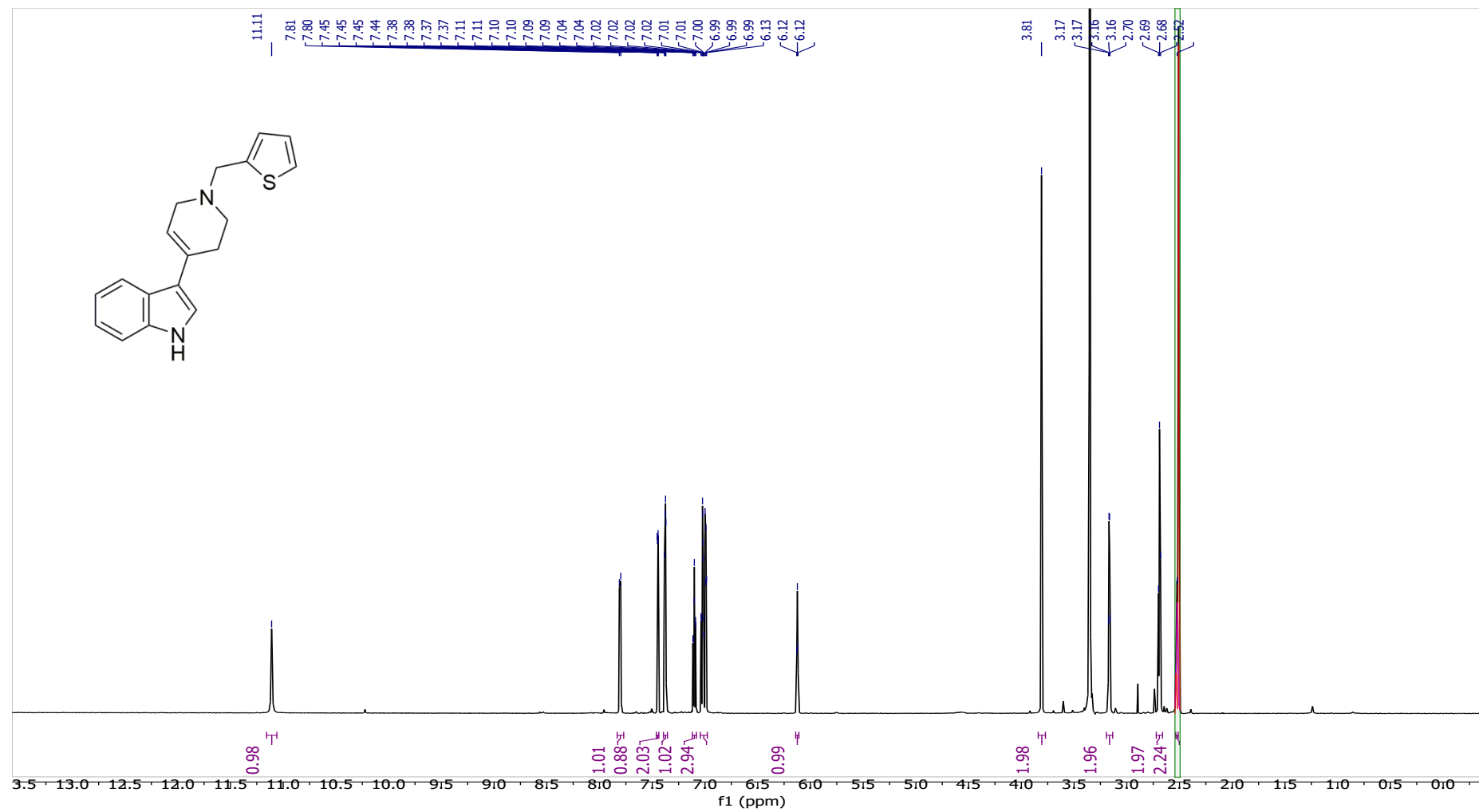
3-(1-(furan-2-ylmethyl)-1,2,3,6-tetrahydropyridin-4-yl)-5-isopropoxy-1H-indole (4)



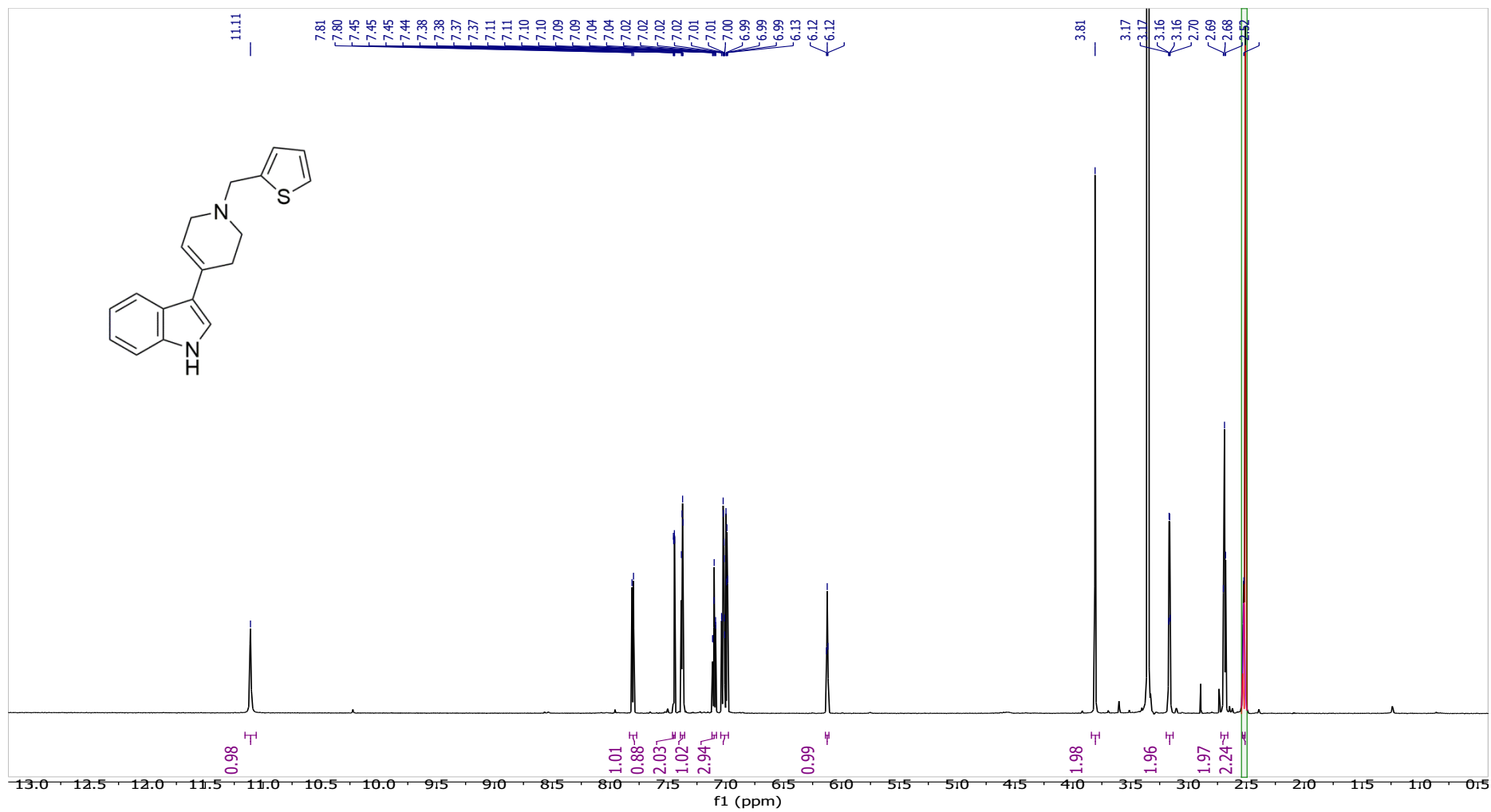
3-(1-(furan-2-ylmethyl)-1,2,3,6-tetrahydropyridin-4-yl)-5-isopropoxy-1H-indole (4)



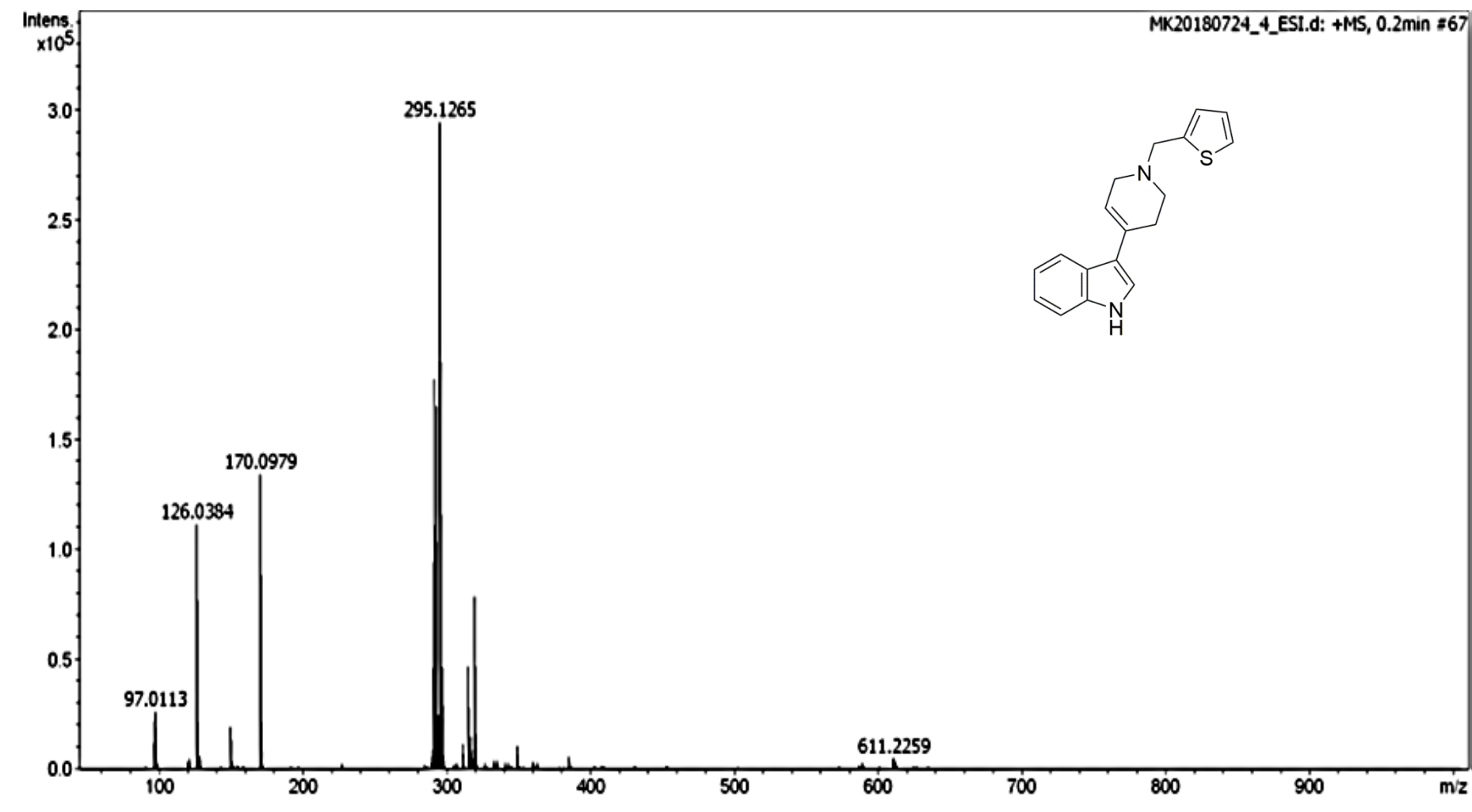
3-(1-(thiophen-2-ylmethyl)-1,2,3,6-tetrahydropyridin-4-yl)-1H-indole (5)



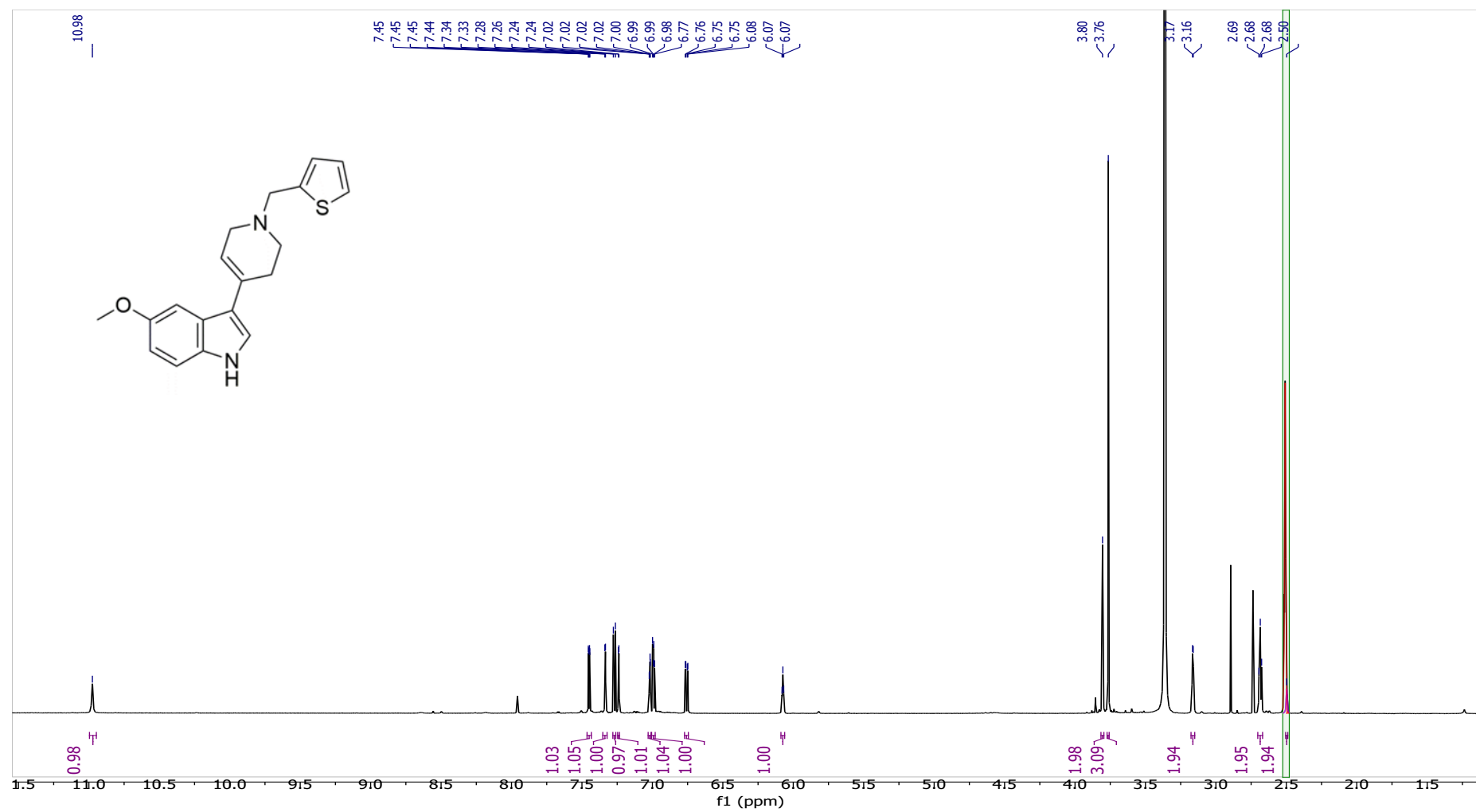
3-(1-(thiophen-2-ylmethyl)-1,2,3,6-tetrahydropyridin-4-yl)-1H-indole (5)



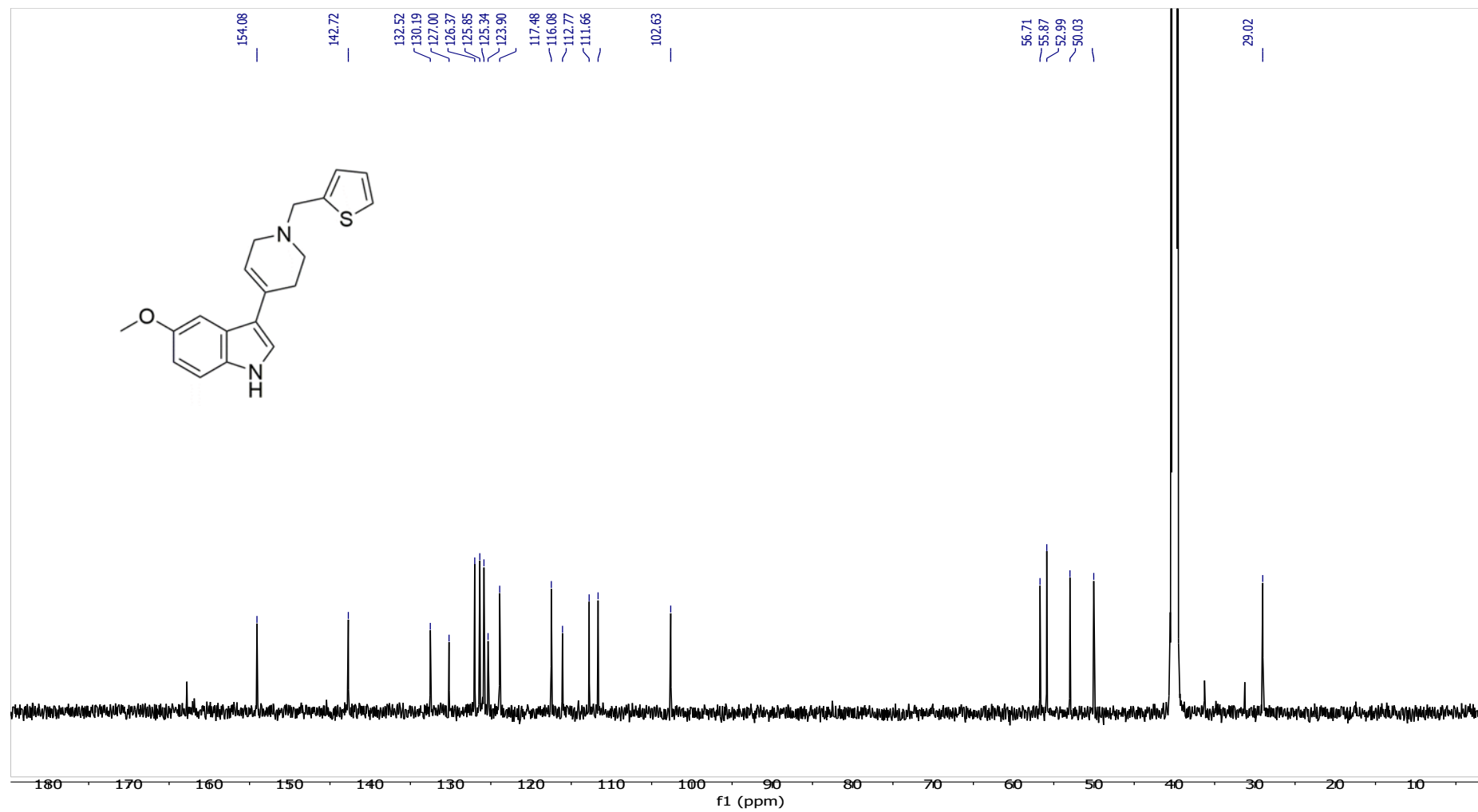
3-(1-(thiophen-2-ylmethyl)-1,2,3,6-tetrahydropyridin-4-yl)-1H-indole (5)



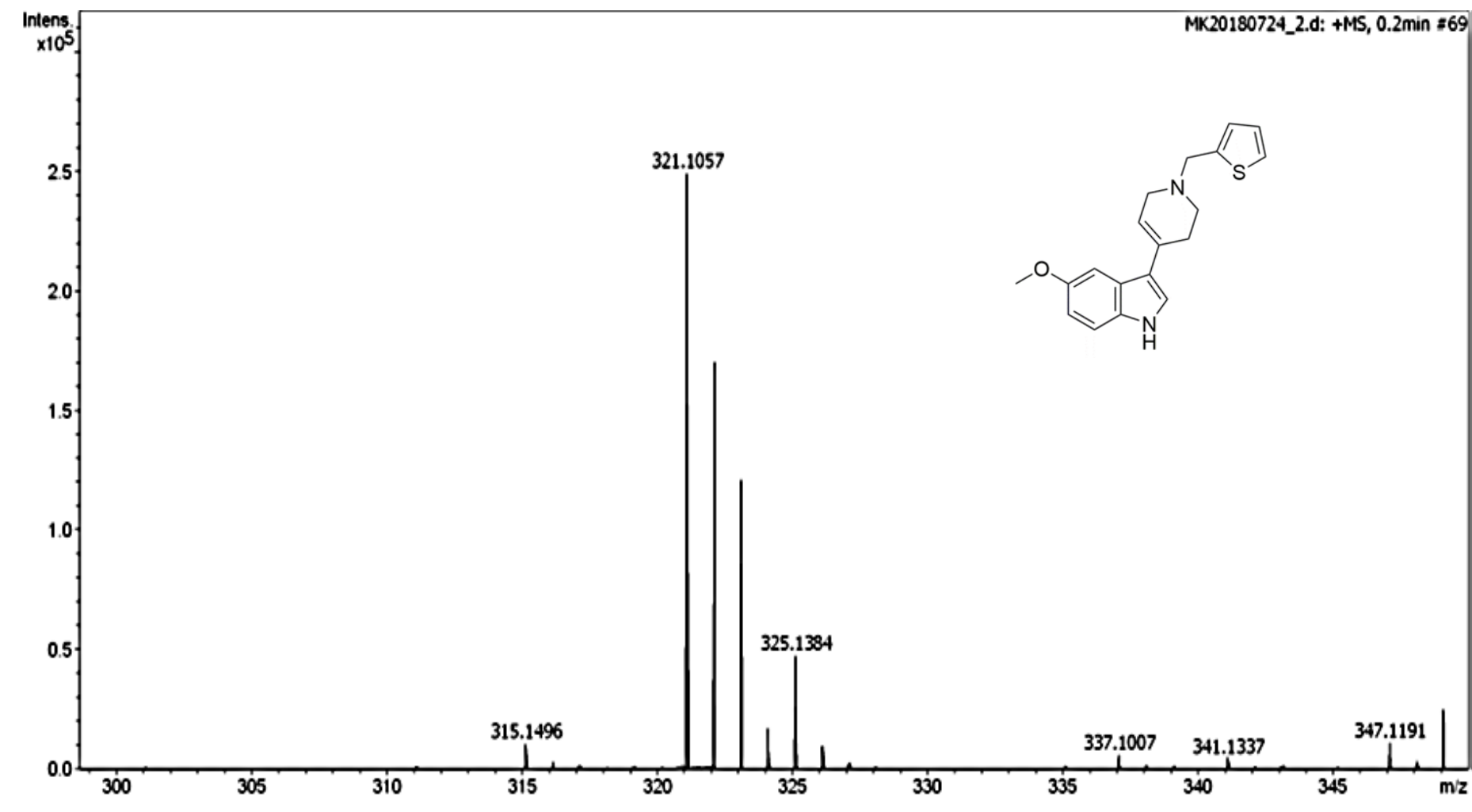
5-methoxy-3-(1-(thiophen-2-ylmethyl)-1,2,3,6-tetrahydropyridin-4-yl)-1H-indole (6)



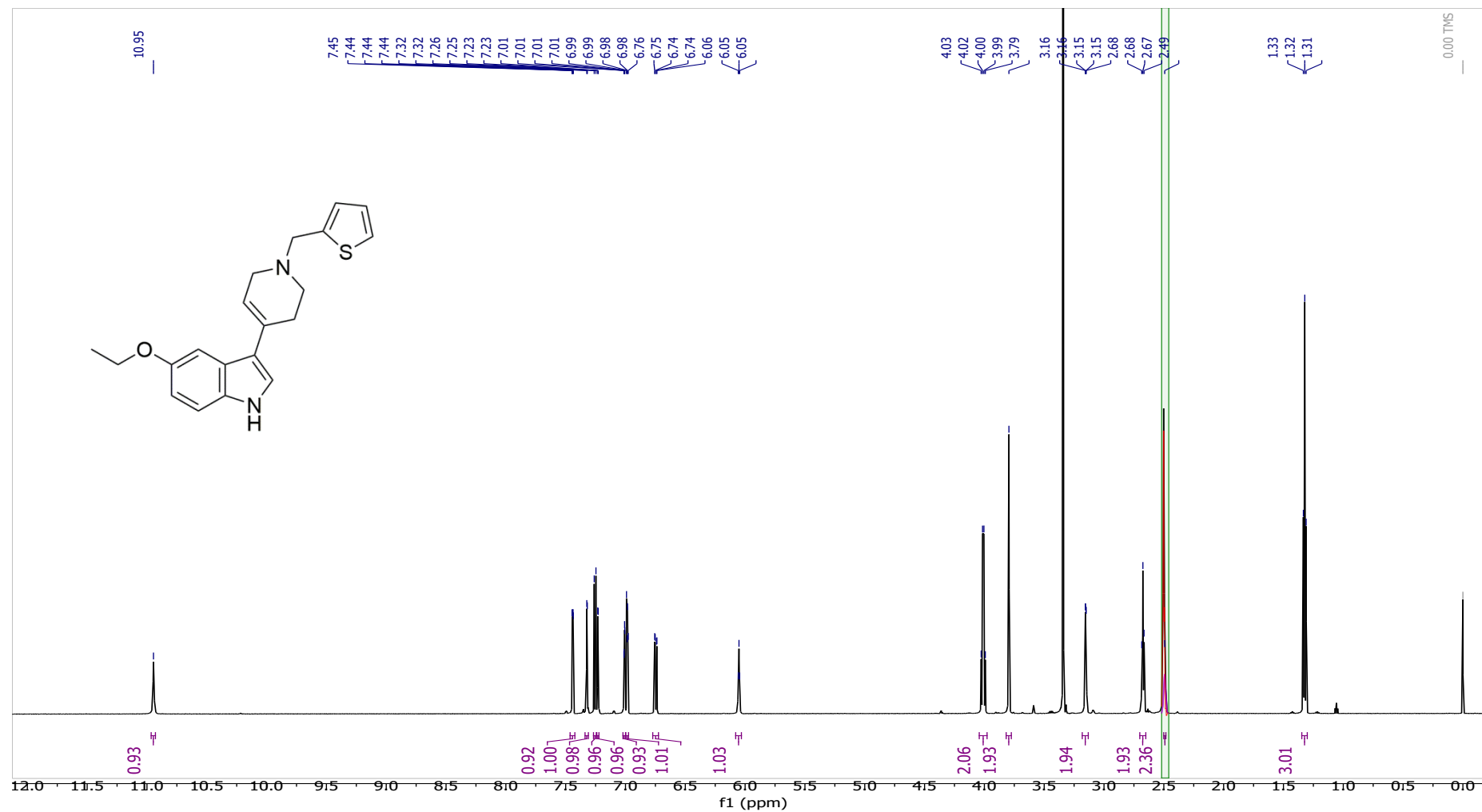
5-methoxy-3-(1-(thiophen-2-ylmethyl)-1,2,3,6-tetrahydropyridin-4-yl)-1H-indole (6)



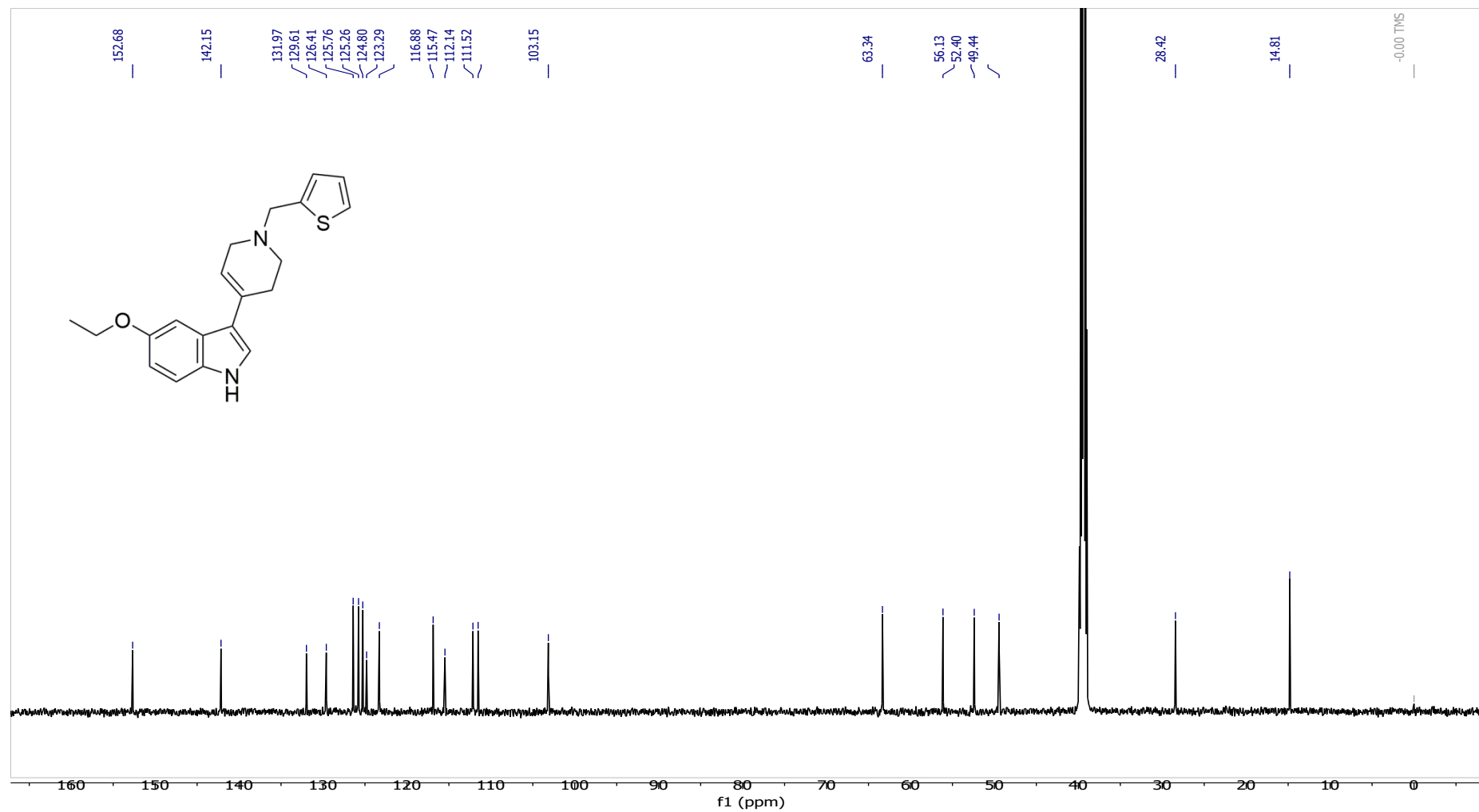
5-methoxy-3-(1-(thiophen-2-ylmethyl)-1,2,3,6-tetrahydropyridin-4-yl)-1H-indole (6)



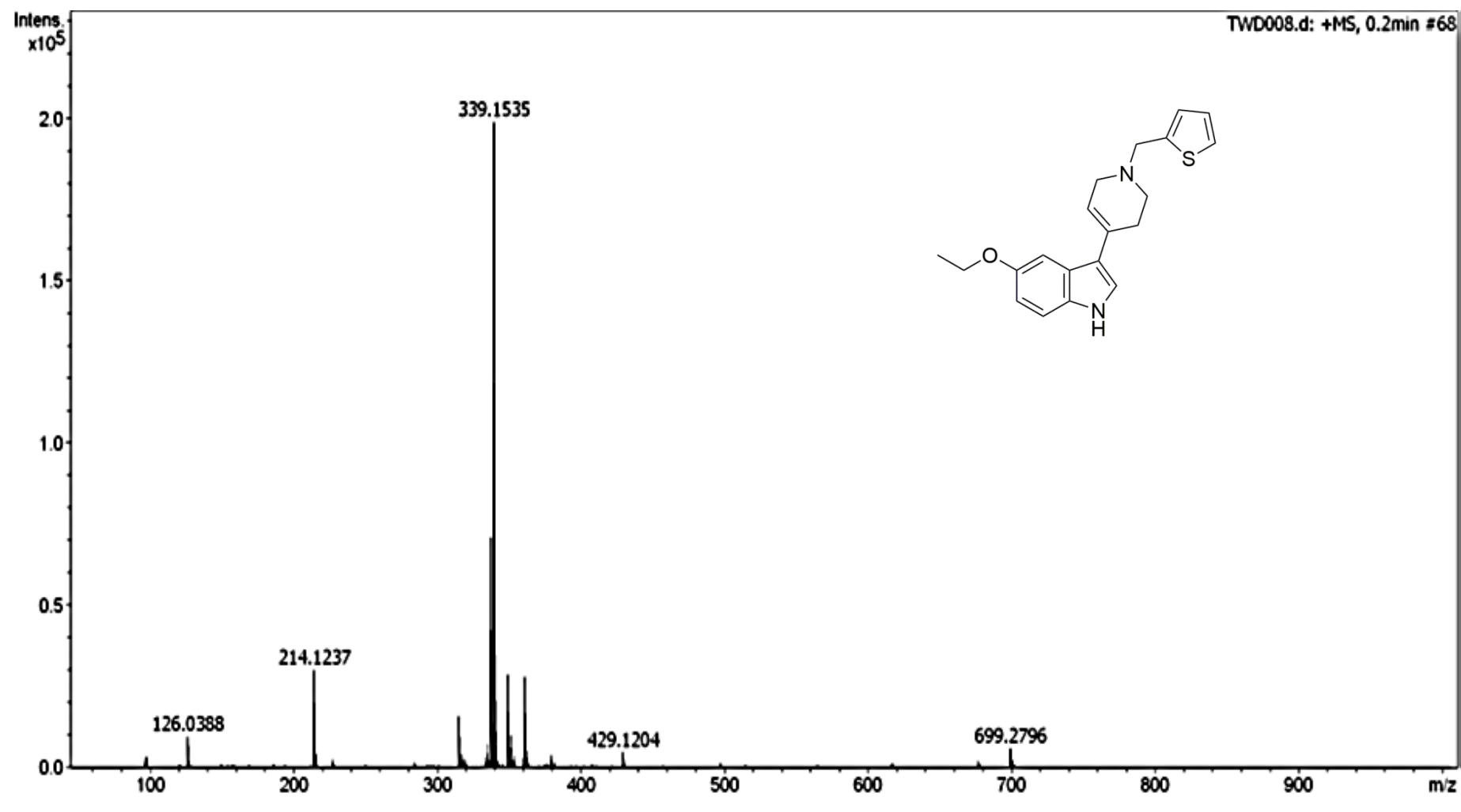
5-ethoxy-3-(1-(thiophen-2-ylmethyl)-1,2,3,6-tetrahydropyridin-4-yl)-1H-indole (7)



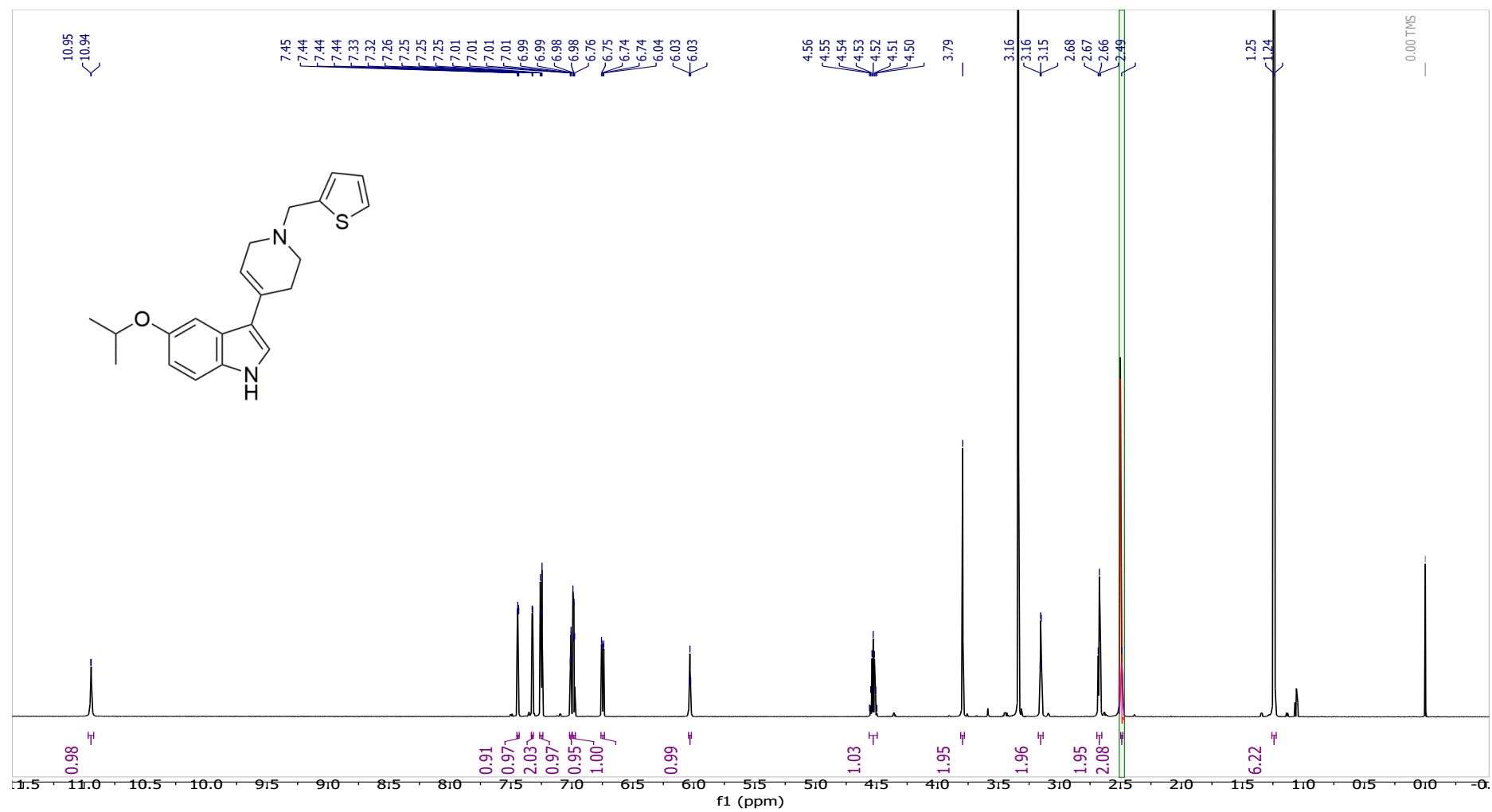
5-ethoxy-3-(1-(thiophen-2-ylmethyl)-1,2,3,6-tetrahydropyridin-4-yl)-1H-indole (7)



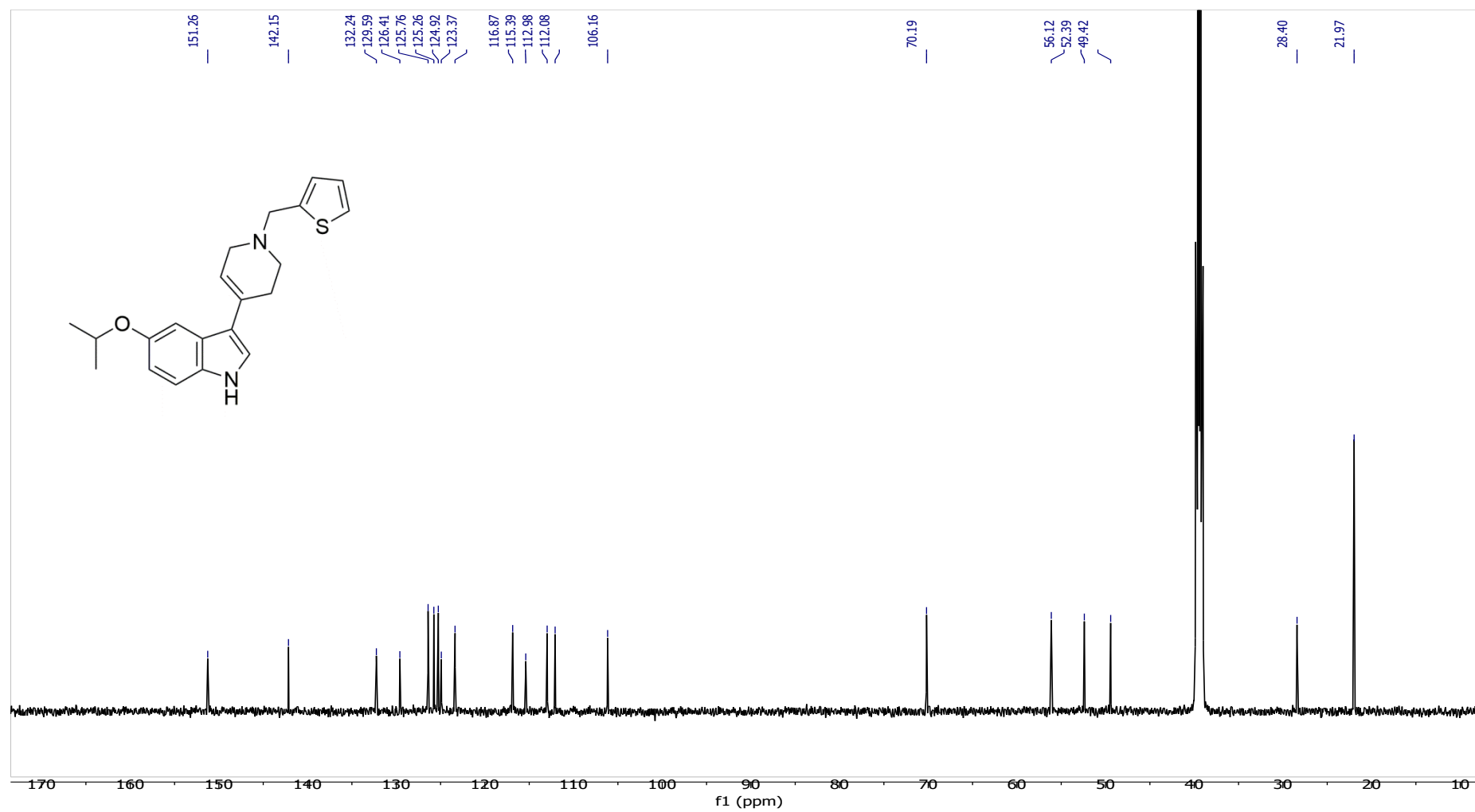
5-ethoxy-3-(1-(thiophen-2-ylmethyl)-1,2,3,6-tetrahydropyridin-4-yl)-1H-indole (7)



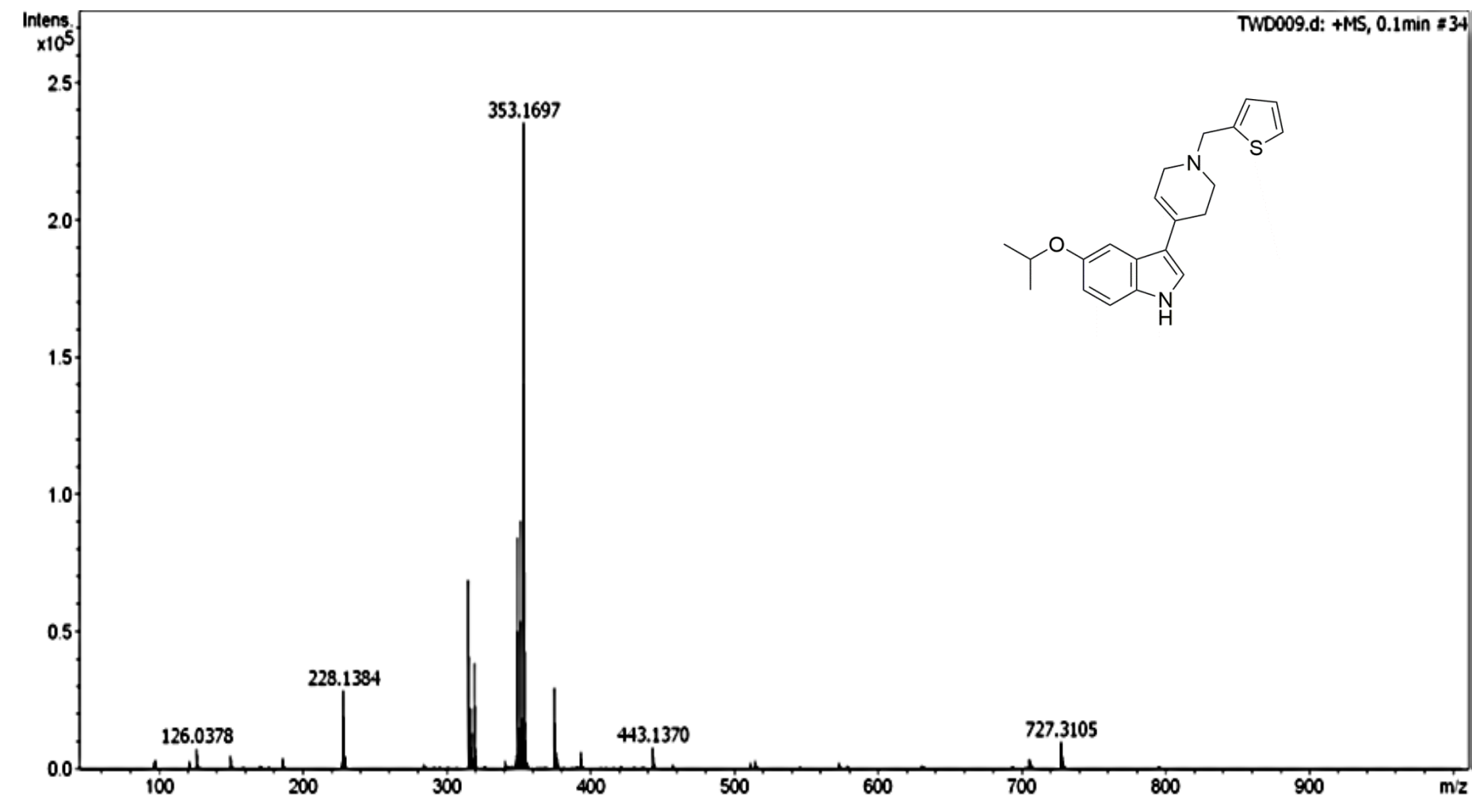
5-isopropoxy-3-(1-(thiophen-2-ylmethyl)-1,2,3,6-tetrahydropyridin-4-yl)-1H-indole (8)



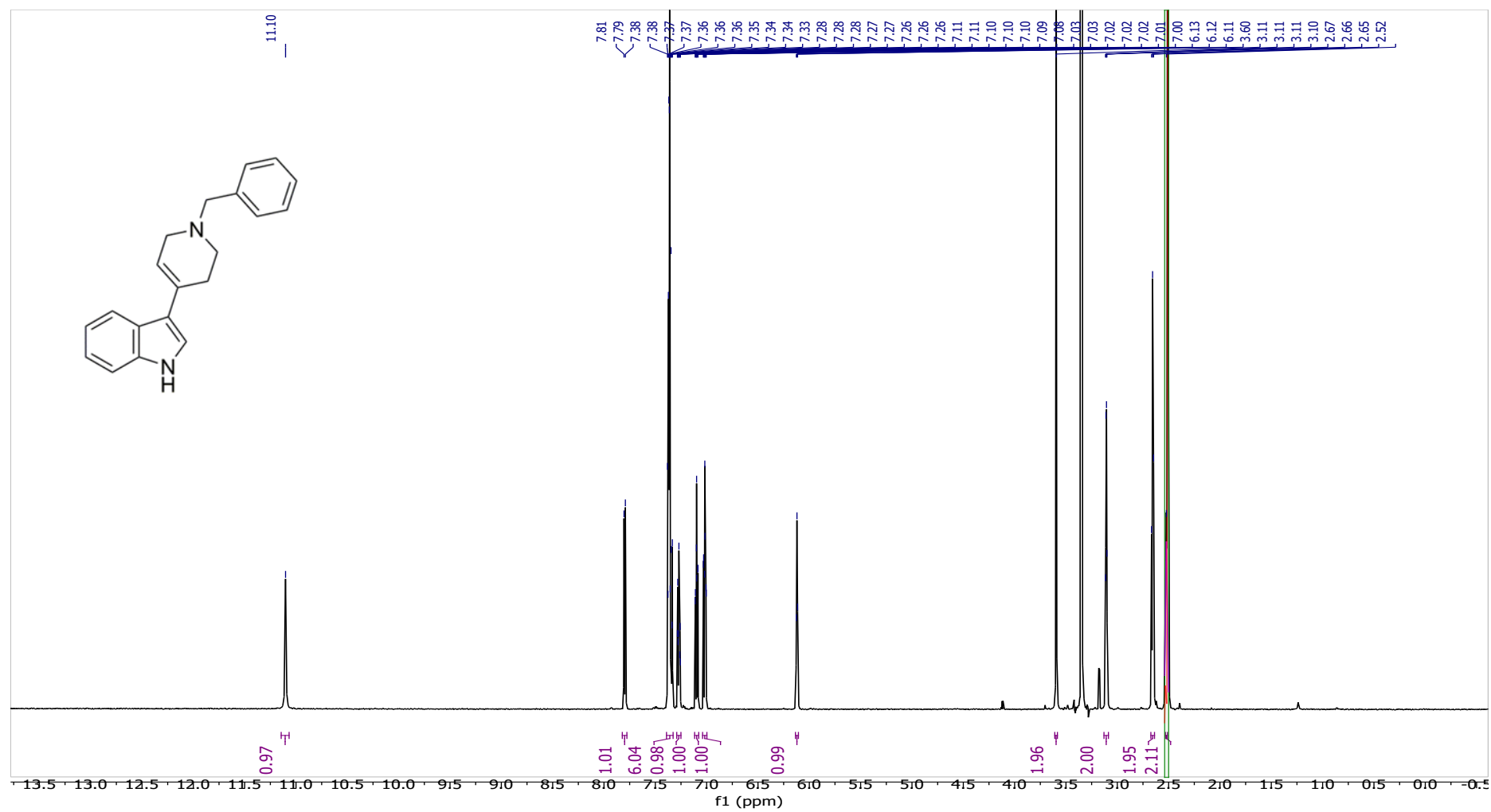
5-isopropoxy-3-(1-(thiophen-2-ylmethyl)-1,2,3,6-tetrahydropyridin-4-yl)-1H-indole (8)



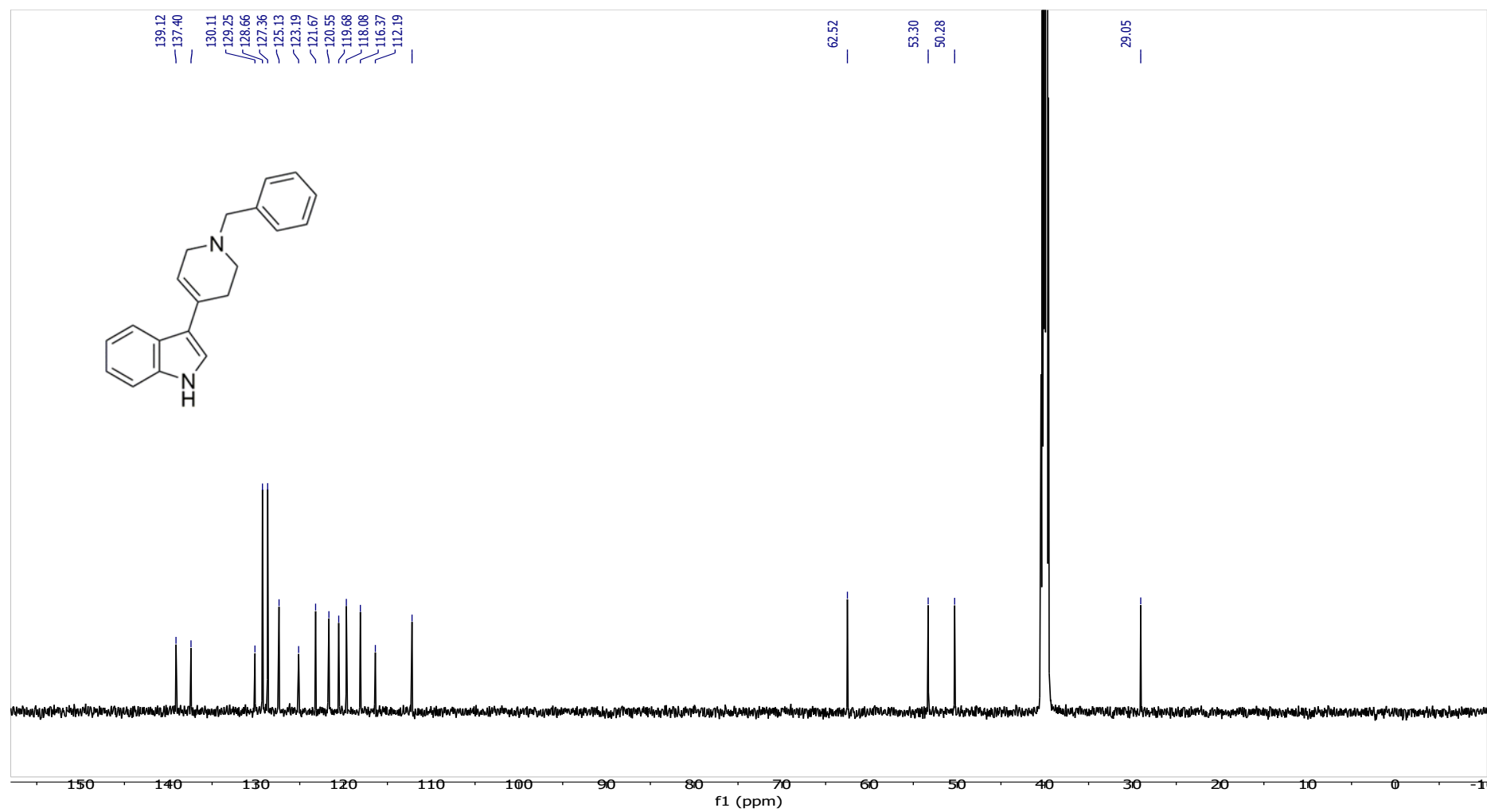
5-isopropoxy-3-(1-(thiophen-2-ylmethyl)-1,2,3,6-tetrahydropyridin-4-yl)-1*H*-indole (8)



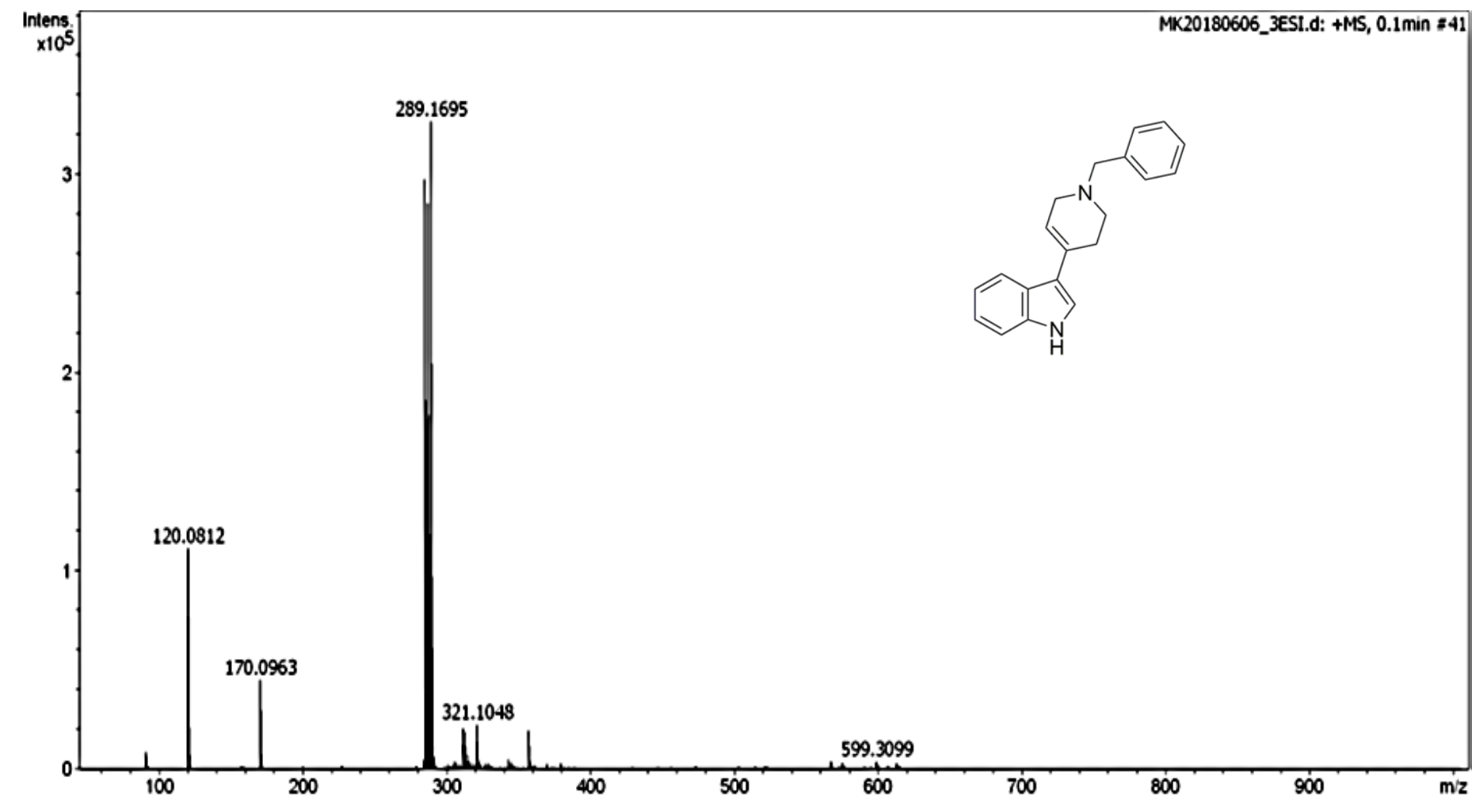
3-(1-benzyl-1,2,3,6-tetrahydropyridin-4-yl)-1H-indole (9)



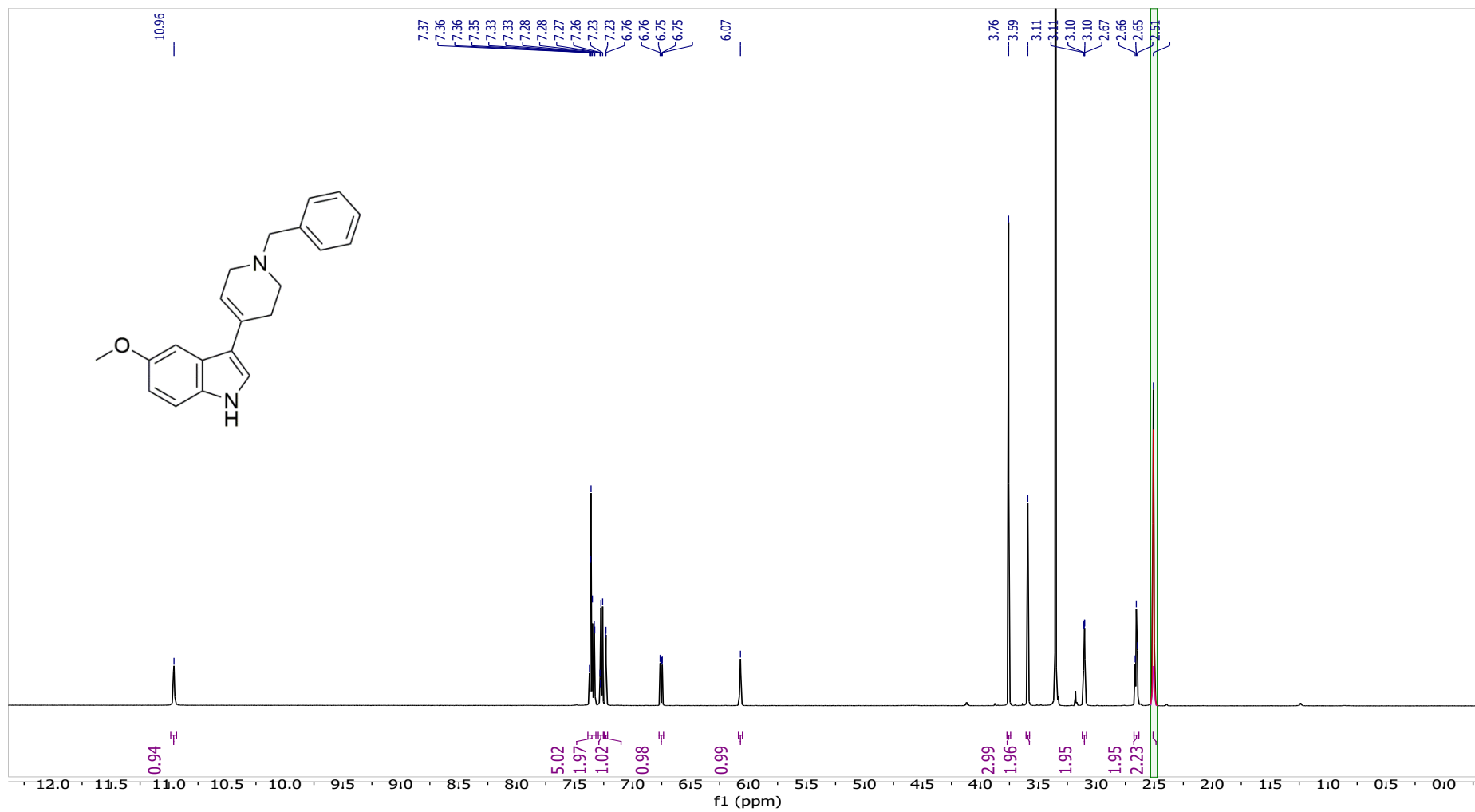
3-(1-benzyl-1,2,3,6-tetrahydropyridin-4-yl)-1*H*-indole (**9**)



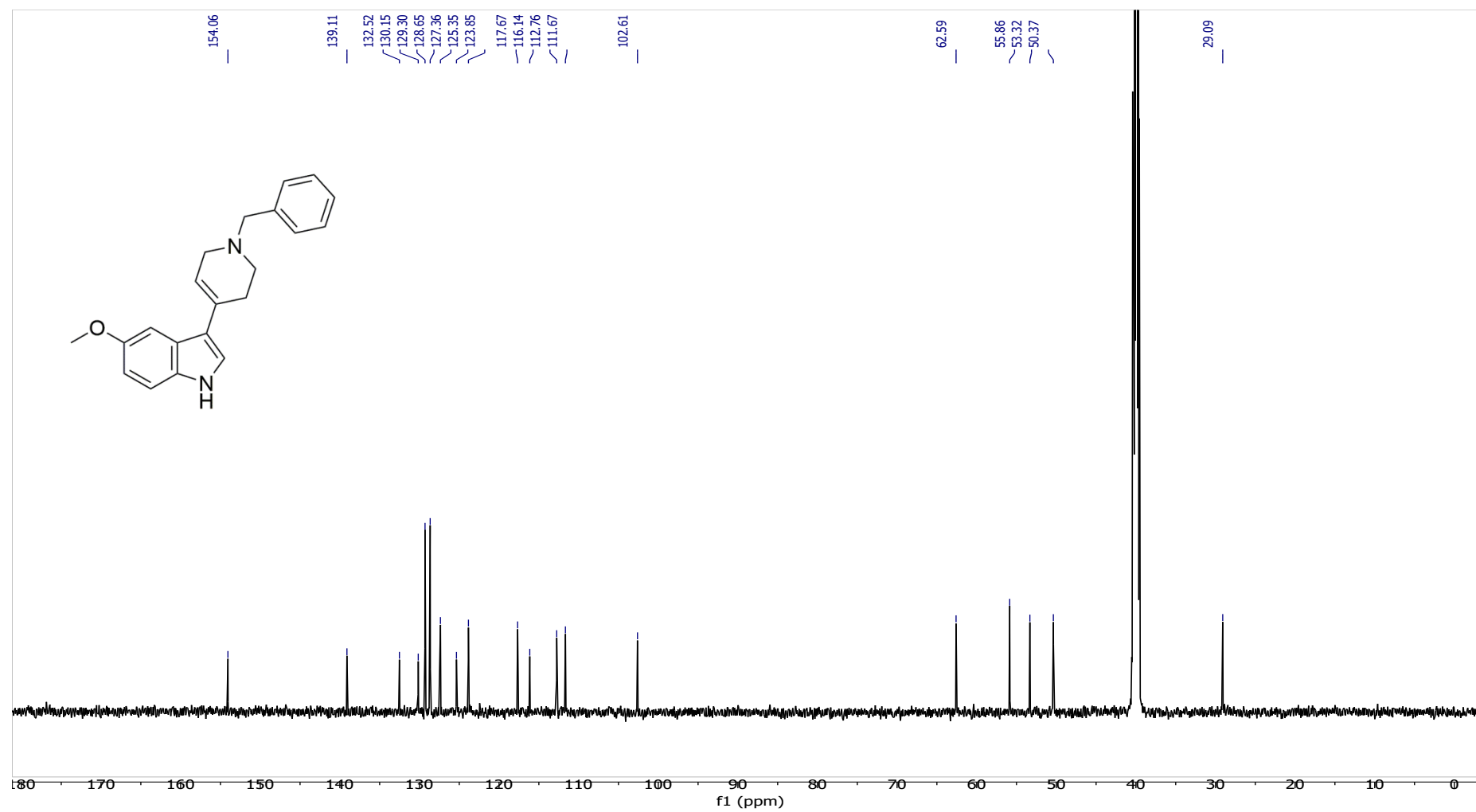
3-(1-benzyl-1,2,3,6-tetrahydropyridin-4-yl)-1H-indole (9)



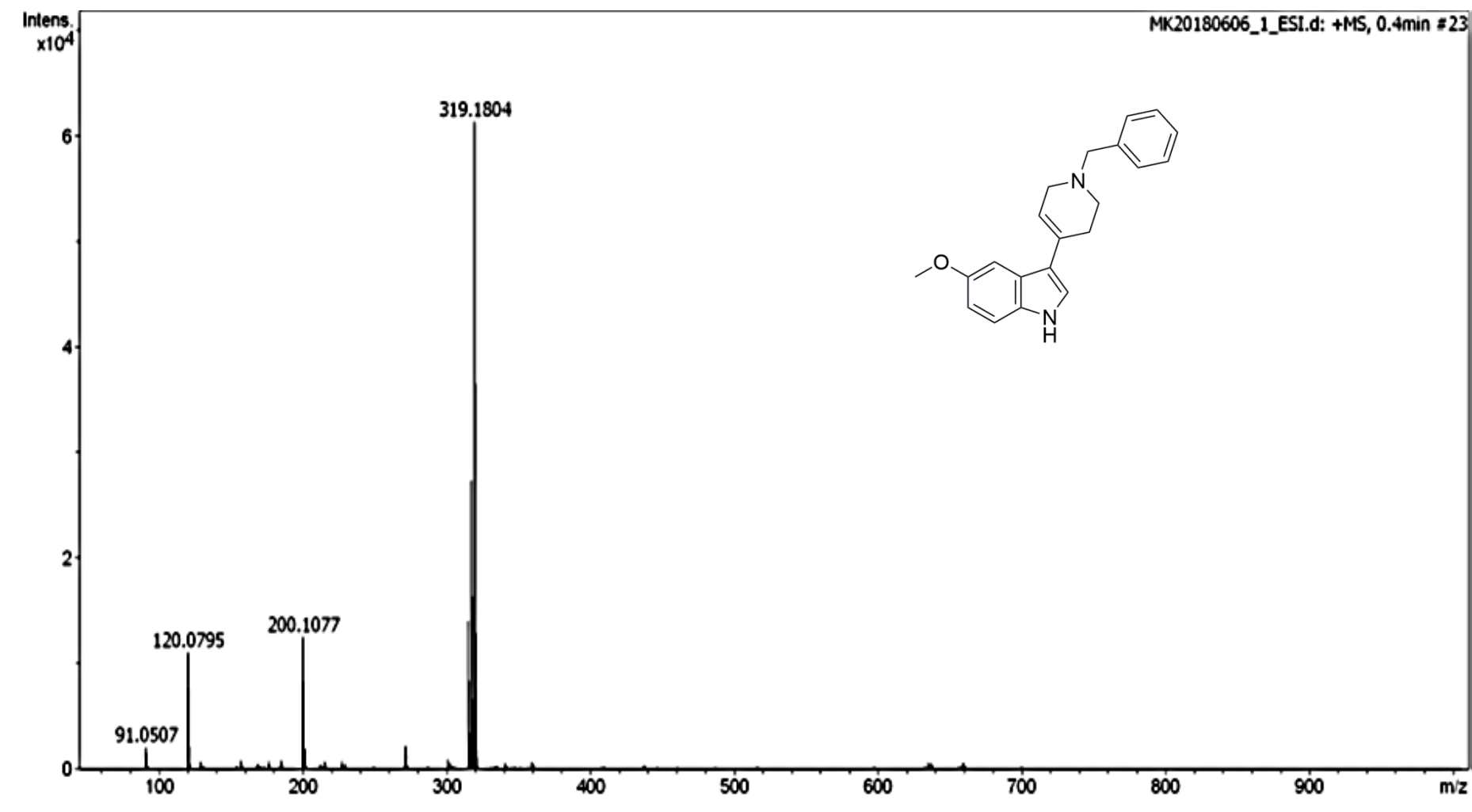
3-(1-benzyl-1,2,3,6-tetrahydropyridin-4-yl)-5-methoxy-1H-indole (10)



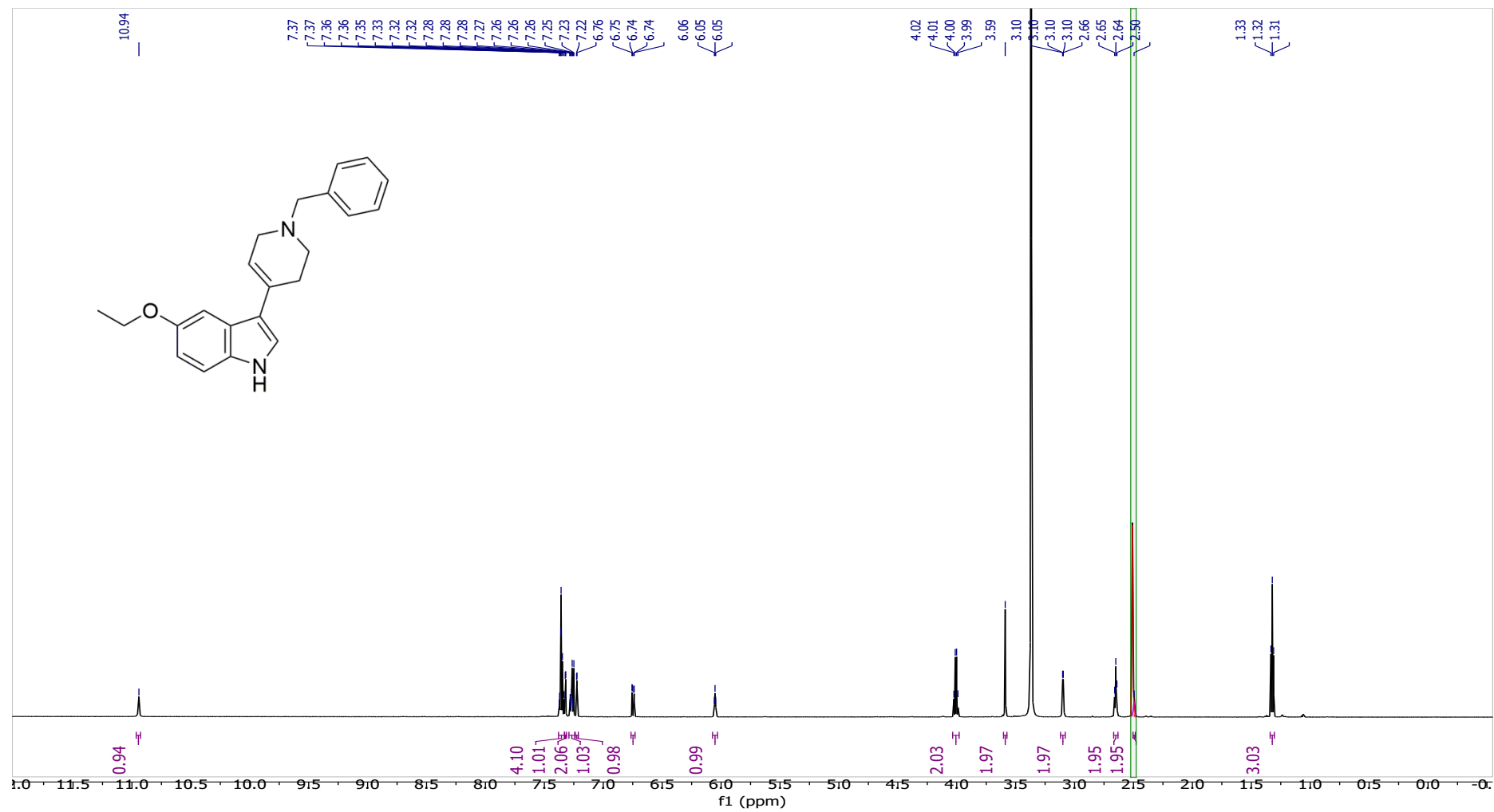
3-(1-benzyl-1,2,3,6-tetrahydropyridin-4-yl)-5-methoxy-1H-indole (10)



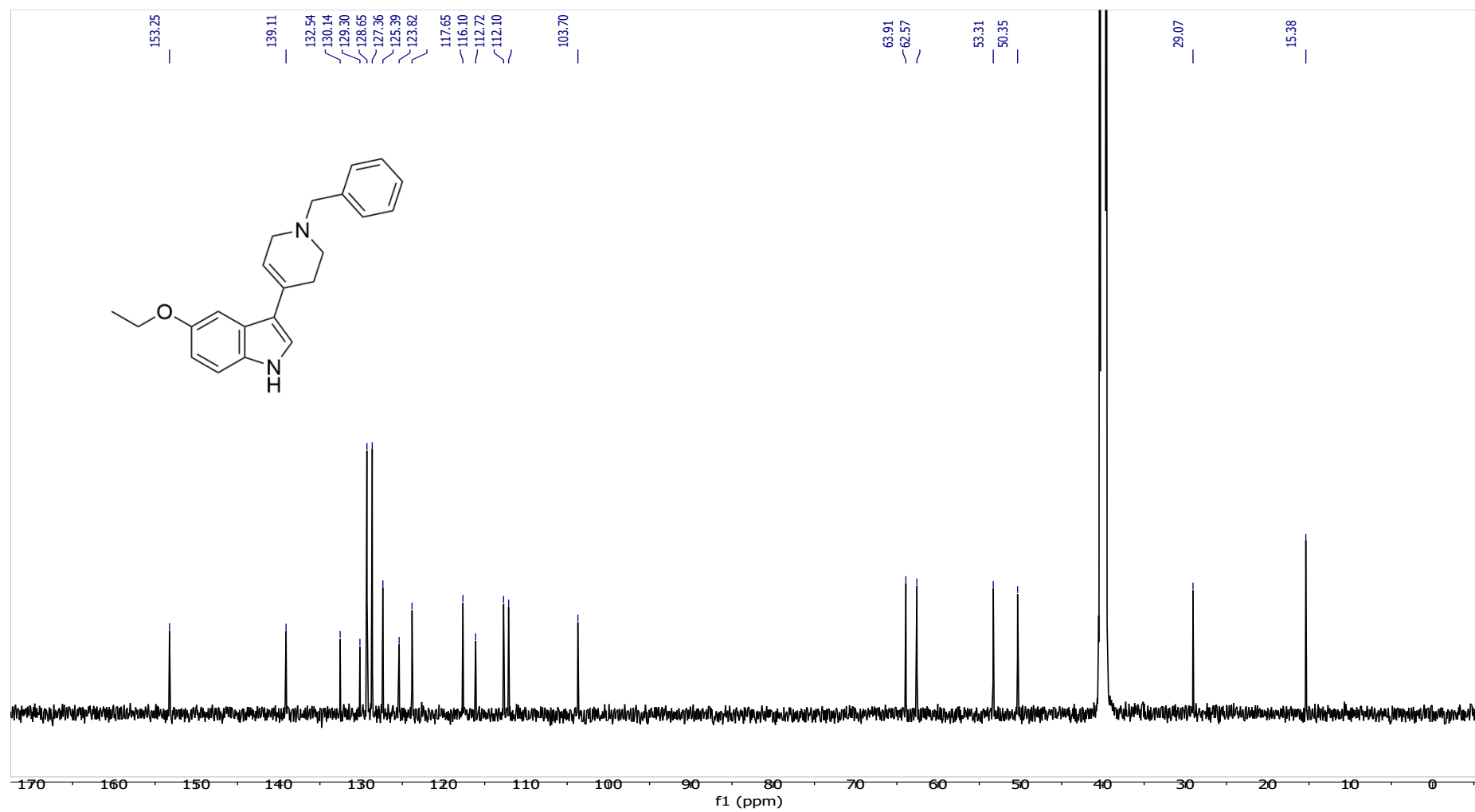
3-(1-benzyl-1,2,3,6-tetrahydropyridin-4-yl)-5-methoxy-1H-indole (10)



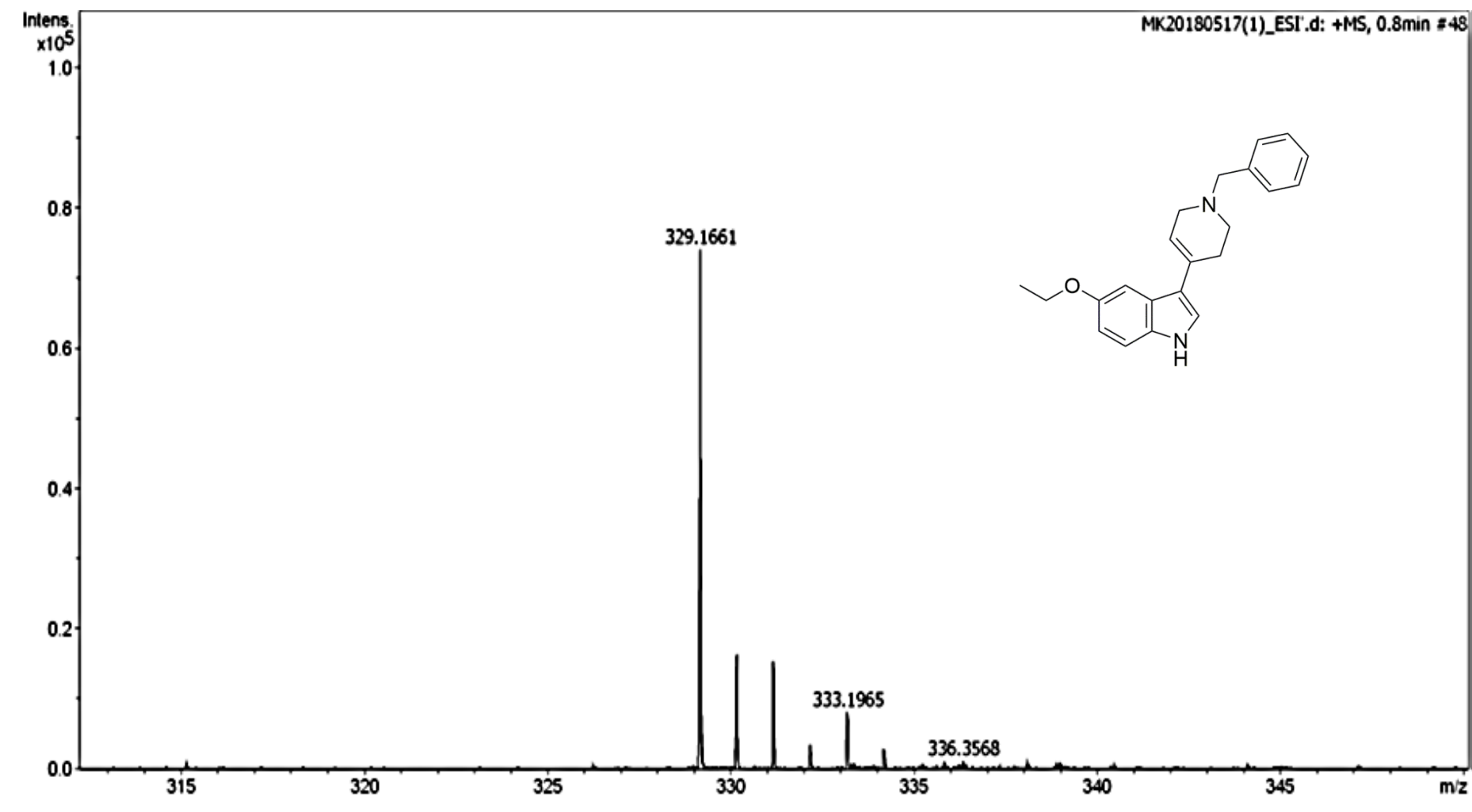
3-(1-benzyl-1,2,3,6-tetrahydropyridin-4-yl)-5-ethoxy-1H-indole (11)



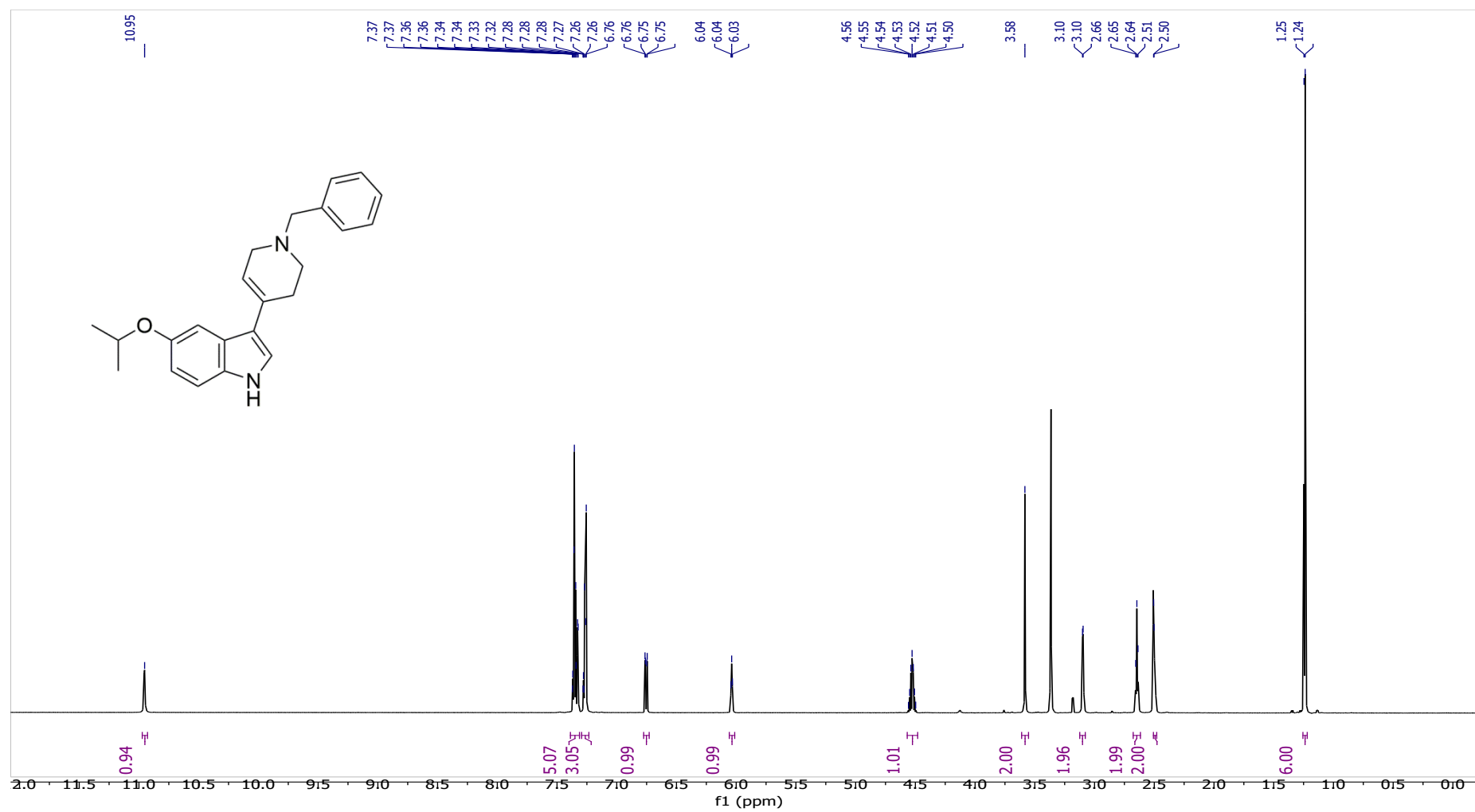
3-(1-benzyl-1,2,3,6-tetrahydropyridin-4-yl)-5-ethoxy-1*H*-indole (11)



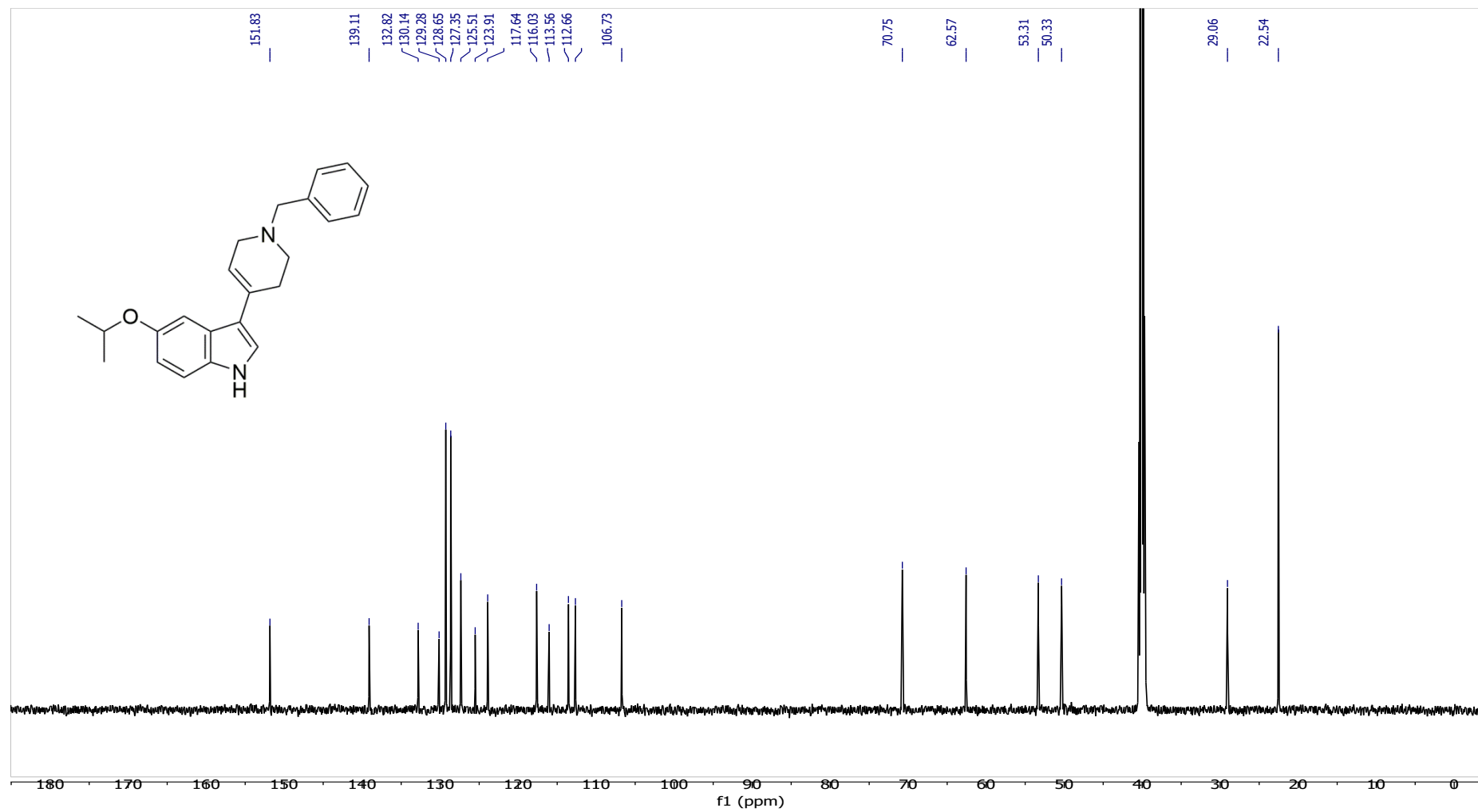
3-(1-benzyl-1,2,3,6-tetrahydropyridin-4-yl)-5-ethoxy-1H-indole (11)



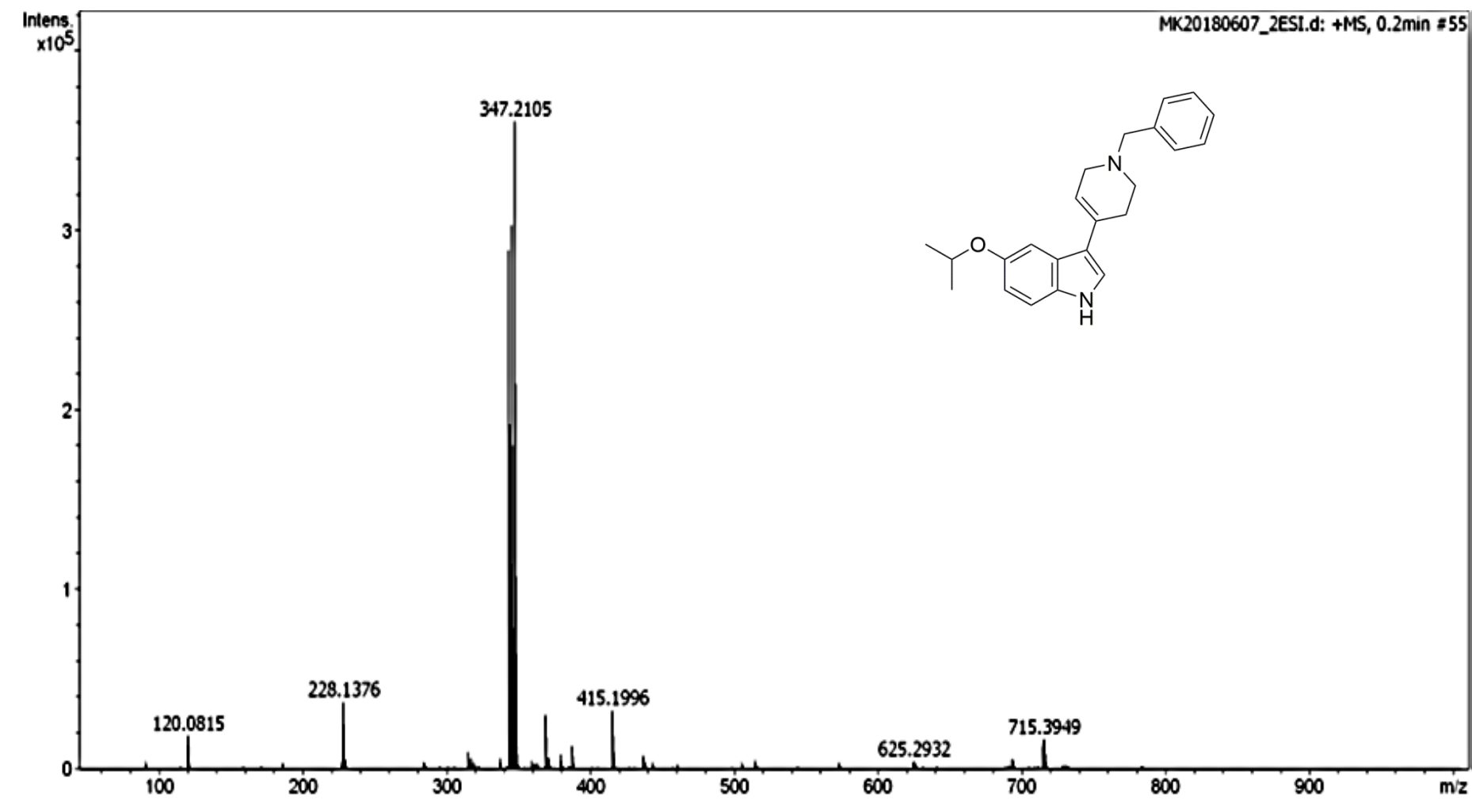
3-(1-benzyl-1,2,3,6-tetrahydropyridin-4-yl)-5-isopropoxy-1H-indole (12)



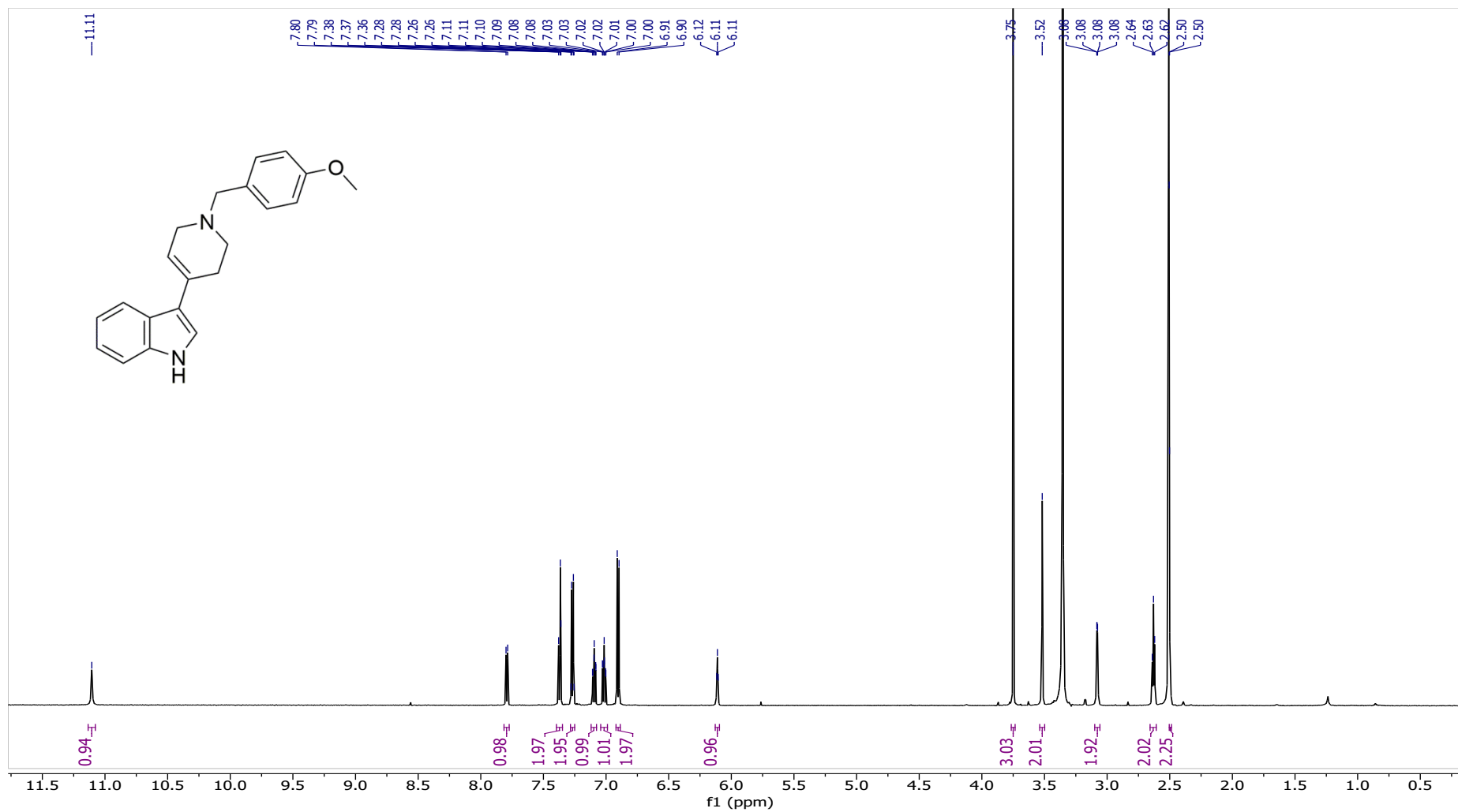
3-(1-benzyl-1,2,3,6-tetrahydropyridin-4-yl)-5-isopropoxy-1H-indole (12)



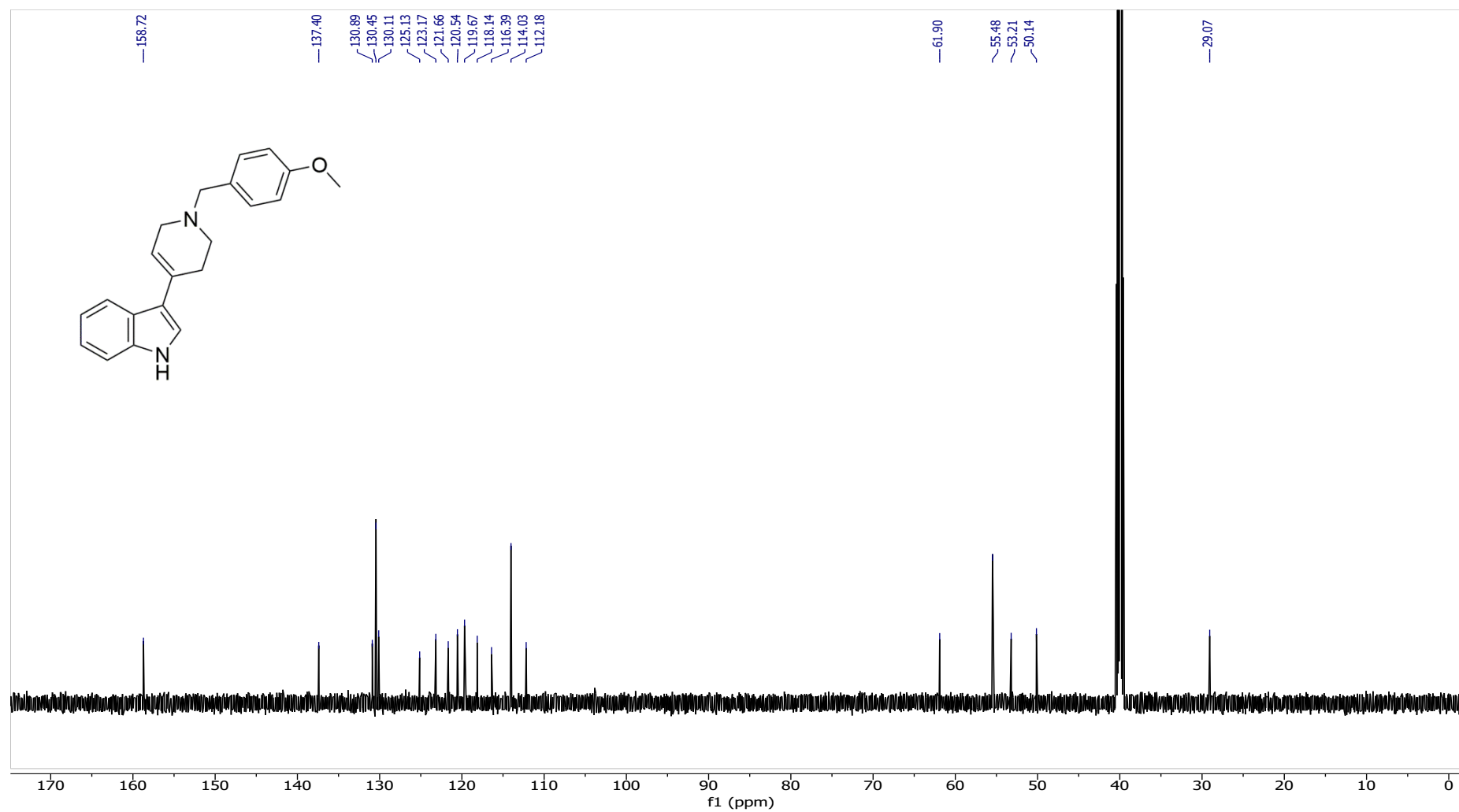
3-(1-benzyl-1,2,3,6-tetrahydropyridin-4-yl)-5-isopropoxy-1H-indole (12)



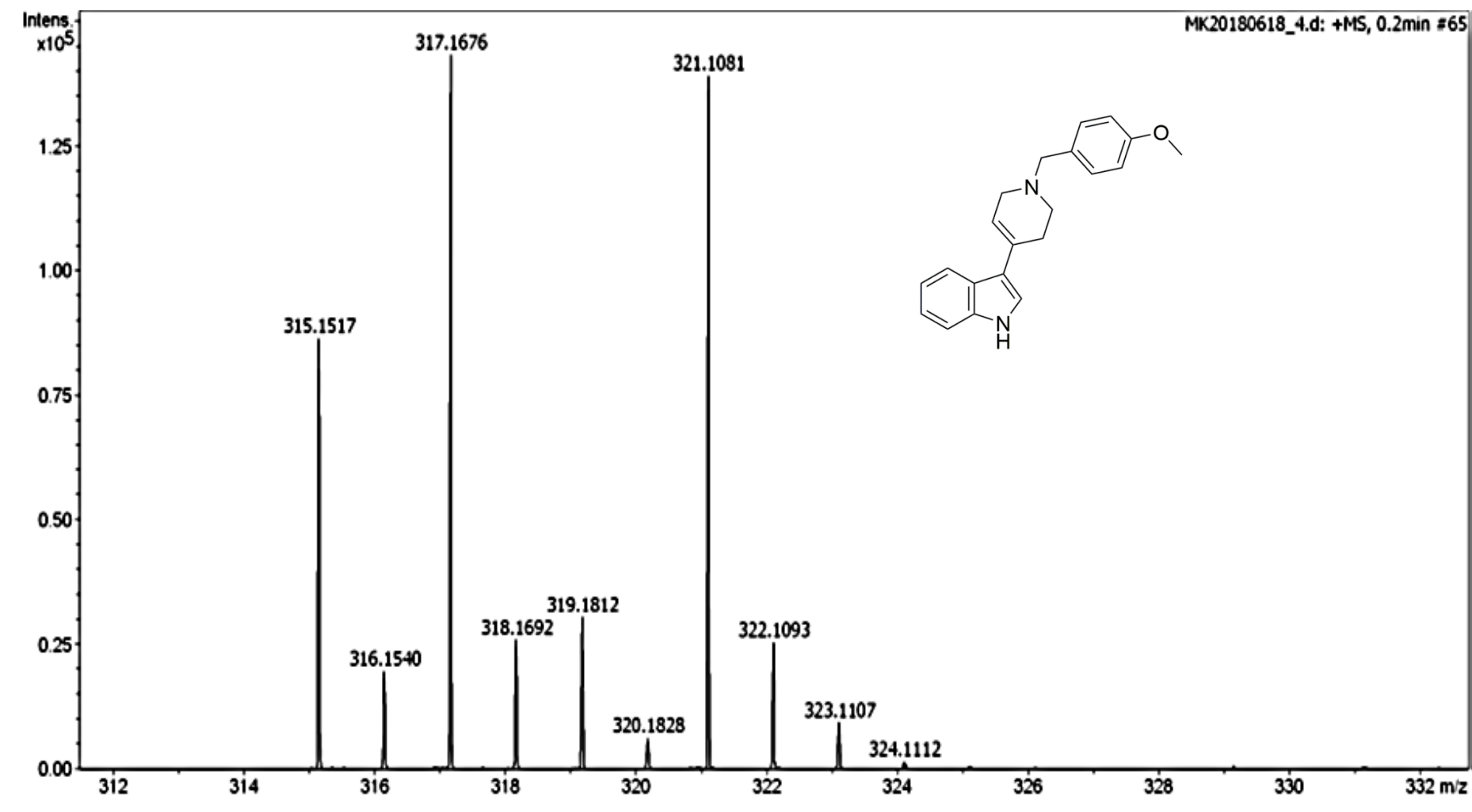
3-(1-(4-methoxybenzyl)-1,2,3,6-tetrahydropyridin-4-yl)-1H-indole (**13**)



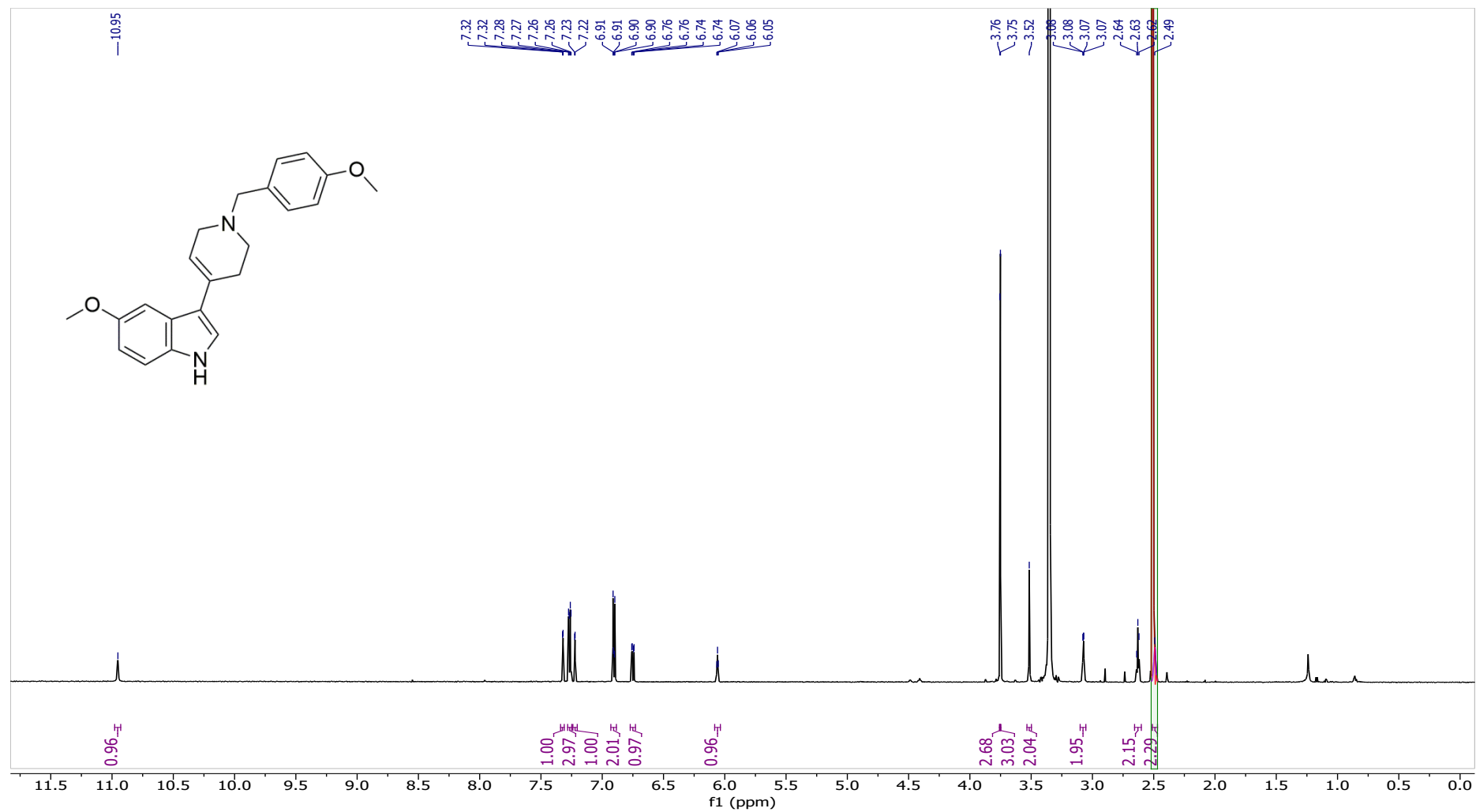
3-(1-(4-methoxybenzyl)-1,2,3,6-tetrahydropyridin-4-yl)-1H-indole (**13**)



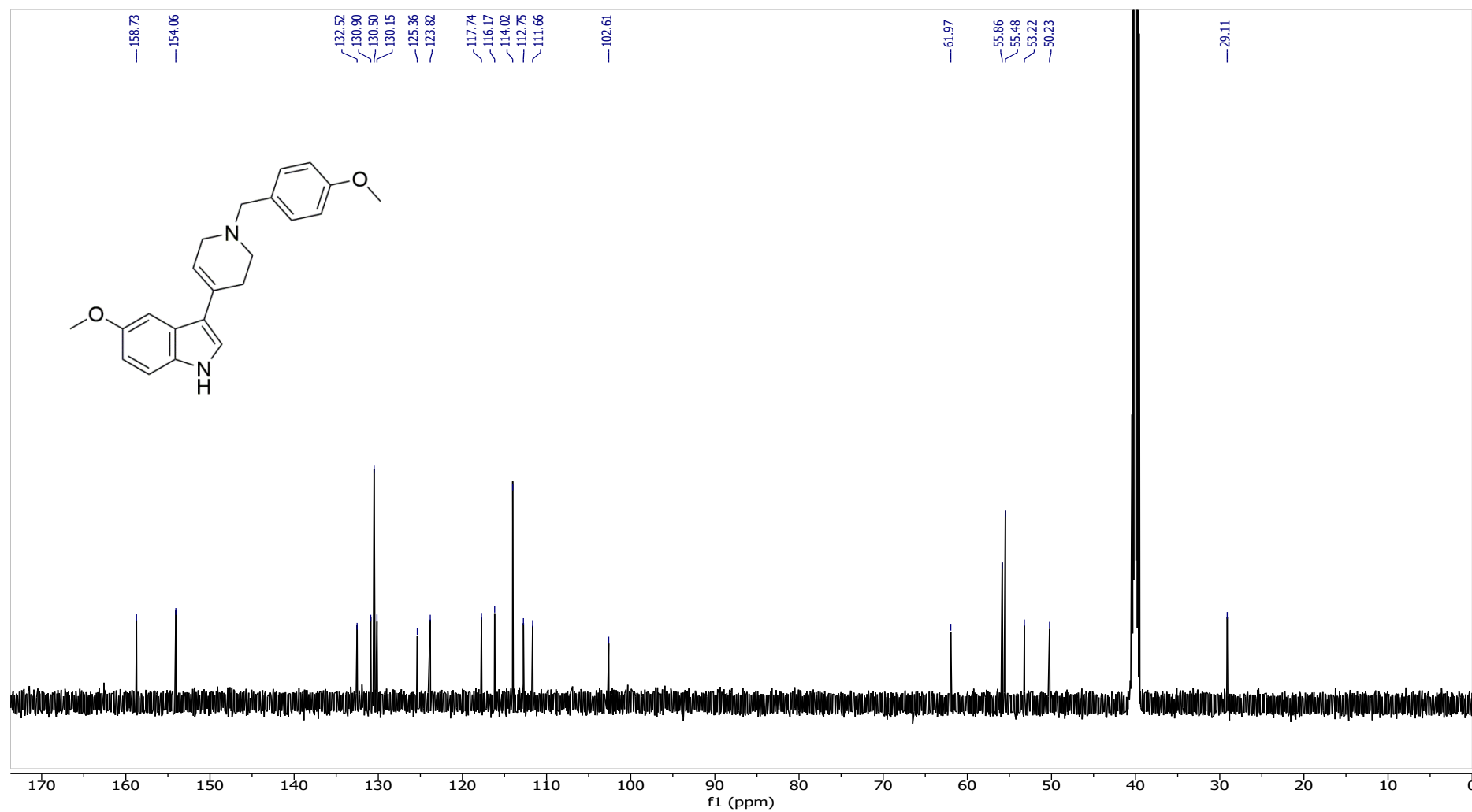
3-(1-(4-methoxybenzyl)-1,2,3,6-tetrahydropyridin-4-yl)-1*H*-indole (**13**)



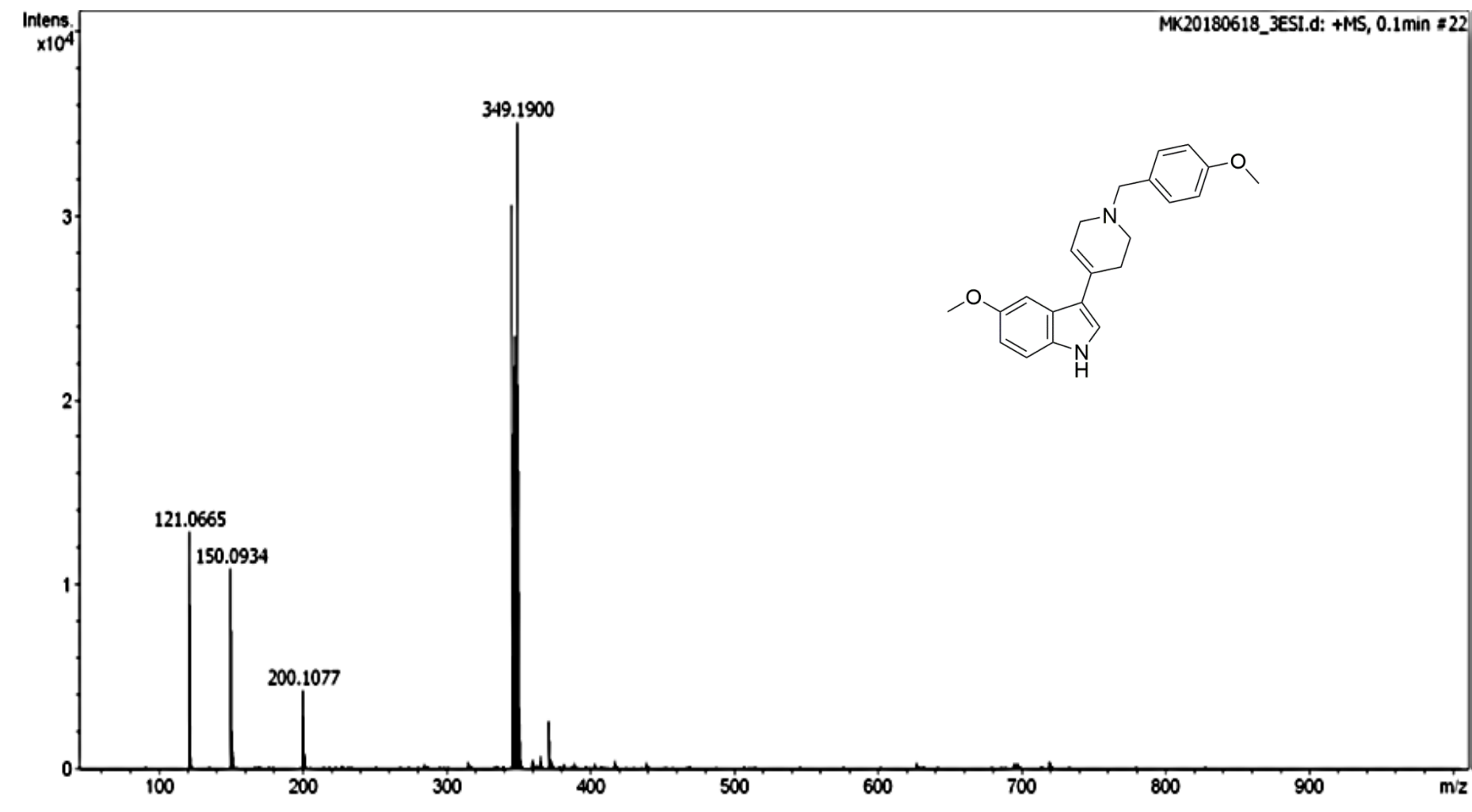
5-methoxy-3-(1-(4-methoxybenzyl)-1,2,3,6-tetrahydropyridin-4-yl)-1*H*-indole (**14**)



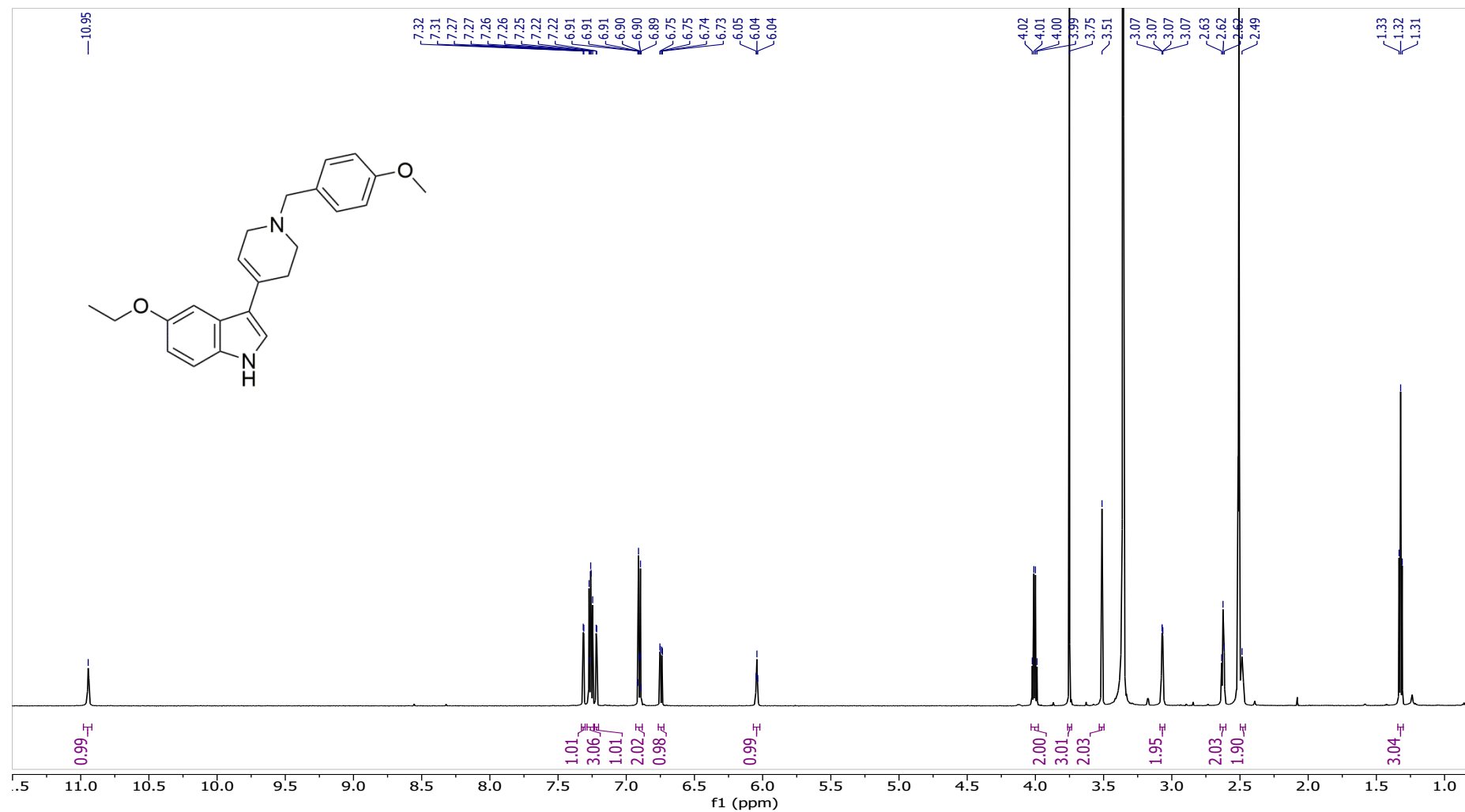
5-methoxy-3-(1-(4-methoxybenzyl)-1,2,3,6-tetrahydropyridin-4-yl)-1H-indole (14)



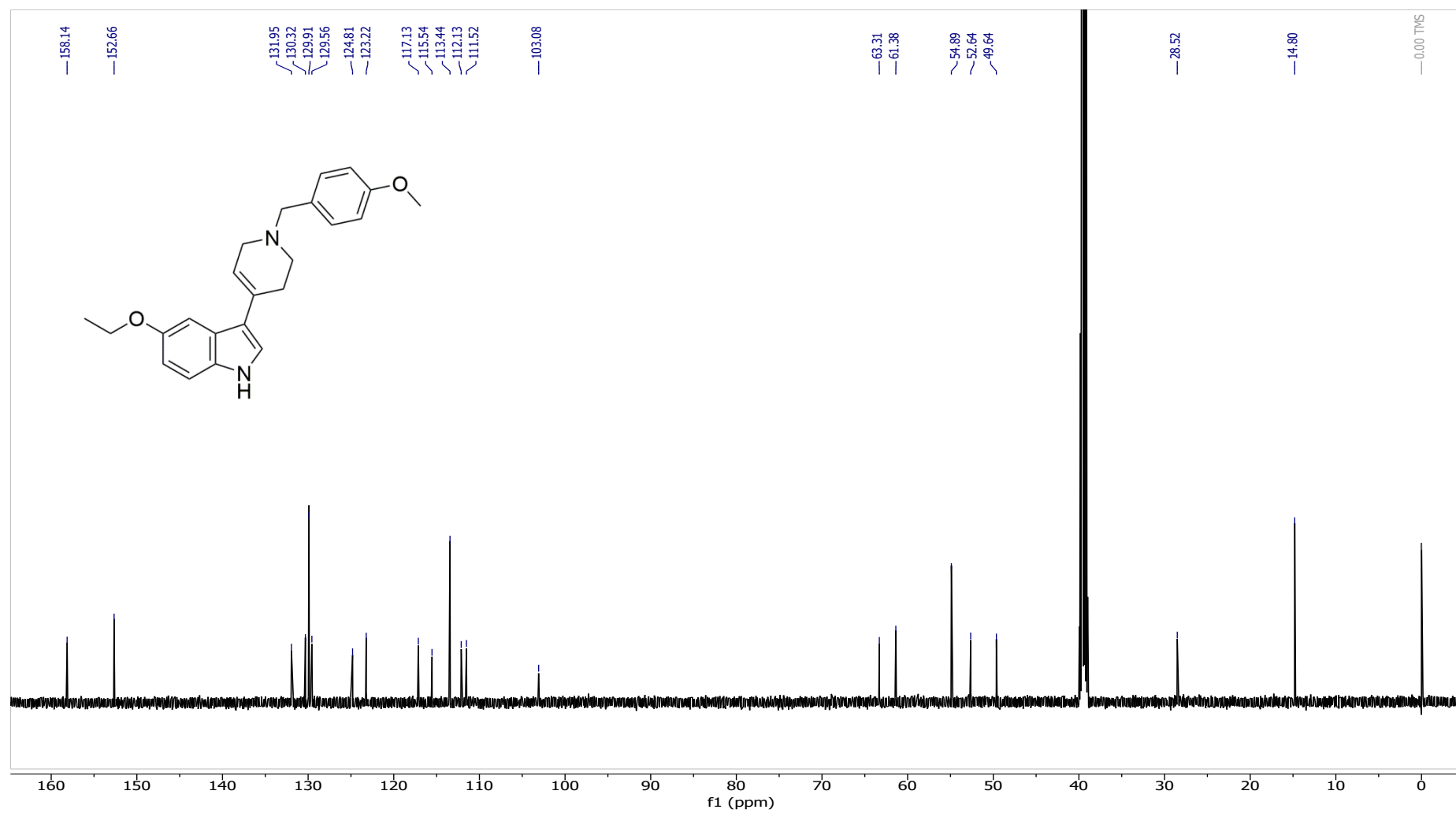
5-methoxy-3-(1-(4-methoxybenzyl)-1,2,3,6-tetrahydropyridin-4-yl)-1H-indole (14)



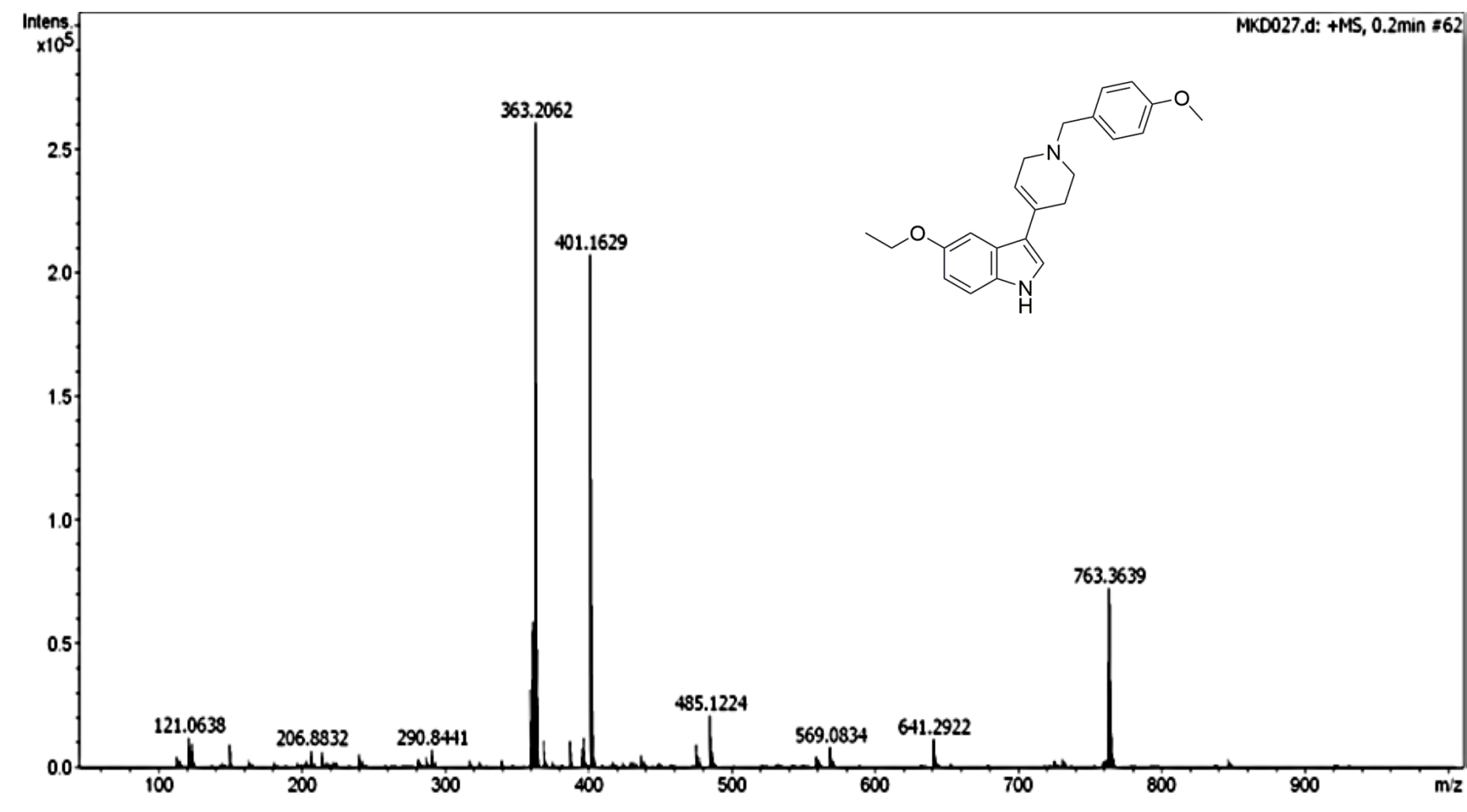
5-ethoxy-3-(1-(4-methoxybenzyl)-1,2,3,6-tetrahydropyridin-4-yl)-1H-indole (15)



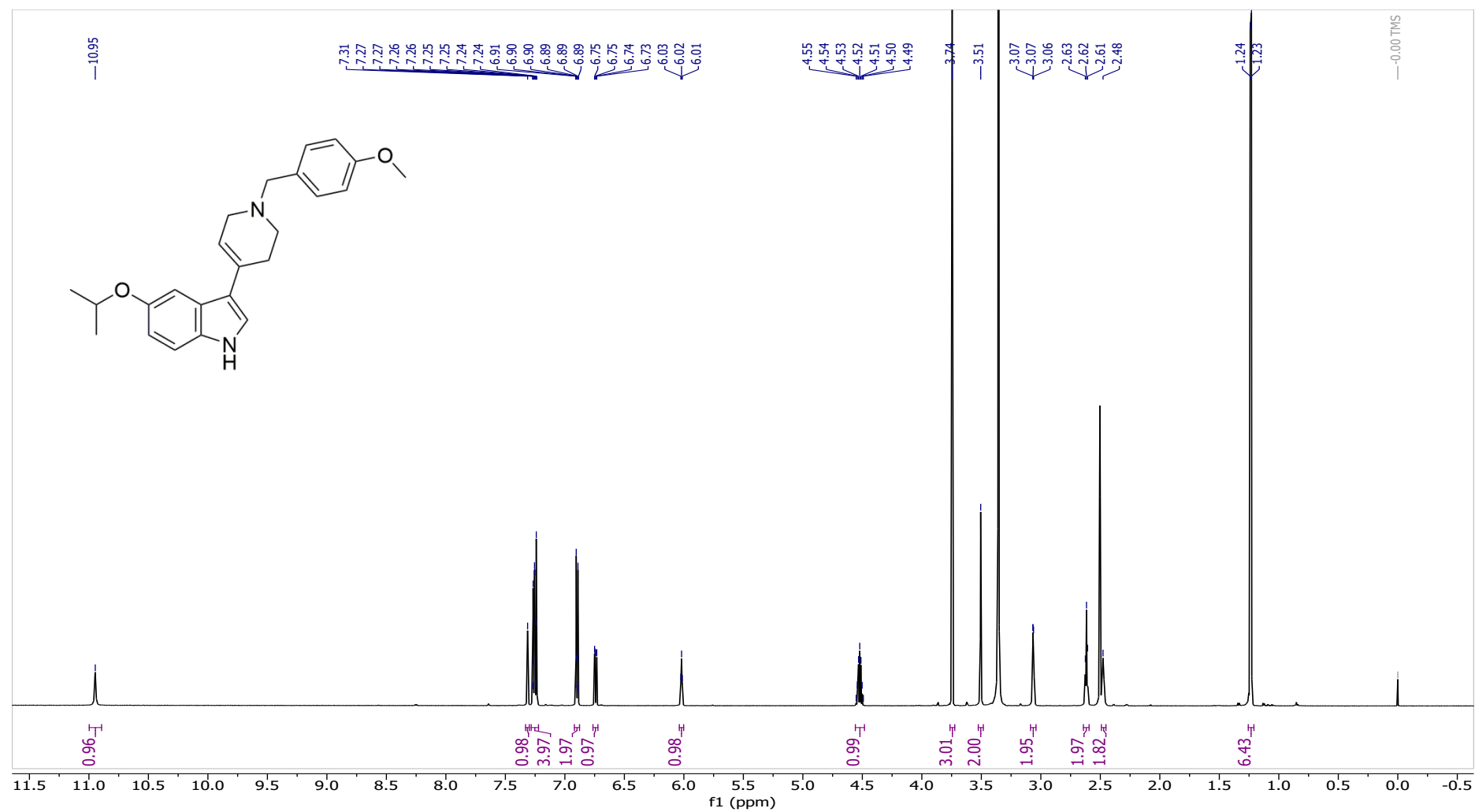
5-ethoxy-3-(1-(4-methoxybenzyl)-1,2,3,6-tetrahydropyridin-4-yl)-1H-indole (15)



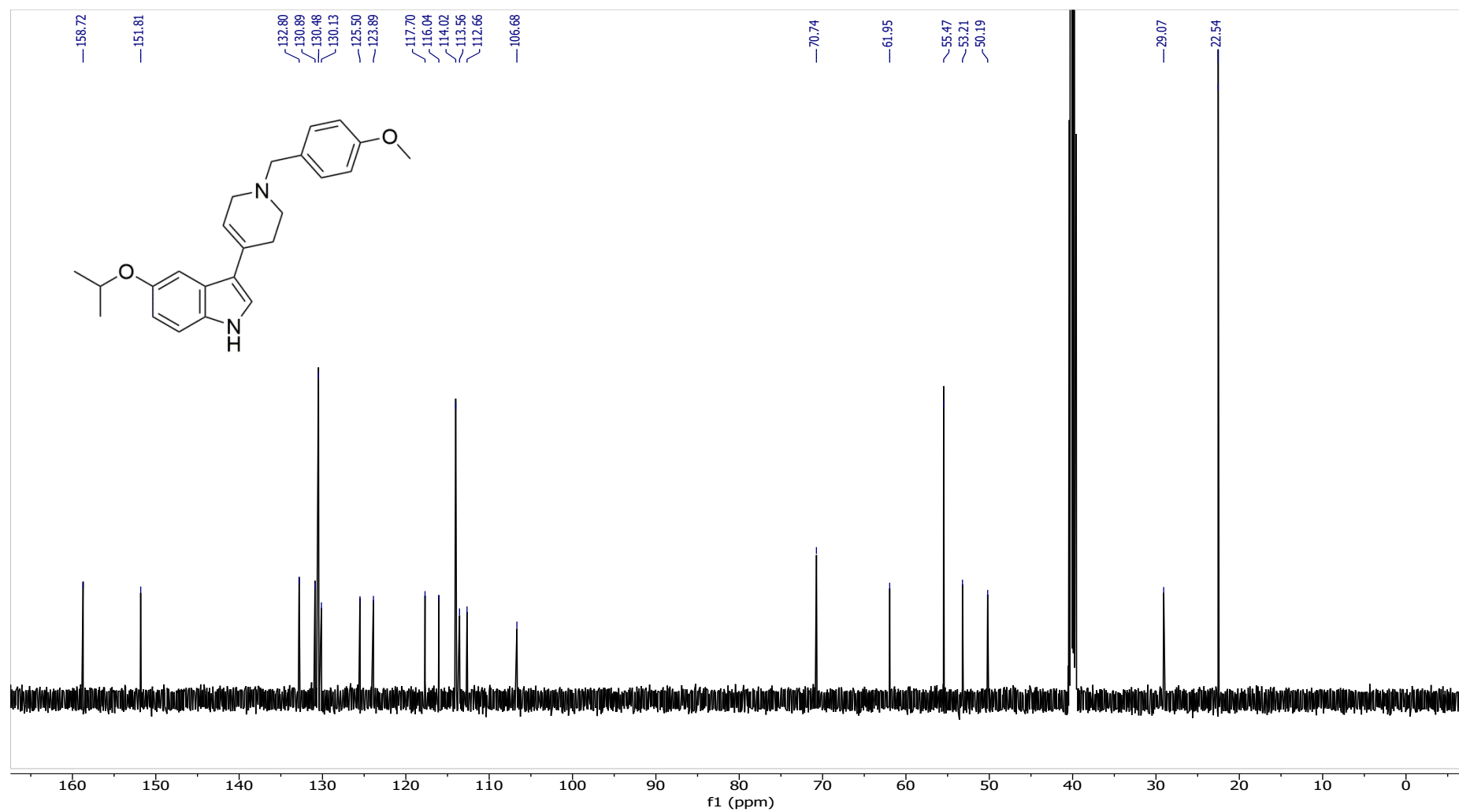
5-ethoxy-3-(1-(4-methoxybenzyl)-1,2,3,6-tetrahydropyridin-4-yl)-1H-indole (15)



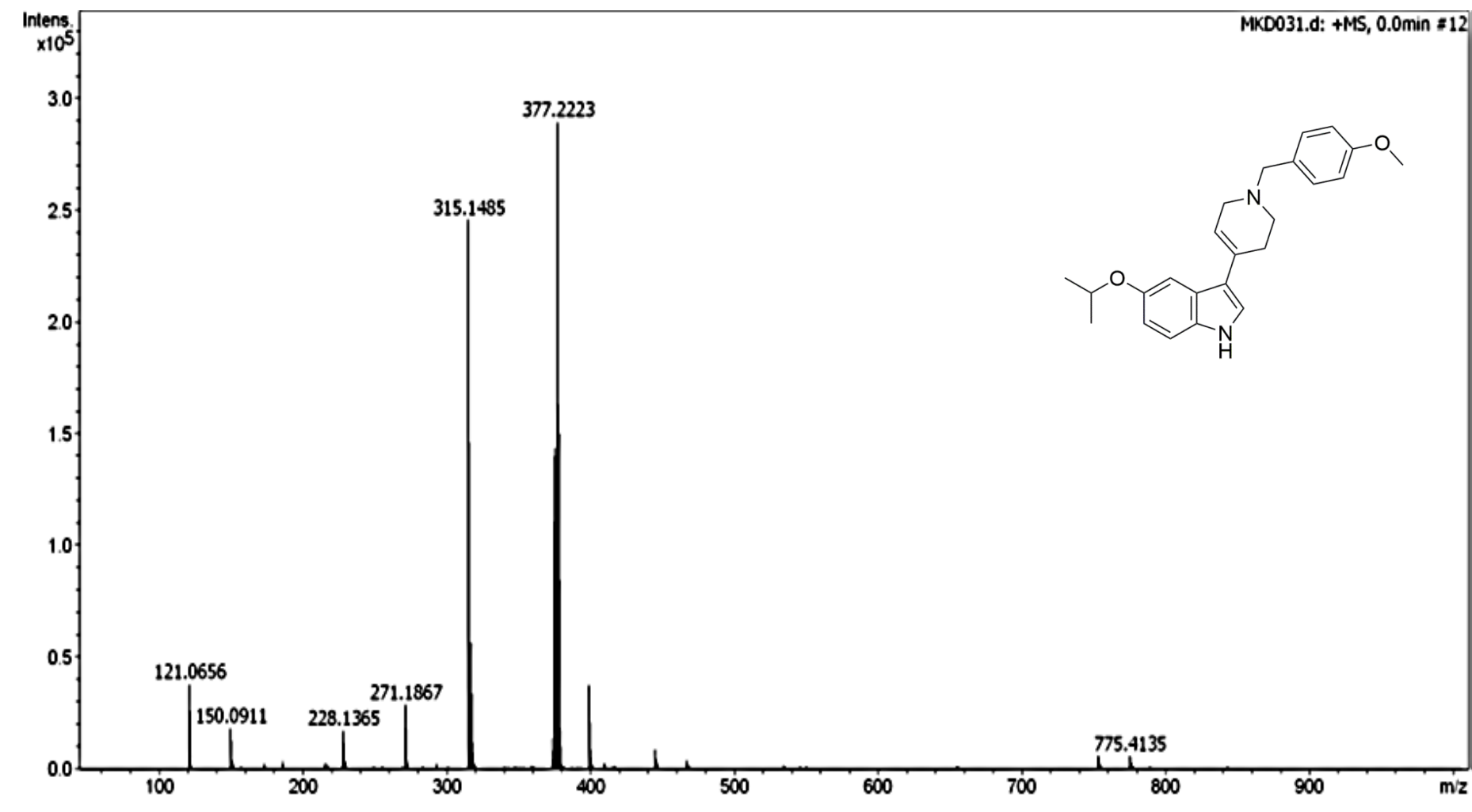
5-isopropoxy-3-(1-(4-methoxybenzyl)-1,2,3,6-tetrahydropyridin-4-yl)-1*H*-indole (**16**)



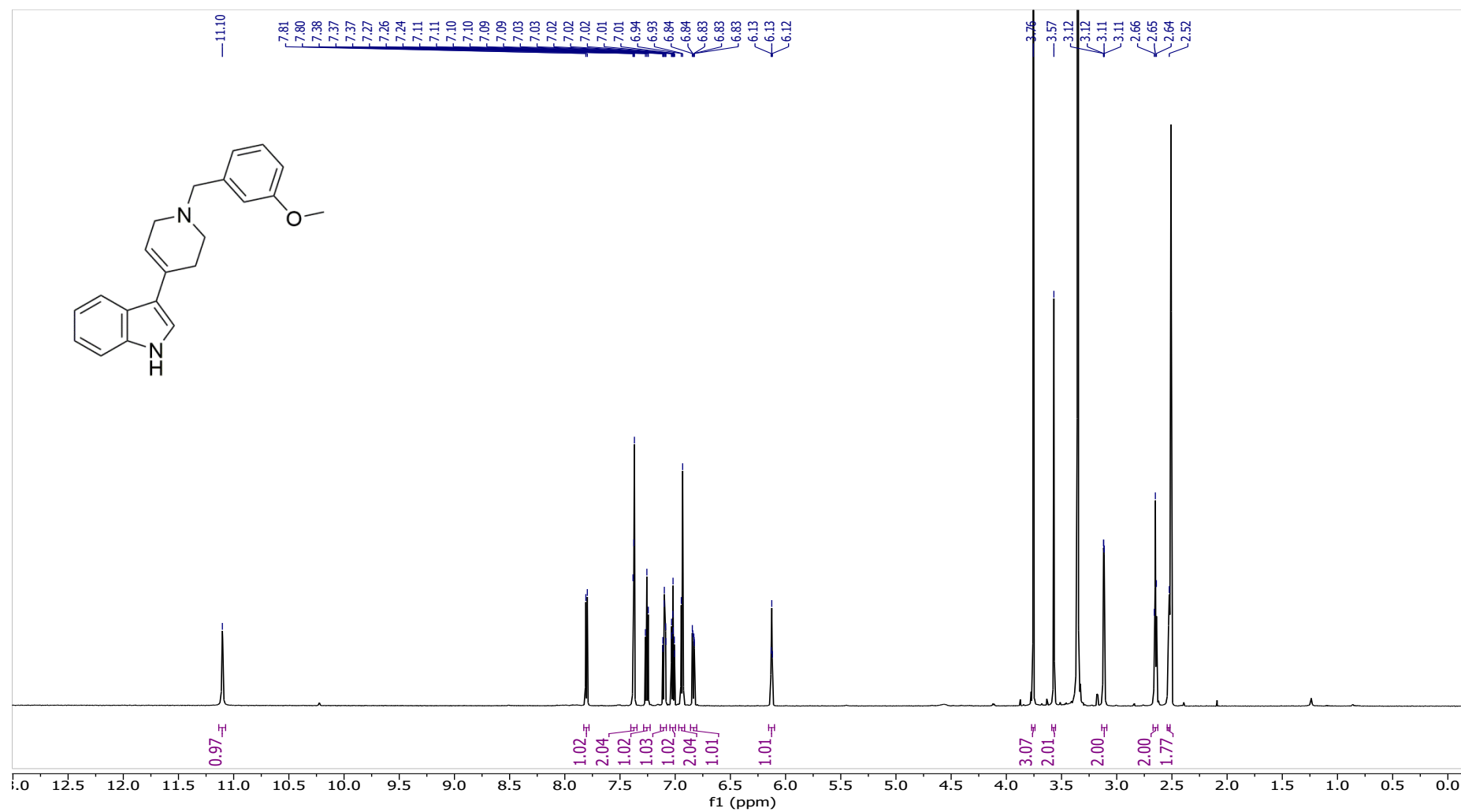
5-isopropoxy-3-(1-(4-methoxybenzyl)-1,2,3,6-tetrahydropyridin-4-yl)-1*H*-indole (**16**)



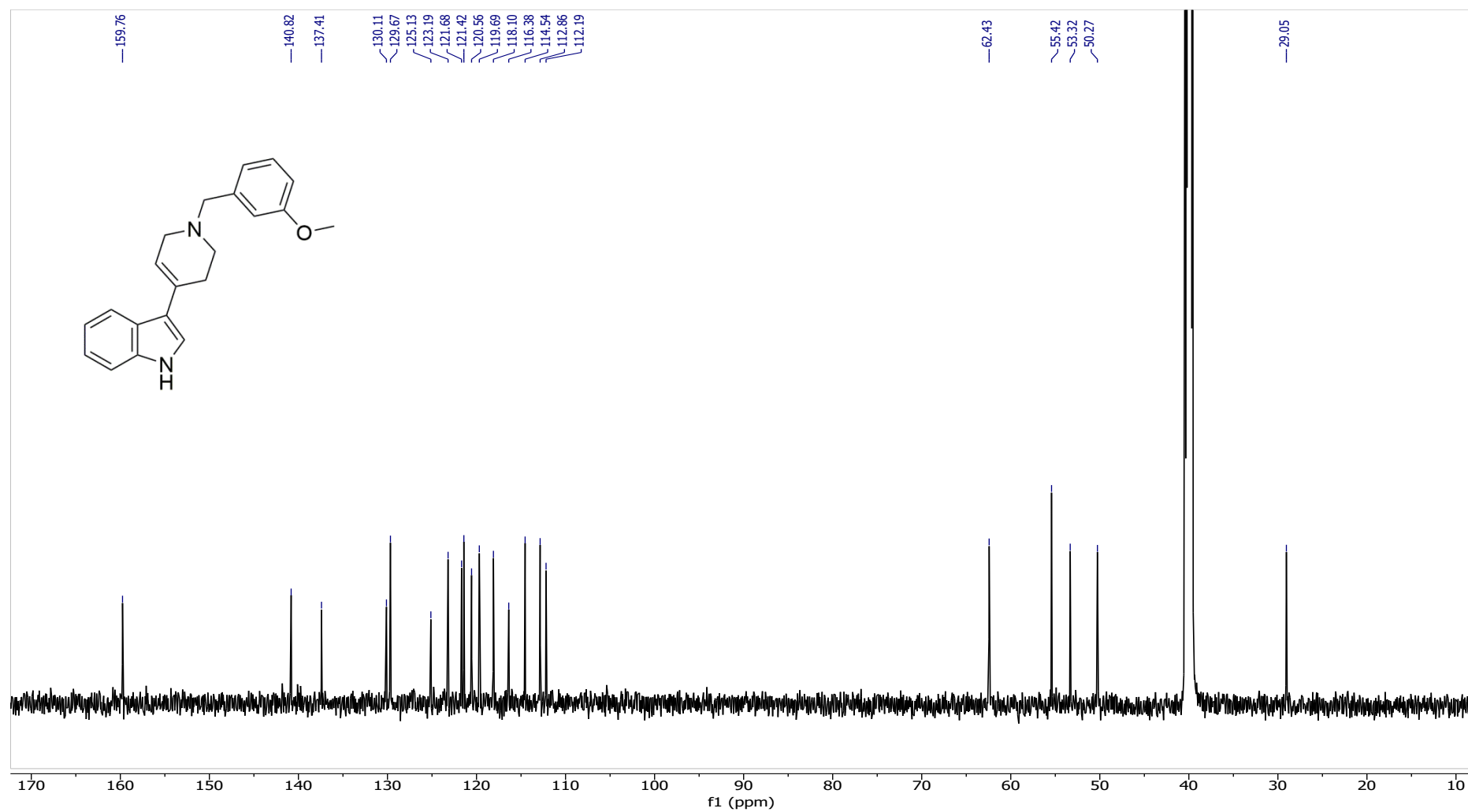
5-isopropoxy-3-(1-(4-methoxybenzyl)-1,2,3,6-tetrahydropyridin-4-yl)-1H-indole (**16**)



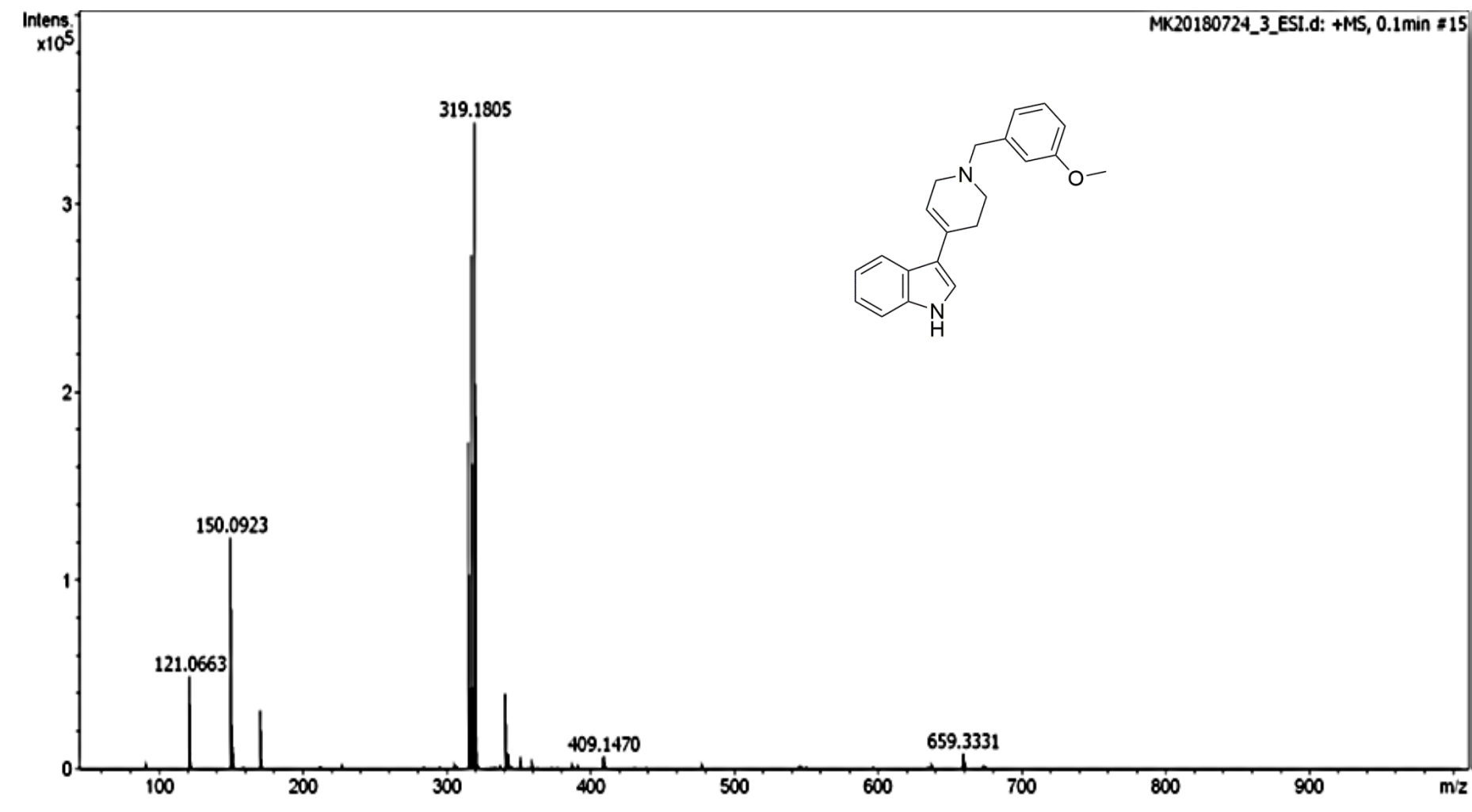
3-(1-(3-methoxybenzyl)-1,2,3,6-tetrahydropyridin-4-yl)-1H-indole (17)



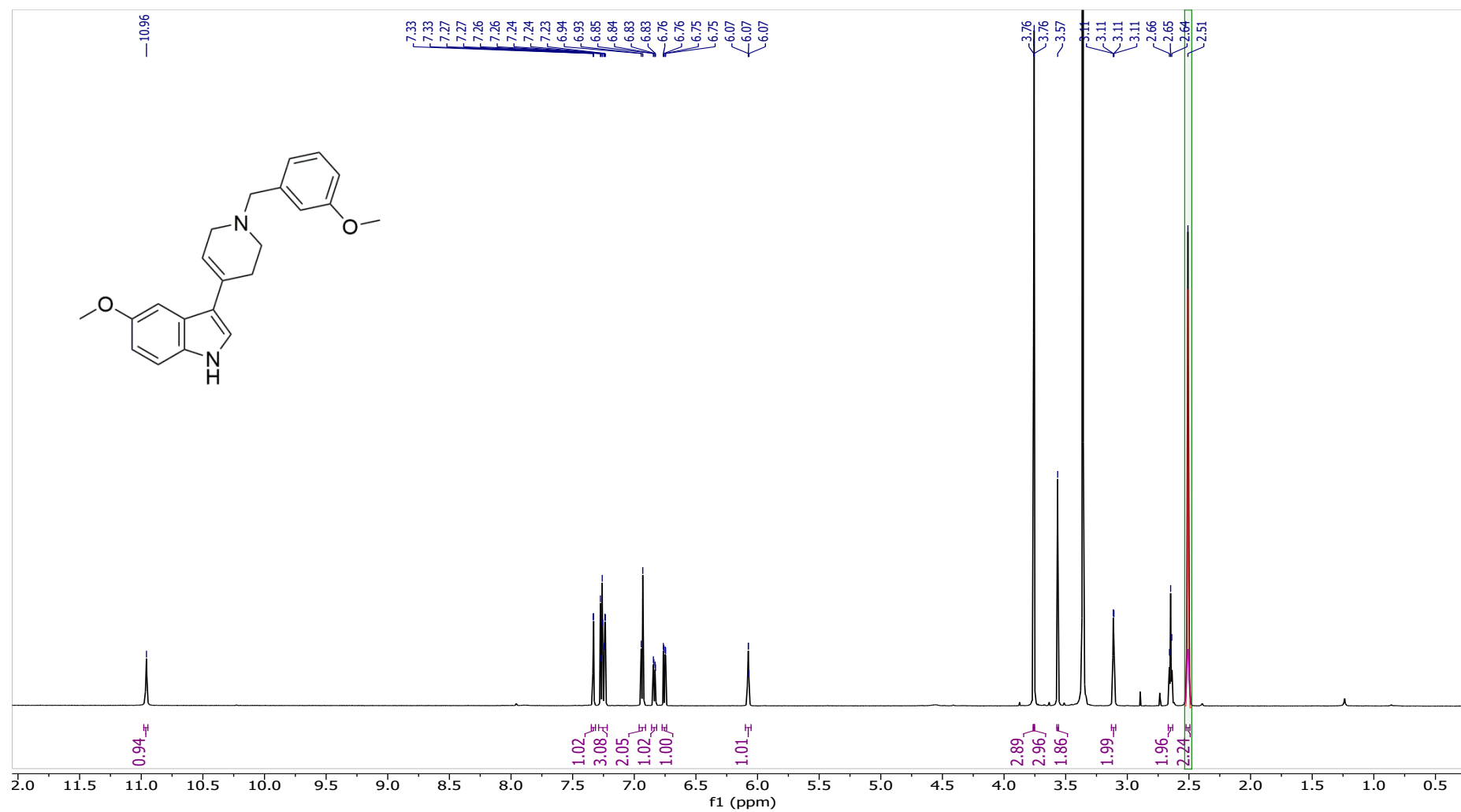
3-(1-(3-methoxybenzyl)-1,2,3,6-tetrahydropyridin-4-yl)-1*H*-indole (17)



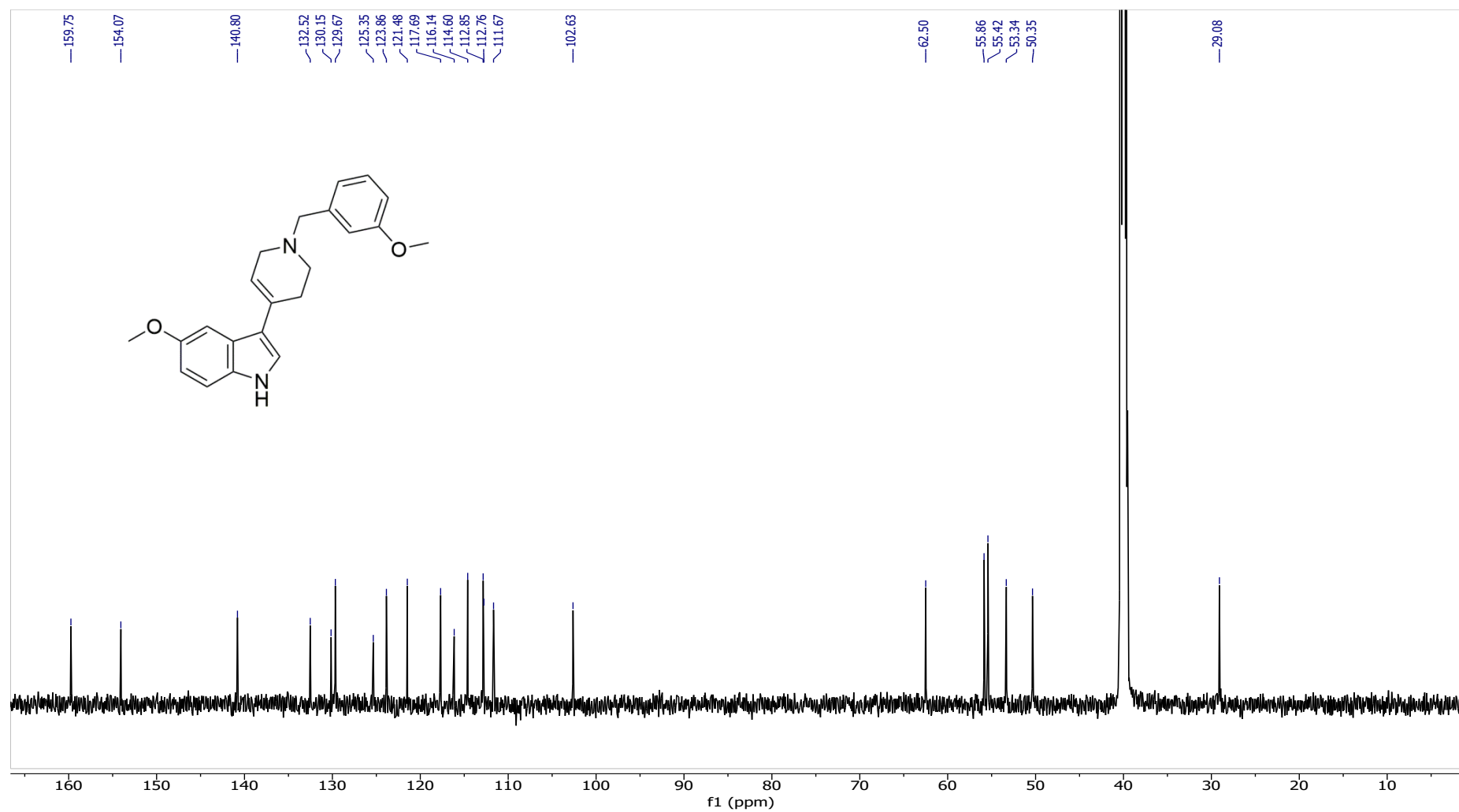
3-(1-(3-methoxybenzyl)-1,2,3,6-tetrahydropyridin-4-yl)-1*H*-indole (17)



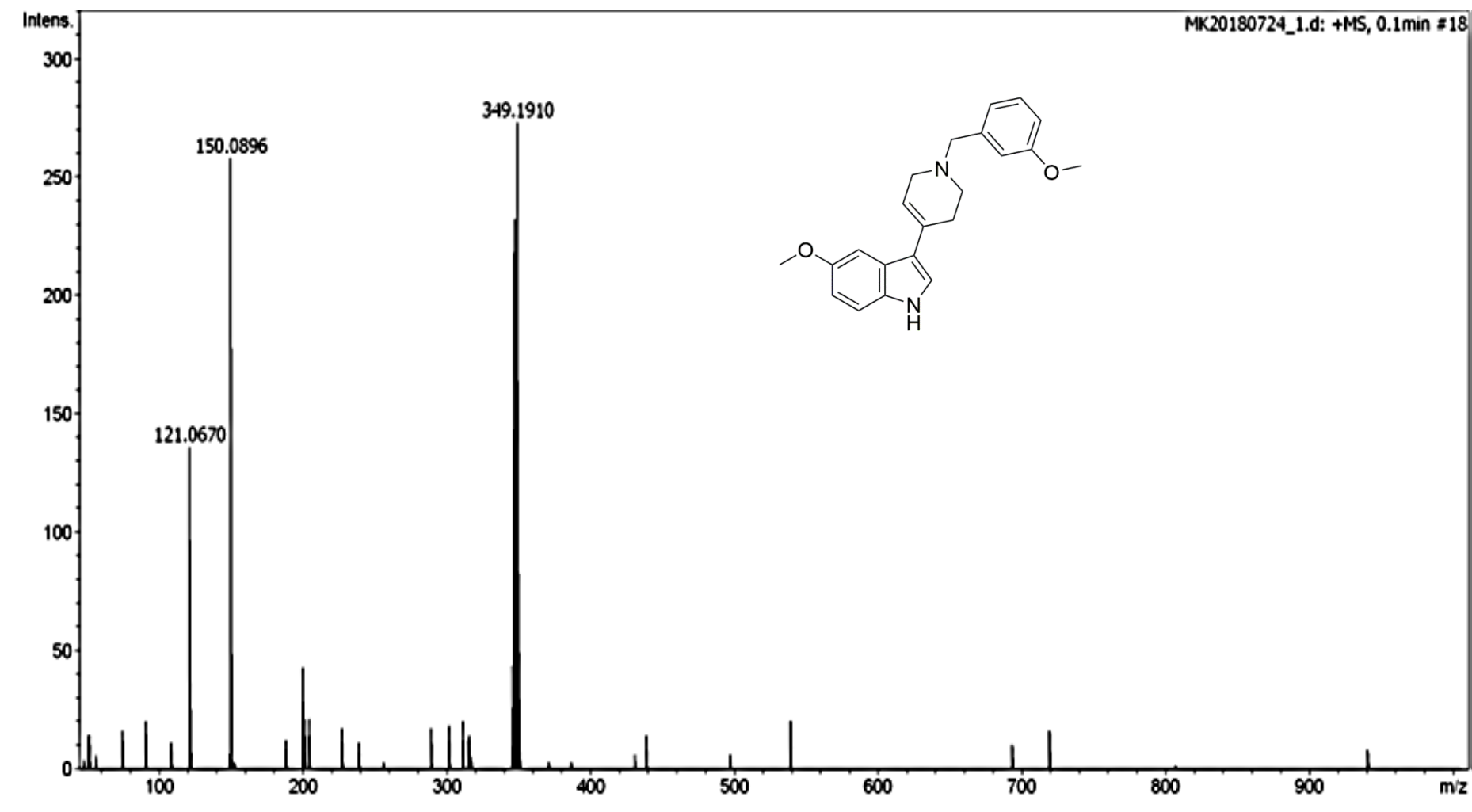
5-methoxy-3-(1-(3-methoxybenzyl)-1,2,3,6-tetrahydropyridin-4-yl)-1H-indole (18)



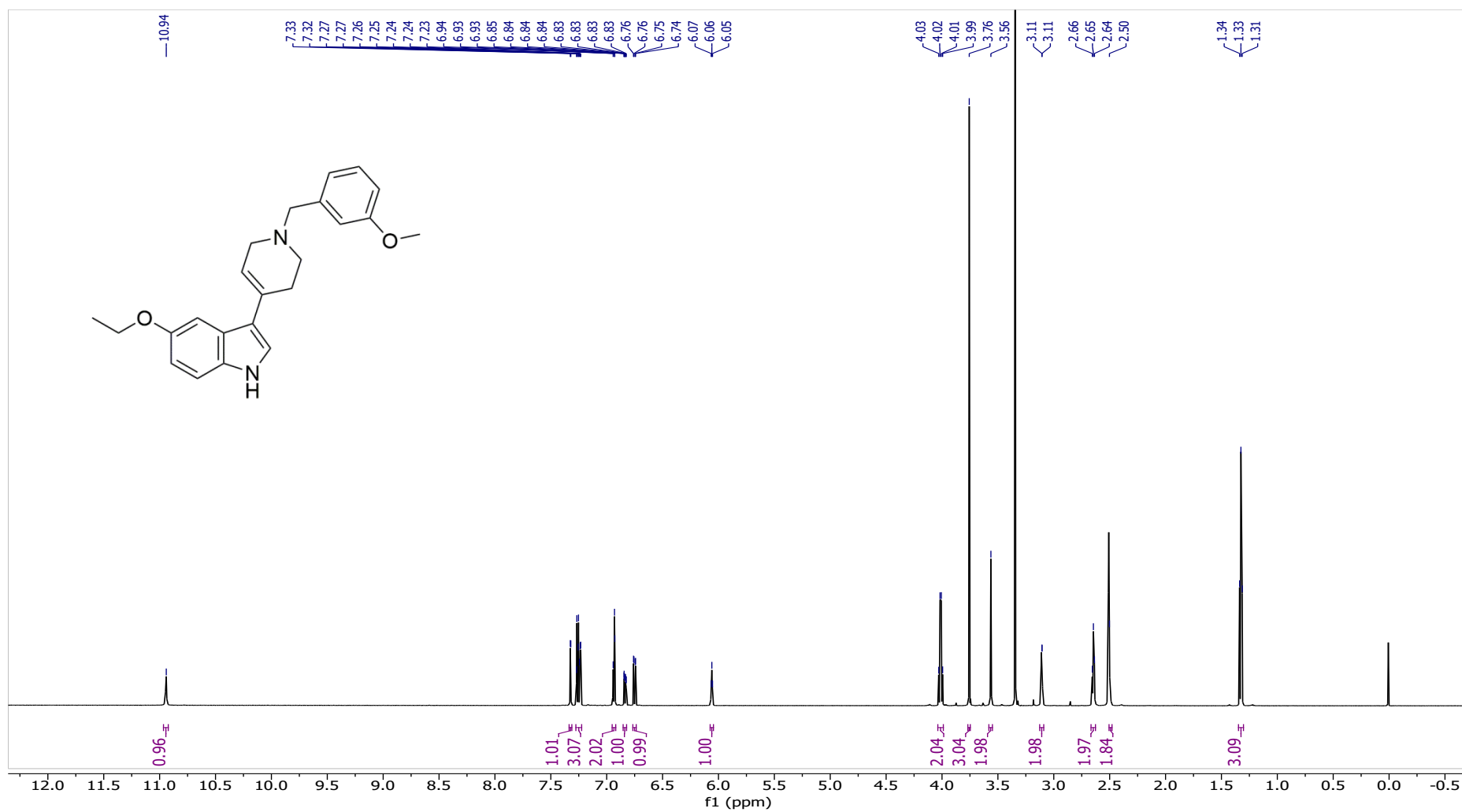
5-methoxy-3-(1-(3-methoxybenzyl)-1,2,3,6-tetrahydropyridin-4-yl)-1H-indole (**18**)



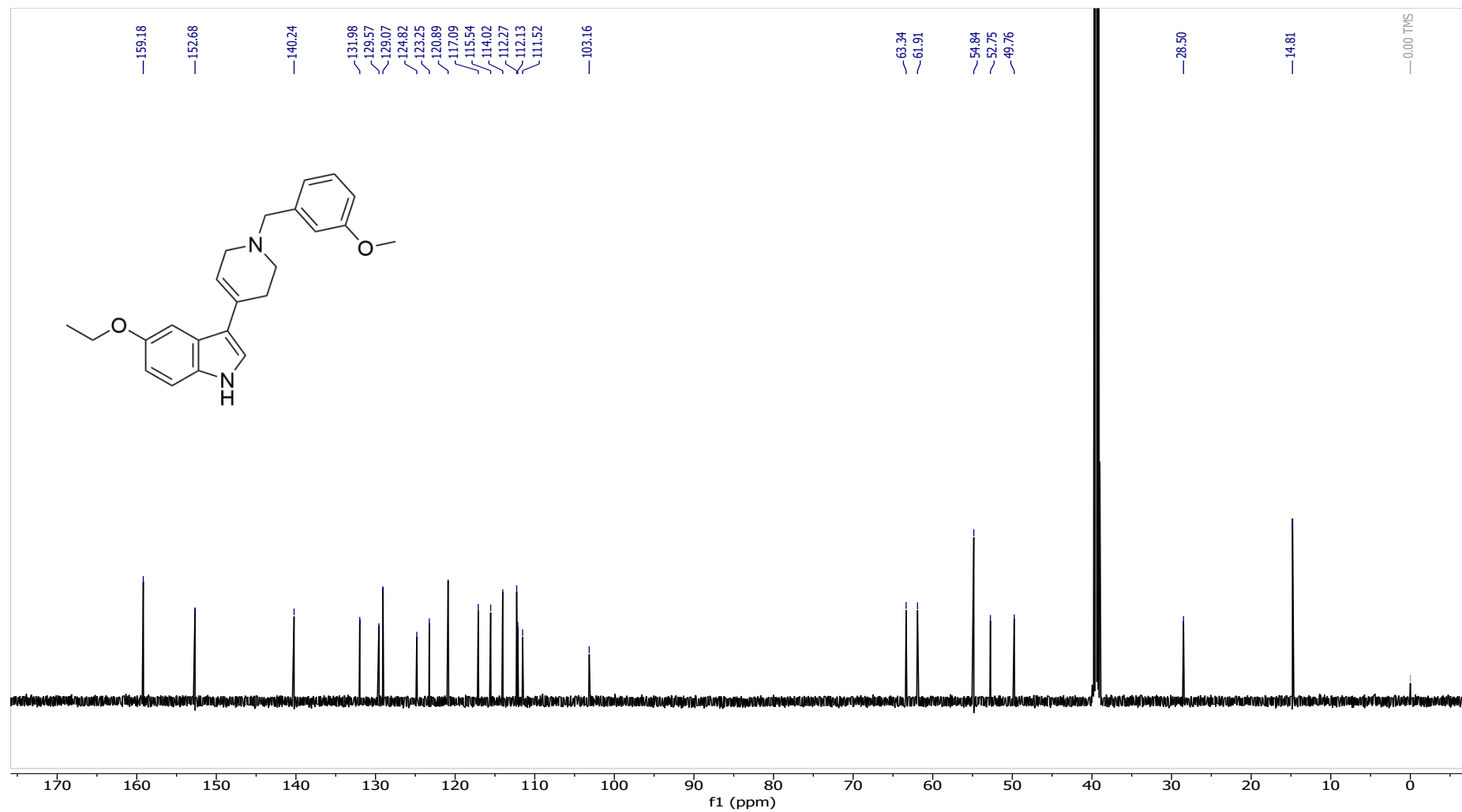
5-methoxy-3-(1-(3-methoxybenzyl)-1,2,3,6-tetrahydropyridin-4-yl)-1H-indole (18)



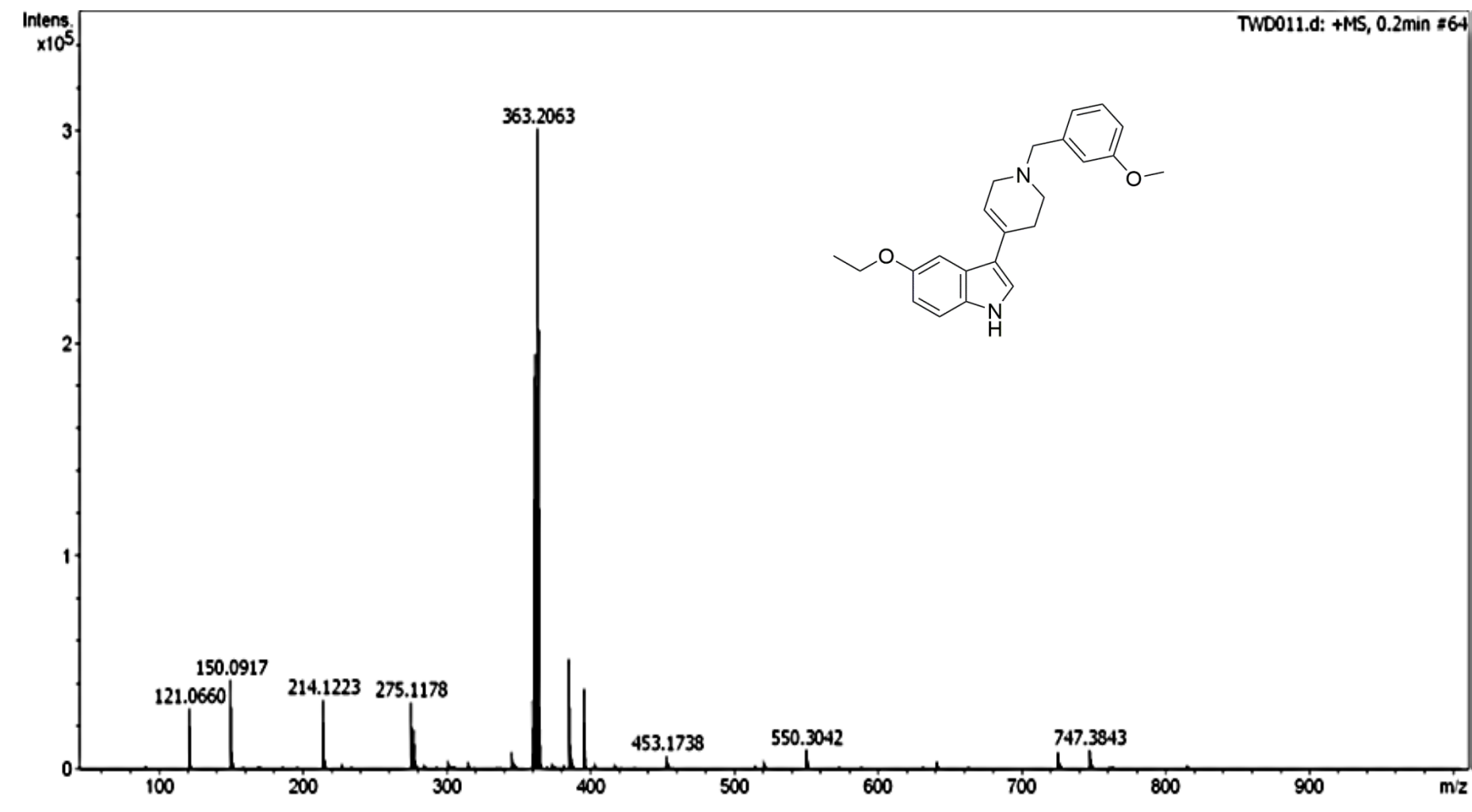
5-ethoxy-3-(1-(3-methoxybenzyl)-1,2,3,6-tetrahydropyridin-4-yl)-1H-indole (19)



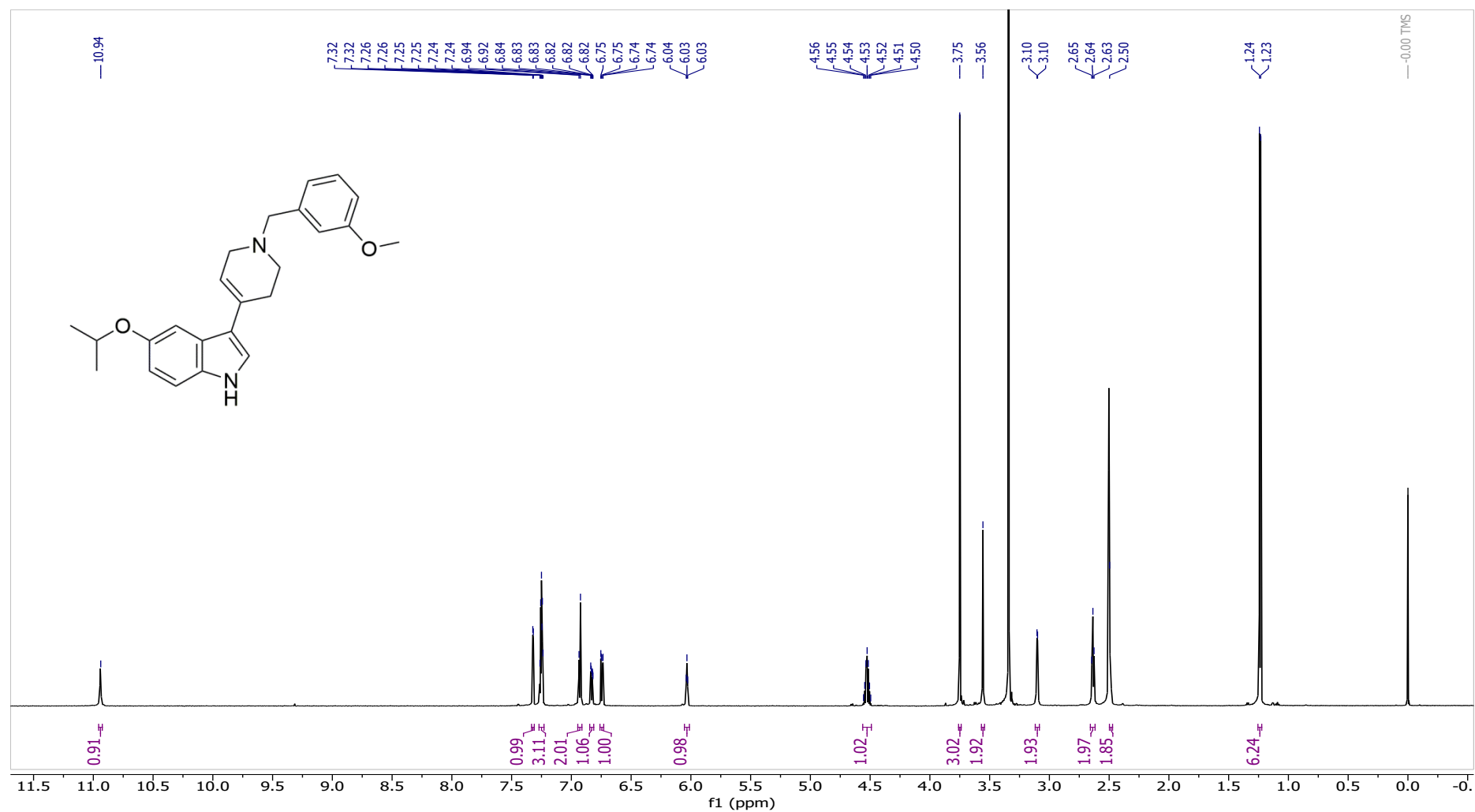
5-ethoxy-3-(1-(3-methoxybenzyl)-1,2,3,6-tetrahydropyridin-4-yl)-1H-indole (19)



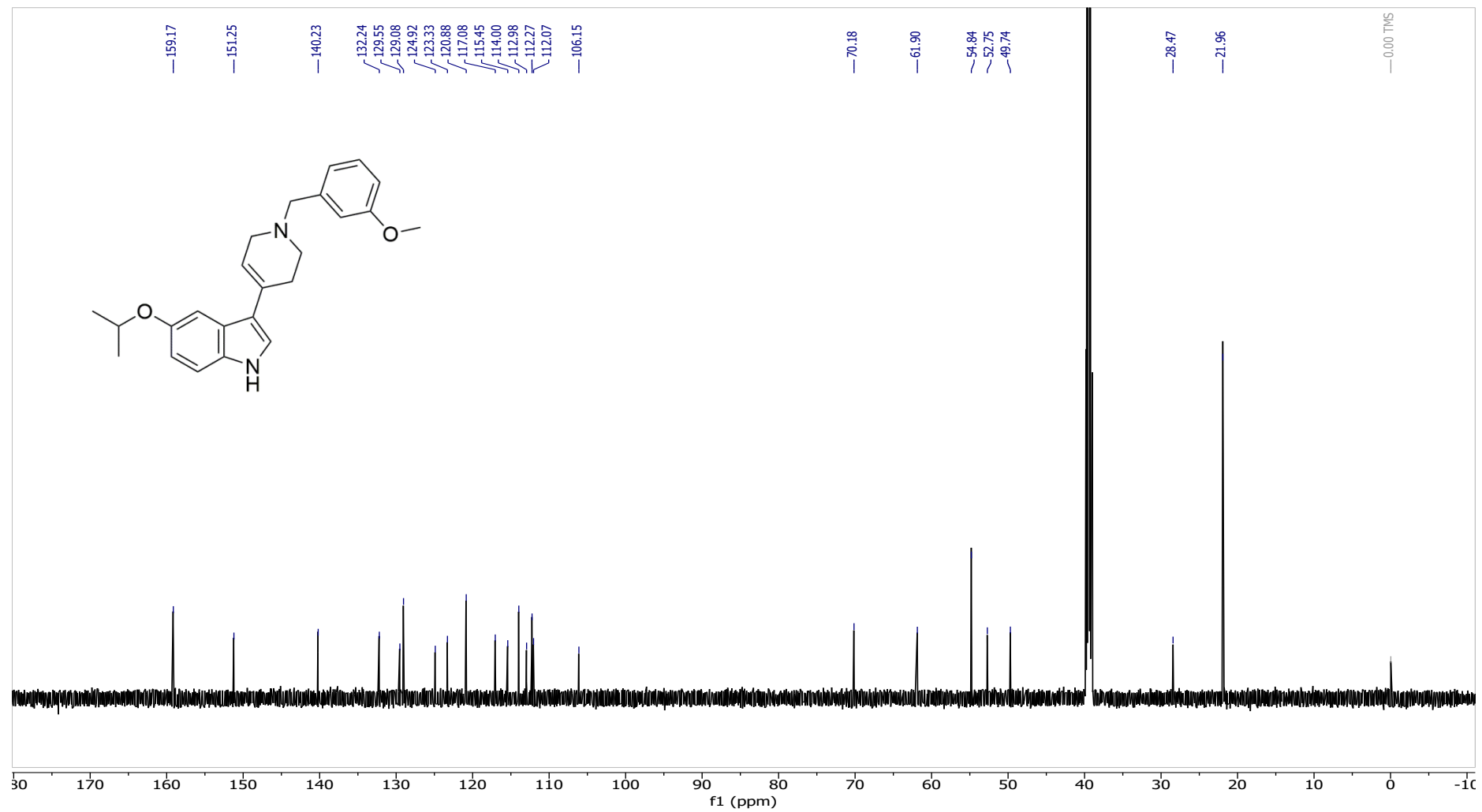
5-ethoxy-3-(1-(3-methoxybenzyl)-1,2,3,6-tetrahydropyridin-4-yl)-1H-indole (19)



5-isopropoxy-3-(1-(3-methoxybenzyl)-1,2,3,6-tetrahydropyridin-4-yl)-1H-indole (20)



5-isopropoxy-3-(1-(3-methoxybenzyl)-1,2,3,6-tetrahydropyridin-4-yl)-1*H*-indole (**20**)



5-isopropoxy-3-(1-(3-methoxybenzyl)-1,2,3,6-tetrahydropyridin-4-yl)-1*H*-indole (**20**)

